University of Naples Federico II

PhD PROGRAM IN NEUROSCIENCE
XXXVII CYCLE

FUNCTIONAL CHARACTERIZATION OF NOVEL K_V7 POTASSIUM CHANNEL MODULATORS DISCOVERED VIA DRUG REPURPOSING AND IN SILICO STRATEGIES

Coordinator: **Prof. Maurizio Taglialatela**

Tutor **Prof. Francesco Miceli**

Candidate **Dr Giusy Carleo**

ACADEMIC YEAR 2023-24

UNIONE EUROPEA
Fondo Sociale Europeo
Ministero dell'Università e della Ricerca
PON RICERCA E INNOVAZIONE 2014 - 2020
REACT EU

La borsa di dottorato è stata cofinanziata con risorse del
Programma Operativo Nazionale Ricerca e Innovazione 2014-2020, risorse FSE REACT-EU
Azione IV.4 “Dottorati e contratti di ricerca su tematiche dell’innovazione”
e Azione IV.5 “Dottorati su tematiche Green”

Index

Abbreviations

3D: three-dimensional

ACMG: American College of Medical Genetics

ADNFLE: autosomal dominant nocturnal frontal lobe epilepsy

AEDs: antiepileptic drugs

AHP: afterhyperpolarization

AIS: axon initial segment

AKAP: A-kinase anchoring protein

ankG: ankyrin G

AP: action potential

ASMs: antiseizures medications

BBR: Benzbromarone

BFNS: *Benign Familial Neonatal Seizures*

BHB: β-hydroxybutyric acid

Ca^{2+}: calcium ion

CaM: Calmodulin

CHO: Chinese Hamster Ovary

CHRNA4: cholinergic receptor nicotinic alpha 4 subunit

Cl^-: chloride ion

CMA: chromosomal microarray

CNS: central nervous system

CNVs: copy number variants

-COOH: carboxy

CryoEM: Cryo-electron microscopy

DAG: diacylglycerol

DEE: developmental and epileptic encephalopathies

DFNA2: deafness nonsyndromic autosomal dominant 2

DNA: Deoxyribonucleic acid

DRE: drug-resistant epilepsy

DRG: dorsal root ganglion

EC_{50}: half maximal effective concentration

EEG: electroencephalogram

EIMFS: Epilepsy of infancy with migrating focal seizures

EMA: European Medicines Agency

FDA: Food and Drug Administration

GABA: γ-amino-butyric acid

$GABA_A$: gamma-aminobutyric acid type A

GABOB: γ-amino-β-hydroxybutyric acid

GCs: granule cells

GoF: gain-of-function

GPCRs: G protein-coupled receptors

GSK: GlaxoSmithKline

GWAS: genome-wide association study

H^+: hydrogen ion

HBA: hydrogen bond acceptor

HBD: hydrogen bond donor

hERG: human Ether-à-go-go-Related Gene

HTS: high throughput screening

IC_{50}: half maximal inhibitory concentration

ID: intellectual disability

I_{KM}: M-current

I_{Ks}: delayed rectifying K^+ current

ILAE: International League Against Epilepsy

IP_3: inositol triphosphate

iPSCs: Induced pluripotent stem cells

IVA: isovaleric acid

K^+: potassium ion

K_{2P}: tandem pore domain potassium channel

K_{Ca} Ca^{2+}-activated K^+ channels

KCC2: potassium-chloride co-transporter 2

K_{ir} inward-rectifier K^+ channels

K_{Na}: Na^+-activated K^+ channels

K_V: voltage-gated K^+-channels

LBDD: ligand-based drug design

LoF: loss-of-function

LQTS: long QT syndrome

LZ: leucine zipper

MD: Molecular Dynamics

MEA: microelecrode array

MES: maximal electroshock seizures

MiRPs: MinK-related peptides

MS: Mass spectrometry

MTX: mallotoxin

Na^+: sodium ion

nAChR: nicotinic acetylcholine receptor

Nedd4-2: neuronal precursor cell-expressed developmentally downregulated

NGS: next-generation sequencing

$-NH_2$: amino

NKCC1: sodium-potassium-chloride co-transporter 1

NMD: non-sense mediated mRNA decay

NMDA: N-methyl-D-aspartate

OHCs: outer hair cells

PB: PiggyBac

PCR: Polymerase Chain Reaction

PD: pore domain

PDB: Protein Data Bank

Pen/strep: penicillin/streptomycin

PIP_2: Phosphatidylinositol 4,5-bisphosphate

PKA: cAMP-dependent protein kinase A

PKC: protein kinase C

PLC: phospholipase C

P_o: maximal probability of opening

PRE: pharmacoresistant epilepsy

PTZ: pentylenetetrazole

Rs: arginine residues

SAR: structure–activity relationship

SBDD: structure-based drug design

Sec1 or STXBP1: syntaxin binding protein 1

SeLFIS*: Self-limited Familial Infantile Seizures*

SeLFNE *self-limited Familial Neonatal Epilepsy*

SeLFNIS: *Self-limited Familial Neonatal-Infantile Seizures*

SID: subunit interaction domain

SQTS: short QT syndrome

SUDEP: sudden unexpected death in epilepsy patients

syx-1A: syntaxin-1A

TEA: tetraethylammonium

Tl^+: thallium ion

TM: Transmembrane

UHPLC: Ultra High Performance Liquid Chromatography

$V_{1/2}$: half-activation potential

VSD: Voltage Sensing Domain

VUS: variant of unknown significance

WES: whole-exome sequencing

WGS: whole-genome sequencing

WHO: World Health Organization

WT: wild type

ZnPy: Zinc Pyrithione

Amino acids

Alanine	Ala	A	Leucine	Leu	L
Arginine	Arg	R	Lysine	Lys	K
Asparagine	Asn	N	Methionine	Met	M
Aspartic acid	Asp	D	Phenylalanine	Phe	F
Cysteine	Cys	C	Proline	Pro	P
Glutamic acid	Glu	E	Serine	Ser	S
Glutamine	Gln	Q	Threonine	Thr	T
Glycine	Gly	G	Tryptophan	Trp	W
Histidine	His	H	Tyrosine	Tyr	Y
Isoleucine	Ile	I	Valine	Val	V

ABSTRACT

K_v7 potassium channels, encoded by the KCNQ gene family, play a fundamental role in neuronal excitability and are implicated in various neurological disorders, including epilepsy and developmental encephalopathies. This study aims to identify and characterize novel K_v7 modulators using a combined approach of drug repurposing and computational modeling. High-throughput screening (HTS) of a repurposing library led to the discovery of promising K_v7 activators, which were further evaluated through electrophysiological techniques, including manual patch-clamp and multi-electrode arrays. The most effective compound, C4, was examined for its selectivity, binding site, and functional effects on iPSC-derived cortical excitatory neurons and pre-clinical seizure models. Additionally, in silico-guided synthesis was employed to design CPRET-106, a novel $K_v7.2$ modulator, which was assessed for its effects on wild-type and gain-of-function mutant channels. The findings contribute to the pharmacological understanding of K_v7 channels and highlight potential therapeutic candidates for epilepsy and related disorders.

INTRODUCTION

The action potential (AP) is a fundamental electrophysiological process that facilitates rapid and coordinated communication in excitable cells, such as neurons and muscle fibers. It is characterized by a transient and reversible shift in the membrane potential, which propagates along the plasma membrane through the orchestrated opening and closing of selective ion channels. While voltage-dependent sodium (Na^+) channels drive the rapid depolarization that moves the membrane potential closer to the AP threshold, voltage-dependent potassium channels activate with a delay, permitting the efflux of K^+ ions. Potassium channels play pivotal role during the phases of **repolarization** and **membrane potential stabilization** in the action potential cycle.

1.1 POTASSIUM CHANNELS

The most diverse and functionally varied type of ion channels found in both prokaryotic and eukaryotic cells are potassium (K+) channels. They regulate the flux of K^+ ions across cellular membranes and are involved in various physiological processes such as cell volume, proliferation, differentiation and survival in both excitable and non-excitable cells. Over 70 genes that encode for K^+ channel subunits have been found in humans. They respond to various physicochemical stimuli and exhibit distinct gating mechanisms tailored to their respective functions, despite sharing a highly conserved selectivity filter for K^+ ions within the pore. Voltage fluctuations in case of K_v channel increases in intracellular levels of calcium (Ca^{2+}) or sodium (Na^+) in case of K_{Na} channel, cellular mediators in case of K_{ir} channel, or temperature in case of K_{2P} channel can all activate K^+ channels. They can be divided into many subfamilies according to their structural and functional properties (Figure 1.1).

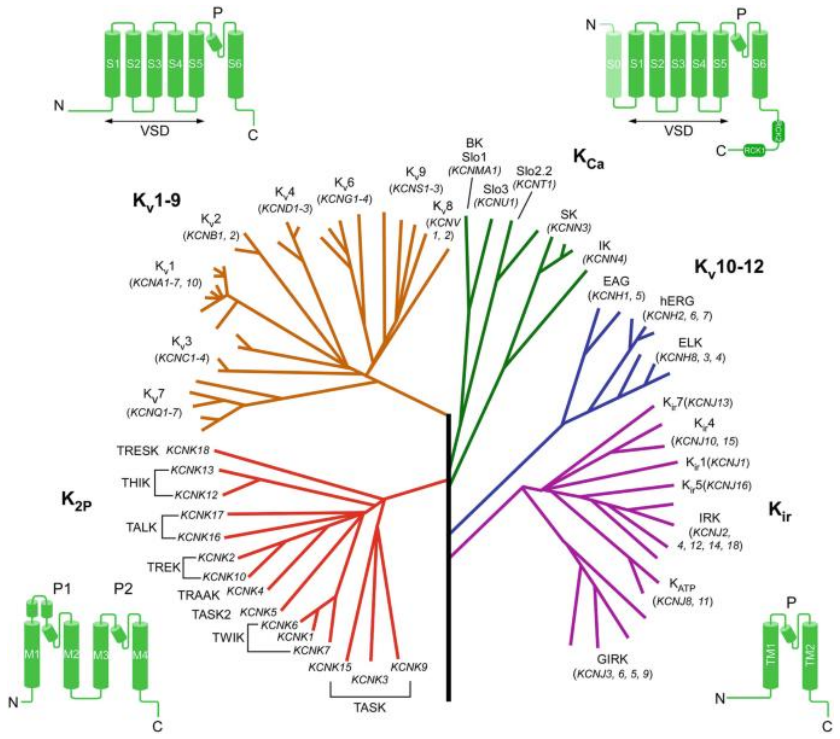

Figure 1.1 Dendrogram of the different families of potassium channels (Gamper et all, 2024)

K^+ channels can assemble into a tetrameric (K_V, K_{Ca}, K_{Na}, and K_{IR} channels) or tetramer-like (K_{2P} channels) architecture based on the transmembrane topology of their subunits, K^+ channels can be classified in:

I) *channels with six transmembrane segments subunits* (6TM): includes voltage-gated K^+ channels (K_V channels; K_V1–K_V12), small conductance Ca^{2+}-dependent K^+ channels (K_{Ca}) and Na^+-dependent K^+ channels (K_{Na});

II) *channels with two transmembrane segments subunits* (2TM): composed by the inward-rectifier channels ($K_{ir}1$–$K_{ir}7$), structurally homologous to the S5–S6 segments of K_V channels and voltage-independent as they lack the voltage-sensing domain (VSD);

III) *channels with four transmembrane segments subunits* (4TM): includes at least 15 different genes ($K_{2P}1$–$K_{2P}17$), topologically characterized by the tandem repetition of two pore domains.

Nonetheless, K^+ channel structural and functional variability is not exclusive to these three categories. Large-conductance Ca^{2+}-dependent K^+ channels, for instance, are tetramers of subunits with seven transmembrane segments (Gamper et al., 2021).

1.1.1 K_V7 POTASSIUM CHANNELS

The KCNQ genes (KCNQ1–5) encode five members of the voltage-gated potassium channel subfamily called $K_V7.1–7.5$. These channels generate a current with slow activation/deactivation kinetics and no inactivation that activates at about -60 mV. This current is essential for regulating the excitability of neurons and muscle cells (Delmas, 2005; Gamper & Shapiro, 2015). Before the KCNQ genes were discovered, K_V7 currents were recorded and examined in neuronal, cardiac, and epithelial cells. Initially, a slow, non-inactivating K^+ current fraction was found in bullfrog sympathetic neurons. This K^+ current was named "M-current" (I_{KM}) (Brown, 1980), because activation of muscarinic receptors, inhibited this voltage-sensitive K^+ current. Later, a K^+ current with even slower kinetics than I_{KM} was found in the heart tissue and was called "I_{Ks}" (Walsh, 1988).

1.1.1.1 REGULATION OF K_V7 CHANNELS

K_V7 channels are characterized by a notably long intracellular C-terminal region, organized into four conserved α-helical domains (A–D helices), shared by all K_V7 family members (Yus-Najera et al., 2002). The C-terminus serves as a critical platform for interactions with various molecules and proteins, essential for Kv7 channel functionality and regulation (Figure 1.2).

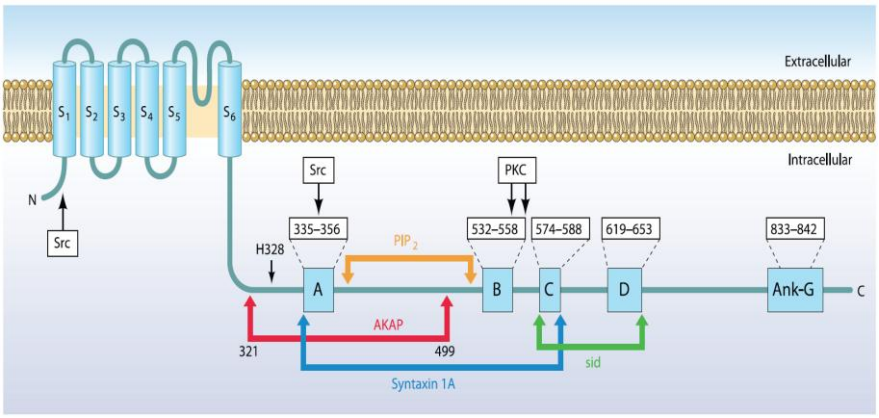

Figure 1.2 Schematic representation of a single $K_V7.2$ subunit. The approximate position of the binding domain for PIP_2 in the COOH terminus is indicated. A, B, C, and D correspond to the four hypothetical α-helical regions. Sid, subunit interaction domain; CaM, calmodulin; AKAP, A-kinase-anchoring protein; PKC, protein kinase C; Ank-G, ankyrin-G; PIP_2, phosphatidylinositol-(4,5)-bisphosphate; Src, proto-oncogene tyrosine-protein kinase (Soldovieri et al., 2011).

Calmodulin (Calcium-modulated protein, or CaM): CaM is a small, soluble, and thermostable protein that binds calcium ions. Structurally, it features two globular domains, the N-lobe and C-lobe, each containing two EF-hand motifs responsible for the binding of Ca^{2+} ions. All K_v7 family subunits interact with CaM, which binds to two distinct sites located on helices A and B (HA and HB) . The site on helix A contains a canonical IQ-binding motif (IQXXXRXXXXR), while helix B includes two overlapping 1-5-10 CaM-binding motifs (Yus-Najera et al., 2002). CaM is essential for proper channel trafficking; mutations in $K_v7.2$-CaM binding sites can reduce export from the endoplasmic reticulum to the plasma membrane (Etxeberria et al., 2008). Additionally, CaM regulates the enrichment of $K_v7.2/K_v7.3$ channels at the axonal initial segment (AIS) in hippocampal neurons (Liu and Devaux, 2014). It also plays a crucial role in generating functional M-current (Gamper et al., 2005).

Phosphatidylinositol-(4,5)-bisphosphate (PIP_2): PIP_2 is a negatively charged phospholipid located on the intracellular leaflet of the plasma membrane and is critical for K_v7 channels activation. It enhances the opening probability of both homomeric and heteromeric channels, with differences in single-channel open probability attributed to varying intrinsic PIP_2 affinities (Li et al., 2005). First studies identified a PIP_2 binding site in a region localized between the S6 transmembrane segment and the A helix of $K_v7.2$channels. This region is enriched of basic residues and substitution of the histidine-328 (His367 in $K_v7.3$) with cysteine reduced PIP_2 sensitivity (Zhang et al., 2003). Later studies identified additional PIP_2-binding regions: one in the A-B helix linker, where PIP_2 phosphate headgroups form electrostatic bonds with a "cationic cluster" (Hernandez et al., 2009), and others in the S2-S3 and S4-S5 loops. PIP_2 binds the S2-S3 loop in the closed state and shifts to the S4-S5 loop during channel activation (Zhang et al., 2013). Structural analyses of PIP_2-bound K_v7 channels reveal the presence of at least two distinct PIP_2 binding sites, designated as PIP_2–I and PIP_2–II. The PIP_2–I site has been identified in various $K_v7.1$ structures and is located within a cleft formed by the S2–S3 linker, S3, S4, and the S4–S5 linker, where the inositol 1,4,5-trisphosphate head group of PIP_2 interacts with positively charged residues on the S2–S3 and S4–S5 linkers (Sun et al., 2020). In addition to PIP_2–I, the PIP2–II site has been observed in the structure of KCNQ4 (Zheng et al.,, 2022). This site is situated in a cleft defined by S1, S4, and S5 from an adjacent subunit and establishes polar interactions with positively charged residues on S0, S1, S4, S5, and S6. Notably, PIP_2–II directly interacts with a conserved lysine residue in S6 (Lys333 in KCNQ4) (Zheng et al., 2022).

AKAP79/150: AKAP79/150 (A-kinase anchoring protein) modulates K_v7 channel function by binding to the Kv7.2 C-terminus and forming a trimeric complex with protein kinase C (PKC). PKC activation phosphorylates serine residues on helix B, suppressing $K_v7.2$ currents. Removing two PKC phosphorylation sites on helix B largely prevents this effect (Hoshi et al., 2003).

Syntaxin-1A (Syx-1A): is a plasma membrane SNARE protein involved in neurotransmitter release. It interacts with neuronal Sec1 (STXBP1) to form a complex facilitating membrane fusion. In $K_v7.2$ and $K_v7.3$ subunits, Syx-1A binds helix A and exerts opposing effects. It reduces $K_v7.2$ currents by approximately 50% but has no inhibitory effect on $K_v7.3$ currents. This difference may result from additional Syx-1A binding sites on $K_v7.2$, particularly in its N-terminus, absent in $K_v7.3$ (Regev et al., 2009).

Ankyrin-G (AnkG): is an adaptor protein responsible for localizing $K_v7.2$ and $K_v7.3$ subunits at the axon initial segment (AIS) and nodes of Ranvier, both critical for action potential generation and propagation. AnkG binds selectively to the distal part of helix D in the $K_v7.2/K_v7.3$ C-terminus (Devaux et al., 2004; Pan et al., 2006).

Nedd4-2: Nedd4-2, a ubiquitin-protein ligase, regulates the surface expression of $K_v7.2/K_v7.3$ and $K_v7.3/K_v7.5$ channels by promoting their ubiquitination, internalization, and degradation. While the PY domain in the $K_v7.1$ C-terminus is crucial for this process, its role in $K_v7.2/K_v7.3$ remains less defined (Ekberg et al., 2007).

1.1.1.2 VOLTAGE GATING OF K_v7 channels

K_v channels are gated by variations in the voltage across the plasma membrane. The S1–S4 segments form the voltage-sensing domain (VSD), while S5–S6 constitute the pore domain (PD) (Figure 1.3 A-B). A peculiar aspect of the architecture of these channels is the interaction between the VSD of one subunit and the PD of the adjacent subunit, a configuration known as "domain-swapped," common to many K_v channel families. The VSD is fundamental to change conformation, which in turn allows the pore to open. The VSD passes from a resting downward position to an activated, outward position during depolarization, when the positively charged S4 segment of the VSD follows the electrostatic force and moves through the membrane. The intracellular S4-S5 linker is pulled by the positively charged Rs in S4 (numbered from the outer side of the cell membrane to the inner cytoplasmic side, see Figure 1.3 A) which then transmits these mechanical forces to the distal region of S6 of a neighbor subunit, causing pore opening. The channel returns to its resting state when the membrane potential reaches its resting potential. Although the exact changes that take place in the VSD during activation are still unclear, theories suggest that ionized hydrogen bonds between the positive Rs in S4 and groups of highly conserved negatively charged residues in the adjacent segments stabilize both the resting and activated states (Tao X et al., 2010).The activated VSD configuration is stabilized by hydrogen bonds formed between arginine residues R4, R5, and R6 and an internal negative amino acid cluster primarily provided by E1 and E2 in S2 and D1 in S3, while the R2 residue stabilizes the resting VSD states by forming an intricate network of electrostatic interactions with neighboring negatively charged residues (Long et al., 2007; Miceli et al., 2015a; Nappi et al., 2020).

In addition to membrane depolarization, K_v7 channel opening requires endogenous ligands such as the membrane lipid phosphatidylinositol 4,5-bisphosphate (PIP_2), which binds to distinct channel regions in the VSD and the PD and induce large and complex structural rearrangements. These structural rearrangements include the following key changes (Figure 1.4):

1. HA, HB, and their surrounding CaM undergo an almost 180° rotation, with HB shifting from the right side to the left side of HA;
2. S6 helices and HA form a continuous helix;

3. bending of the S6 Helix: Along with these structural rearrangements, the C-terminal part of S6 bends at the conserved ‘‘PAG’’ segment, resulting in the opening of the activation gate;
4. after the rotation, CaM, which attaches to the VSD in the closed state, is released from the VSD;
5. as HC is directly connected to HB, it also undergoes a ~90° rotation during the rearrangements, forming a coiled-coil structure.

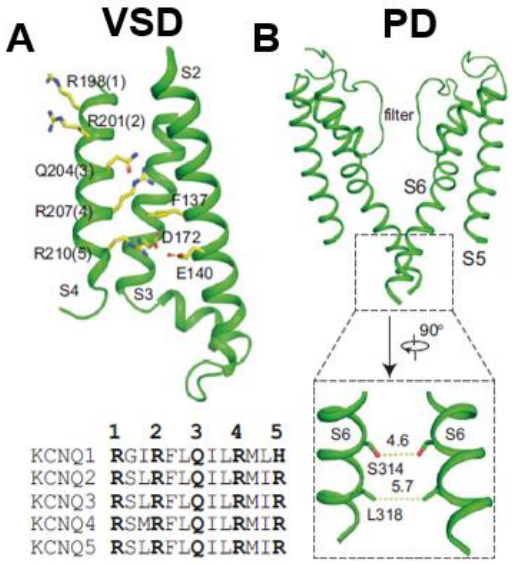

Figure1.3 The apo-state structure of Kv7.2. A) Representation of the differential role of ionized hydrogen bonds involving arginines (R) in the proximal (R2) and distal (R4, R5, R6) portions of the S4 transmembrane segment on VSD movement during K_v7 channel gating (adapted from Li et al. 2020)

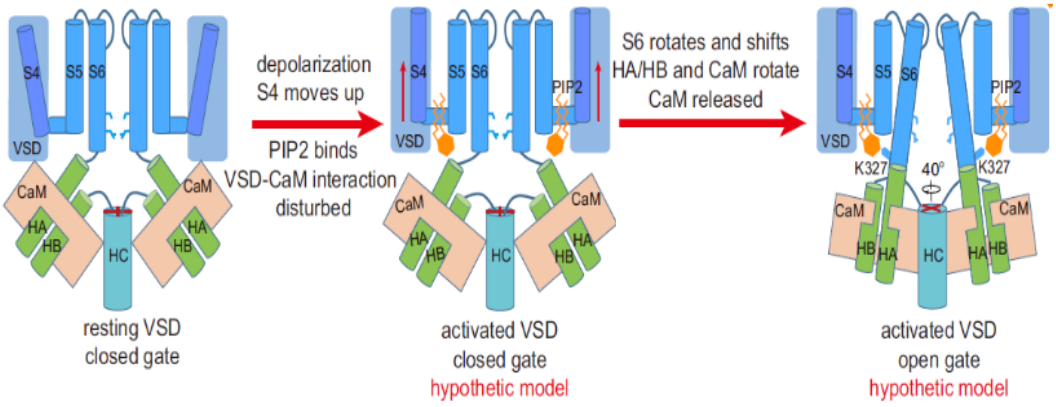

Figure 1.4 The activation mechanism of $K_v7.2$.

Several cryo-EM structures of K_V7.1 (Sun et al., 2017; Sun et al., 2020; Ma et al., 2022; Mandala et al., 2023; Willegems et al., 2022), Kv7.2 (Li et al., 2021; Ma et al., 2023; Zhang et al., 2024), and K_V7.4 (Li et al., 2021; Zheng et al., 2022) have been reported confirming in more details the structure and the activation mechanism of these class of ion channels (Figure 1.5 B-C).

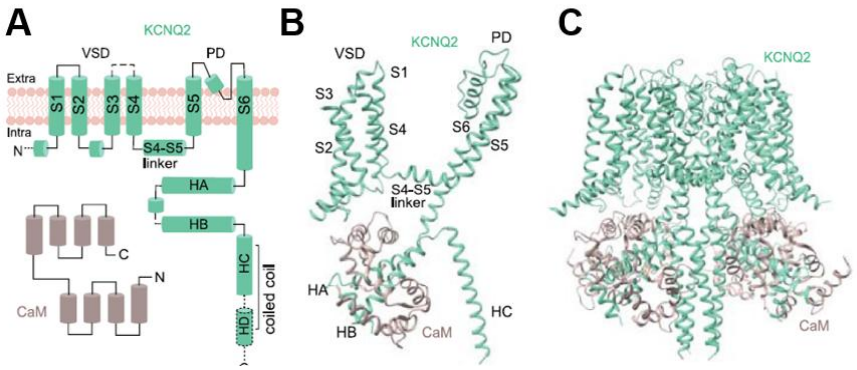

Figure 1.5. K_V7 channel architecture A) Subunit topology of KCNQ2-CaM **B)** Single subunit structure of HsKCNQ2-CaM apo. S1–S6, HA–HC, and CaM are labeled **C)** The cartoon model of the HsKCNQ2-CaM apo complex in the side view (Yuan Huang, 2023).

1.1.1.3 DISTRIBUTION AND PHYSIOLOGICAL ROLE OF K_V7 CHANNELS

K_V7 channels are not uniformly expressed throughout the body (Figure 1.6). Although initially identified in neurons and cardiac myocytes, K_V7 channels have traditionally been classified as “cardiac” ($K_V7.1$) or “neuronal” ($K_V7.2$–$K_V7.5$) channels. However, growing research into their physiological and pathological roles highlights that this classification is overly simplistic, as K_V7 channels play crucial roles in various cell types. The $K_V7.1$ subunit, encoded by the KCNQ1 gene, is primarily expressed in cardiomyocytes, where it forms complexes with KCNE1 β-subunits. Together, these proteins generate the slow component of the delayed rectifying K^+ current (I_{Ks}), which is essential for repolarizing the cardiac action potential (Sanguinetti et al., 1996). The critical role of I_{Ks} in heart function is underscored by the severe consequences of mutations in KCNQ1 or KCNE genes, which are associated with cardiac arrhythmias, syncope, and sudden death. The majority of $K_V7.1$ loss-of-function variations lengthen the ventricular action potential duration, which results in the long QT syndrome (LQTS), by decreasing the amplitude of the repolarizing outward I_{Ks} current; on the other hand, infrequent severe gain-of-function mutations in $K_V7.1$ channels decrease the duration of the ventricular action potential by boosting I_{Ks} channel activity, which results in short QT syndrome (SQTS) and atrial fibrillation (Dvir et al., 2014). Additionally, $K_V7.1$ subunits can be found in non-cardiac organs like the pancreas, thyroid gland, gastrointestinal system, and inner ear. $K_V7.1$/KCNE2 and Kv7.1/KCNE3 complexes produce constitutively open channels in the voltage range of -80 to +80 mV, in contrast to $K_V7.1$/KCNE1 heteromers (Abbott et al., 2015; Abbott et al., 2016a). $K_V7.1$/KCNE2 channels control the production of thyroid hormones in thyrocytes and participate in the apical K^+ recycling linked to the H^+-K^+-ATPase, which is necessary for acid secretion in gastric parietal cells (Roepke et al., 2006). $K_V7.1$/KCNE3 channels are found on the basolateral membrane of colonic crypt cells in the gut. When constitutively activated and not inactivated, these channels serve as a K^+ recycling channel that promotes electrogenic intestinal Cl^- secretion (Preston et al., 2010). The functions of KCNE4 and KCNE5 β-subunits in vivo are currently being investigated, even though all five KCNE proteins control the activity of the Kv7.1 channel (Abbott et al., 2016b). Co-expression of KCNE4 inhibits $K_V7.1$ channel function by shifting the voltage sensitivity toward positive membrane values, according to in vitro experiments (Grunnet et al., 2002). KCNE5 alters $K_V7.1$'s voltage dependency and modulates $K_V7.1$ activation and inactivation in a temperature-dependent manner (Angelo et al., 2002).

Both the central and peripheral nervous systems exhibit significant levels of expression for the $K_V7.2$ and $K_V7.3$ subunits. In neuronal cells, $K_V7.2$ and $K_V7.3$ are found at subcellular

locations like the perisomatic area, the AIS, nodes of Ranvier, and synaptic terminals that are crucial for controlling neuronal transmission (Soldovieri et al., 2011). Adult neurons mostly contain $K_v7.2$ and $K_v7.3$ channels, which are assembled into heteromeric $K_v7.2/7.3$ channel that underlying the so-called M-current (I_{KM}).

There are several observations that support this theory:

1) when expressed in heterologous systems heteromeric $K_v7.2/7.3$ currents show pharmacological and biophysical characteristics mostly recapitulating those of the native I_{KM} current (Wang et al., 1998; Shapiro et al., 2000; Hadley et al., 2003).

2) $K_v7.2$ or $K_v7.3$ homomers produce extremely small currents in heterologous cells and neurons, while their co-expression results in higher current density (Schwake et al., 2000). A recent study suggests that the composition of $K_v7.2$ and $K_v7.3$ channels varies throughout development, depending on the nervous system area and cell type. These channels may be expressed in neurons, and their expressions vary with age. $K_v7.2$ is present in the mouse brain three days after birth, increasing until adulthood (Tinel et al., 1998). $K_v7.2$ and $K_v7.3$ are found in excitatory and inhibitory cells in the cortex and hippocampus, except for the GABAergic cell in vasoactive intestinal polypeptide (VIP) interneurons (Tasic et al., 2016; Goff et al., 2019). Most thalamic and forebrain cells express both $K_v7.2$ and $K_v7.3$ channels, but subcortical regions may not, and conflicting evidence suggests higher Kv7.2 channel expression in brainstem and spinal cord. (Saganich et al., 2001; Verneuil et al., 2020). $K_v7.2$, but not $K_v7.3$ subunits expressed by other neuronal populations, such as a subpopulation of dorsal root ganglion neurons (King et al., 2014) and large sciatic nerve axons (Schwarz et al., 2006). All these studies lend credence to the idea that homomeric $K_v7.2$ and $K_v7.3$ channels have distinct roles in the neuronal membrane and are expressed in different regions and at different stages of development. The $K_v7.4$ subunit, which is encoded by the KCNQ4 gene, is strongly expressed in the cochlea's sensory outer hair cells (OHCs), where it regulates their intrinsic excitability (Housley et al., 1992). It is also found in inner hair cells (IHCs) at a lesser level (Kimitsuki et al., 2010).

Additionally, $K_v7.4$ subunits have been found in skeletal muscle cells, where they control proliferation, differentiation, and response to myotoxic stimuli (Iannotti et al.,2010; Iannotti et al., 2013), as well as in vascular and visceral smooth muscle, where they are involved in the regulation of basal tone and in response to myogenic stimuli (Ipavec et al., 2011; Jepps et al., 2011; Svalø et al., 2013) (Paventi et al., 2022) (Testai et al., 2016).

The $K_v7.5$ subunit, which is encoded by the KCNQ5 gene, was the last member of the K_v7 family to be discovered. As previously stated, the $K_v7.5$ subunit exhibits a cellular pattern of expression that overlaps with that of the $K_v7.2$ and $K_v7.3$ subunits in neurons and brain regions (Lerche et al., 2000). These subunits are found in the perisomatic region, the AIS, the nodes of Ranvier, and the synaptic terminals of neurons. The Kv7.5 subunit can form heteromeric channels with Kv7.2 (Soh et al., 2022) and $K_v7.3$ subunits and has been linked to I_{KM} molecular heterogeneity. (Lerche et al., 2000; Schroeder et al., 2000). Moreover, $K_v7.5$ has been identified as a key component of medium and slow afterhyperpolarization (AHP) currents that follow an action potential in hippocampal neurons. These currents play a role in restoring the membrane potential to baseline levels after neuronal activation, thereby limiting the firing rate of neurons and preventing excessive excitability (Tzingounis et al., 2010). Additionally, $K_v7.4/7.5$ heteromeric channels were discovered in non-neuronal tissue, such as skeletal and smooth muscle cells, where they may be involved in the hyperpolarizing K^+ current in vascular smooth muscle cells that triggers vasodilation by inhibiting $Ca2^+$-dependent contraction (Stott et al., 2014). More proof that $K_v7.5$ plays a critical role in controlling neuronal excitability has recently been found in individuals with severe epileptic problems who had both gain-of-function and loss-of-function mutations in the KCNQ5 gene (Wei et al., 2022; Lehman & Guella, 2017).

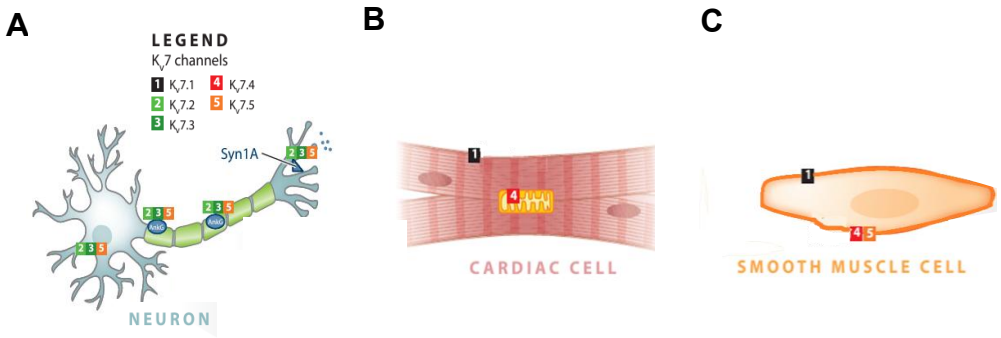

Figure 1.6 Schematic representation of the distribution of K_v7 channels in the different tissues. A) The $K_v7.2$, $K_v7.3$ and $K_v7.5$ subunits were detected at the AIS, nodes of Ranvier and presynaptic terminals in neuron. **B)** $K_v7.1$ subunit was discovered in cardiac cell. **C)** $K_v7.4$ and $K_v7.5$ subunits were detected in smooth muscle cell.

1.1.1.4 THE ROLE OF THE M-CURRENT

As described before, heteromeric $K_v7.2/K_v7.3$ channels underline the M-current, which acts as a powerful brake against excessive neuronal activity. In particular, this current is involved in the following physiological process:

1) spike-frequency adaptation

An action potential consists of a gradual depolarization toward a threshold value, followed by a rapid rising phase, an overshoot, and a repolarization phase. This process is succeeded by a brief afterhyperpolarization (AHP) phase, during which K^+ channels remain open. AHP can be subdivided into three phases:

1. a **fast phase (fAHP)** lasting 1–5 ms, primarily mediated by calcium- and voltage-dependent BK channels;
2. a **medium phase (mAHP)** lasting 50–200 ms, mediated by Kv7 and HCN channels;
3. a **slow phase (sAHP)** lasting 0.5 seconds to several seconds, mediated by Kv7 and SK Ca2+ channels.

K_v7 channels, the primary mediators of the M-current (I_{KM}), contribute significantly to both the mAHP and sAHP, influencing the refractory period and neuronal firing frequency (Tzingounis and Nicoll, 2008). Therefore, slow activation of I_{KM} reduces the frequency of neuronal firing in response to sustained stimuli, a phenomenon known as spike-frequency adaptation.

K_v7 channels are expressed in presynaptic terminals, where they regulate neurotransmitter release. Martire and coll. (2004) established that activation of presynaptic I_{KM} hyperpolarizes hippocampal nerve terminals, reducing calcium influx through voltage-gated $Ca2^+$ channels. This, in turn, diminishes the release of noradrenaline, GABA, and D-aspartate. In a subsequent study, the same authors (2007) highlighted the role of $K_v7.2$ subunits in dopamine release from rat striatal synaptosomes. They observed that the I_{KM} activator retigabine inhibited [^{3}H] dopamine release, whereas I_{KM} blockers such as TEA and XE991 enhanced [^{3}H] dopamine release and counteracted retigabine-induced inhibition.

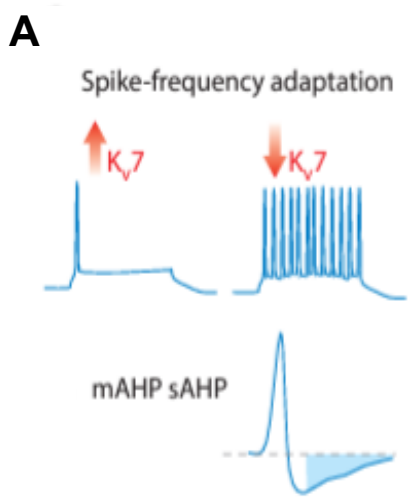

Figure 1.7 Summary of I_{KM} current electrophysiological effects in neurons. (Adapted from Barrese et al, 2017))

1.1.1.6 KCNQ2, KCNQ3 AND KCNQ5-RELATED CHANNELOPATHIES

KCNQ2 mutations cause a wide range of neurodevelopmental and epileptic phenotypes, from more benign forms like *self-limited familial neonatal epilepsy* (SeLFNE, previously known as Benign Familial Neonatal Seizures, BFNS) to more severe phenotypes, such as *developmental and epileptic encephalopathy* (DEE). SeLFNE is characterized by multifocal seizures starting around the third day of life and disappearing within a few weeks or months; however, 10-15% of affected children show seizures later in life (Plouin et al., 1994). Seizures are generally brief, lasting one to two minutes, and the motor activity may be confined to one body part, migrate to other body regions, or generalize. The neuropsychological development is usually normal (Miceli, 2018).

On the other hand, DEE is characterized by pharmaco resistant seizures that begin in the first week of life and remit between nine months and four years of age. Contrary to SeLFNE, patients with DEE show moderate to severe developmental impairment (Weckhuysen et al., 2012). Additionally, KCNQ2 mutations have been identified in several individuals with Ohtahara syndrome (Saitsu et al., 2012), the most severe and the earliest developing age-related epileptic encephalopathy, characterized by tonic seizures occurring within the first three months of life, often within the first two weeks. In SeLFNE, KCNQ2 mutations are inherited from affected parents through a classical autosomal dominant pattern. These mutations predominantly include missense and frameshift/deletion variants, splice variants, nonsense mutations, and exon deletions have. The mutations associated with SeLFNE are distributed throughout the $K_V7.2$ sequence, often clustering in the VSD between the S2 and S3 segments. These mutations typically result in a mild loss of function effect (LoF) that cannot be compensated by the wild-type allele. Functional studies have indicated that a reduction in I_{KM} by as little as 25% is sufficient to cause SeLFNE (Schroeder et al., 1998). The LoF variants may casue epilepsy by the following mechanism: mutations in the PD can reduce the current density; those in the VSD can reduce the voltage sensitivity (Dedek et al., 2001; Castaldo et al., 2002; Miceli et al., 2013) and mutations in the C-terminus affect the affinity and/or function of modulators such as calmodulin or syntaxin-1A (Alaimo et al., 2009; Soldovieri et al., 2014). The ILAE's more recent definition, "developmental and epileptic encephalopathies," refers to a diverse group of conditions marked by early-onset, frequently severe epileptic seizures and abnormal EEG patterns on a background of developmental impairment that tends to worsen because of epilepsy (Specchio et al., 2022). Pharmacoresistant seizures that start in the first week of life and go away between nine

months and four years of age are the hallmark of KCNQ2-related DEE. Individuals exhibit developmental impairment ranging from mild to severe (Weckhuysen et al., 2022.)

All KCNQ2 variants causing DEE are missense de novo pathogenic variations that are mainly localized in some important channels region, including the PD, the S6 and the intracellular S6-helix A linker (Goto et al., 2019), the S4 in VSD, the proximal C-terminal segment that binds PIP2 and CaM, the B helix also involved in CaM-binding (Millichap et al., 2016). Functional studies revealed that pathogenic variants causing DEE exhibit more severe functional alterations than those associated to SeLFNE (Orhan et al., 2014). In addition to LoF mutations, patients with DEE also had de novo missense variants that caused gain-of-function effects (GoF) (Miceli et al., 2015b; Mulkey et al., 2017).

Although less common (Miceli et al., 2017), mutations in the KCNQ3 gene have been identified in patients with various neurological phenotypes. KCNQ3 variants have been associated with SeLFNE, exhibiting clinical features indistinguishable from K_V7.2-related self-limited syndromes. Most individuals present normal psychomotor development, although some cases report mild intellectual disability (ID) (Miceli et al., 2015b). The mutations show an autosomal dominant inheritance pattern and are predominantly missense variants, and result in a LoF effect in vitro. Unlike KCNQ2, homozygous KCNQ3 variants are compatible with life. For instance, two frameshift variants resulting in LoF were identified in homozygous patients with developmental delay and neonatal seizures (Kothur et al., 2018; Lauritano et al.,2019). Interestingly, in both described families, heterozygous parents carrying the KCNQ3 frameshift variants were unaffected. This greater tolerance for mutations in KCNQ3 compared to KCNQ2 may explain the lower prevalence of epilepsy-associated variants observed in KCNQ3.

In addition to LoF mutations, recent studies have reported de novo missense KCNQ3 mutations causing GoF effects in children with global developmental delay, ASD, and frequent sleep-activated multifocal epileptiform discharges. These mutations are in the VSD at the outermost arginines (R1 and R2) of the K_V7.3 S4 segment, producing GoF effects (Sands et al., 2019).

Mutations in the *KCNQ5* gene have been identified in individuals with intellectual disability (ID) and other neurological conditions. To date, only 12 pathogenic *KCNQ5* variants have been found, a significantly smaller number compared to the hundreds of disease-causing KCNQ2 variants and the several dozens reported in *KCNQ3*. Functional studies indicate

that *de novo* heterozygous missense mutations in *KCNQ5* can result in either loss-of-function (LoF) or gain-of-function (GoF).

Among the reported variants, G239S (LoF), G384R (LoF), and L395V (LoF) have been identified in individuals with ID, with or without seizures (Lehman & Guella, 2017). Additionally, a heterozygous intragenic duplication of *KCNQ5* was detected in a patient with mild ID and a history of absence epilepsy during adolescence, with no abnormalities were observed on electroencephalography (EEG) or magnetic resonance imaging (MRI) (Rosti et al., 2019). Moreover, the L197P (GoF) and Y267H (GoF) variants have been shown to cause significant GoF effects in two individuals diagnosed with developmental and epileptic encephalopathy (DEE) or ID, inthe absence of seizures (Nappi et al., 2022).

Furthermore, a large whole-exome sequencing (WES) study identified five pathogenic *KCNQ5* variants in ten individuals from five unrelated families with genetic generalized epilepsy (GGE): three heterozygous missense mutations P369L (LoF), A406V (LoF), R415H (LoF), one truncating mutation Q469fs (LoF), and one splice-site modification (*c.1375-2A>G* LoF). Notably, the first mentioned was inherited from a assymptomatic parent, the second was found in a patient whose parent presented ID, while the other two arose *de novo*. Functional characterization classified all five newly identified variants as strong LoF (Krüger et al., 2022).

Although *in vitro* functional studies in heterologous cells cannot fully replicate the complexity of *in vivo* phenotypes, identifying and quantifying the effects of loss of function (LoF) or gain of function (GoF) in K_v7 channels can help establish genotype-phenotype correlations. Severe phenotypes are typically associated with pronounced alterations in K_v7 channel function, such as strong GoF or LoF effects, that lead to a dominant-negative effect, whereas milder phenotypes result from more subtle functional changes (Nappi et al., 2020).

This relationship is particularly evident in KCNQ2-related disorders. The growing application of next-generation sequencing (NGS) techniques continues to expand the catalog of KCNQ2 mutations, further refining these correlations.

In contrast, the smaller number of KCNQ3 variants identified to date have a less definedgenotype-phenotype correlation. For KCNQ5, the situation is even more challenging, as the extremely limited number of identified variants prevents the establishment of this correlation.

1.1.1.7 PHARMACOLOGY OF K_V7 NEURONAL CHANNELS

Considering the significant role that I_{KM} plays in human physiology and pathology, it is not unexpected that neuronal K_V7 potassium channels are important pharmacological target for several neurologic disorders involving neuronal excitability (Barrese et al., 2010).

Activators or blockers of Kv7 currents could have distinct therapeutic applications: activators may be used for treatment of epileptic disorders and other pathological conditions where neuronal hyperexcitability plays a crucial role, like neuropathic pain (Liu et al., 2021), ischemic stroke (Bierbower et al., 2015), and amyotrophic lateral sclerosis (Wainger et al., 2021); whereas blockers were historically developed to treat learning and memory disorders (Figure 1.8).

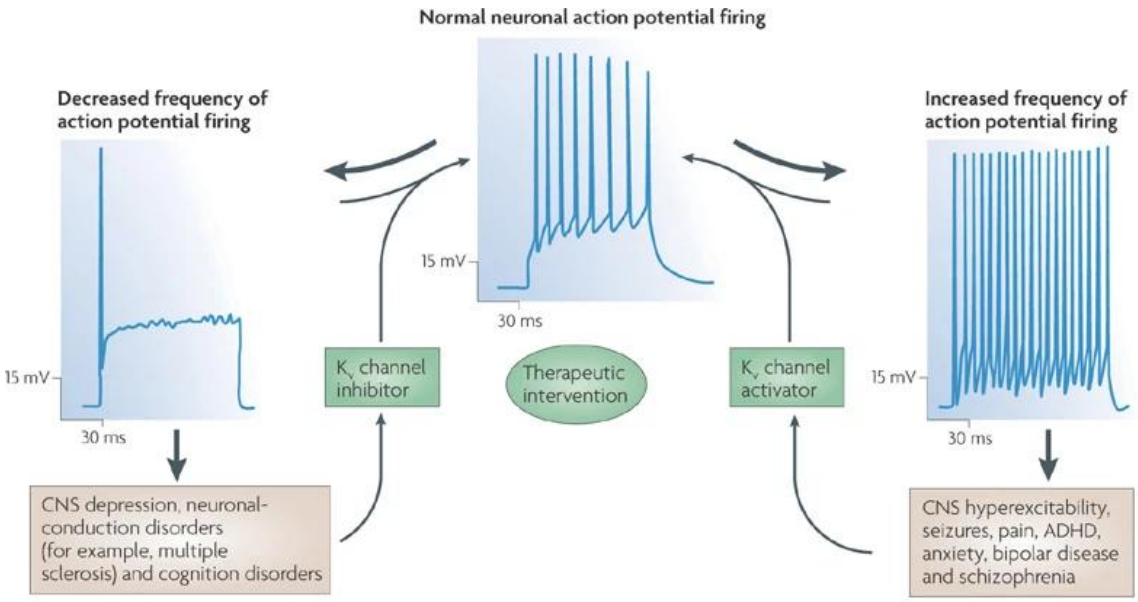

Figure 1.8 Effect of K_V7 channel activators and inhibitors on abnormally altered neuronal activity (from *(Wulff, 2009)*).

1.1.1.7.1 I_{KM} ACTIVATORS

Flupirtine and retigabine

Even though flupirtine was developed before K_V7 channels were discovered, it was the first substance to be identified as a K_V7 activator. In the 1980s, the German pharmaceutical company Chemiewerk Homburg first introduced this drug as a non-opioid nonsteroidal antinflammatory analgesic. In 1984, it was the first K_V7 channel agonist to receive clinical approval in Europe due to its distinct analgesic and muscle relaxant properties in contrast to opioids and other non-steroidal anti-inflammatory drugs. Further research has shown that flupirtine increased the activity of I_{KM}, acting on homomeric $K_V7.2$ channels at concentrations

like those attained during standard therapy with this drug (Martire et al., 2004). Originally, the analgesic action of flupirtine was attributed to its ability to act as an agonist of γ-amino-butyric acid ($GABA_A$) receptors or an antagonist of N-methyl-D-aspartate (NMDA) receptors (Szelenyi et al., 2013). Besides analgesic properties, flupirtine also showed neuroprotective effects (Boscia et al., 2006) and anticonvulsant action in both the kainic acid model of neonatal convulsions and pentylenetetrazol-induced seizures (PTZ) mouse models (Raol et al., 2009). Unfortunately, flupirtine causes severe liver toxicity, that limited its use to short-term pain management in 2013, and later in 2018 its marketing authorization was withdrawn by EMA. In order to separate the analgesic actions from the anticonvulsant activity, structure–activity relationship (SAR) studies have performed, allowing to discover that replacement of the basic nitrogen atom in the pyridine ring of flupirtine with carbon atom enhanced the antiepileptic activity, reducing at the same time analgesic activity. Based on this observation the compound retigabine was syntetized. (Figure 1.9). As a pan-K_v7.2–7.5 agonist, flupirtine shares the same pore channel region binding site as retigabine and other K_v7 openers (Kim et al., 2015; Bock et al., 2019).

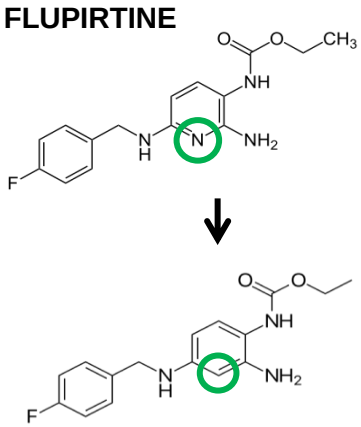

Figure 1.9 Chemical structures of flupirtine and retigabine, as indicated. Green circles indicate pharmacophore modification and retigabine development.

Retigabine, the first licensed anticonvulsant medication that acts on the K_v7 potassium channel, was commercialized by GSK in 2011 under the names Trobalt® in Europe and Potiga® in the US as an adjuvant treatment for patients with partial-onset seizures who were at least 18 years old. Retigabine is an activator of K_v7.2-7.5, but it has no effect on the cardiac K_v7.1 channel. The main effect of retigabine is a hyperpolarizing shift in channel activation, together with an acceleration in channel opening and a slowing down of its deactivation (Main et al., 2000). Its effect on the channel voltage-sensitivity depends on the K_v7 channel subtype: in fact, it is maximum on K_v7.3 (-43 mV), intermediate for K_v7.27.3 (-

30 mV), K_v7.2 (-24 mV), and K_v7.4 (Tatulian et al., 2001) (Table 1.2). In contrast, retigabine was not active on Kv7.1 channels.

	Maximal shift in $V_{1/2}$ (mV)	**Retigabine EC_{50} (μM)**
K_v7.2/7.3	-30.4	1.9 ± 0.2 (n=5)
K_v7.1	-0.7	100.1 ± 6.5 (n=5)
K_v7.2	-24.2	2.5 ± 0.6 (n=5)
K_v7.3	-42.8	0.6 ± 0.3 (n=5)
K_v7.4	-24.6	5.2 ± 0.9 (n=5)

Table 1.2 Quantification of the effects prompted by retigabine on currents expressed by Kv7 channels (from Tatulian, 2001).

Retigabine enhances the amplitude of current in K_v7.5 homomers but does not alter voltage sensitivity (Dupuis DS, 2002).

In conclusion, retigabine stabilizes the open conformation on K_v7.2/7.3 heteromers, increasing the single channel open probability without causing a noticeable change in channel conductance (Tatulian, 2003). Mutagenesis, electrophysiology and cryo-EM studies revealed that retigabine binds into the pore domain of neuronal K_v7, in an intracellular hydrophobic pocket situated between S5 and S6 segments (Main et al., 2000). Within this cavity, a residue of tryptophan (W236 in K_v7.2, W265 in K_v7.3), present at the end of the S5 helix, was found to be crucial for the retigabine effect. Along with this residue, other amino acids, such as L243 in S5, L275 in the pore, L299 and Gly301 in the S6 (based on the K_v7.2 sequence), are also implicated in the binding of retigabine; however, none of them appear to be as important as W236. The binding mode involving this tryptophan residue and retigabine was fully elucidated by Kim and coll. (2015), using unnatural amino acid. They demonstrated that an H-bond interaction occurs between the carbamate group of retigabine, that acts as a H-bond acceptor (HBA) and the amino group of the tryptophan, that acts as a H-bond donor (HBD). This binding mode was recently confirmed by the published cryo-EM structures of the human K_v7.2 and K_v7.4 in complex with retigabine (Li X et al., 2021; Li T et al., 2021). It is interesting to note that additional interaction sites were identified in both models: in both instances, an H-bond interaction took place between the side chain of serine and the aniline group of retigabine. The K_v7.2 S303A mutant exhibited reduced retigabine activity in electrophysiological tests (Li X et al., 2021), but the K_v7.4 S309H mutant exhibited no retigabine activity at all (Li T et al., 2021). Then, the fluorophenyl group of retigabine and

the aromatic ring of F246 (F240 on $K_v7.2$) were also shown to have a π-π stacking contact in $K_v7.4$ MD simulations; the retigabine effect was partially eliminated when F246 was mutated to alanine (Li T et al., 2021) (Figure 1.10).

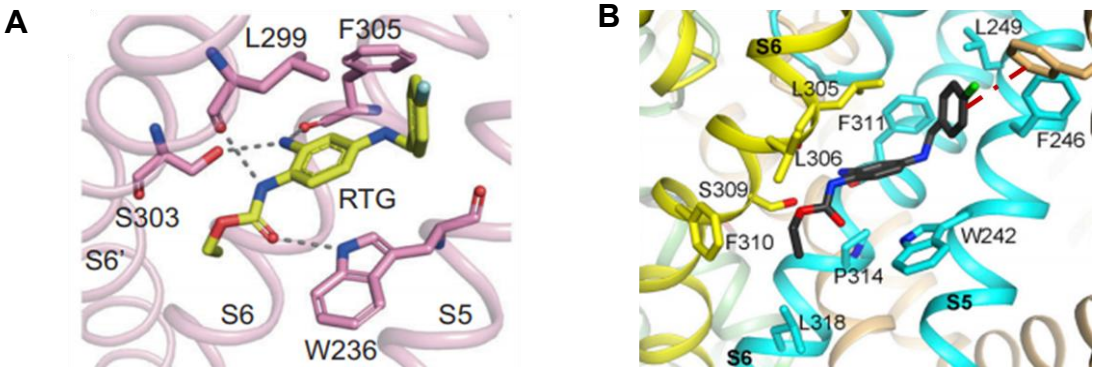

Figure 1.10. Retigabine binding site. 3D representations of the retigabine (RTG) binding site on Kv7.2 (A) or Kv7.4 (B) channels (Li et al., 2021).

Retigabine was an effective anticonvulsant drug, but unfortunately its clinical application was so limited that the company decided to stop producing it in 2017. The restrictions that resulted in a negative risk/benefit ratio for retigabine were:

I) *poor K_v7 subtype selectivity*. Indeed, retigabine-induced activation of $K_v7.4$ and $K_v7.5$ channels expressed in genitourinary smooth muscle caused urinary retention (Brickel et al., 2012; Malysz and Petkov, 2020). Recently, this hypothesis has been questioned by Tykocki and coll. (2019) which suggest that urological side effects of retigabine are due to activation of K_v7 channels in sensory nerves which decreases sensory outflow in the mouse urinary bladder;

II) *short half-life*. A three-times-daily dosage schedule is necessary due to the quick metabolism by phase-II enzymes (acetylation and N-glucuronidation) (Barrese et al., 2010);

III) *poor brain penetration,* due to the limited lipophilicity (log P = 3.08) (Zhou et al., 2015)*;*

IV) *Formation of photoinduced dimers*. The Food and Drug Administration (FDA) warned in 2013 that long-term use of retigabine may cause blue-gray staining of the retina and mucocutaneous tissue. This off-target effect was seen in patients who had received treatment for at least four years (Clark et al., 2015). The effects on vision were not entirely evident, and there was no information available for how long these changes would last (Brickel et al., 2020).

Retigabine Derivatives and other K_v7 Channel activators

SF0034 and RL-81: Potency and Selectivity Enhancements

In 2015, Kalappa and coll. (2015) synthesized SF0034, a fluorinated derivative of retigabine, by introducing a fluorine atom at the 3-position of the aniline ring. This modification enhanced its potency fivefold on $K_v7.2/7.3$ channels compared to retigabine while reducing its affinity for $K_v7.4/7.5$ channels, thus leading to a reduction of urinary retention as side effects. In addition, the presence of the electron-withdrawing fluorine improved chemical stability by reducing oxidation and dimer formation. Notably, when tested in animal models of epilepsy, SF0034 exhibited superior anticonvulsant efficacy compared to retigabine (Kalappa et al., 2015).

By introducing further modifications on the SF0034 structure, Kumar and coll. (2016) synthesized RL-81, which incorporates a CF3 group at the 4-position of the benzylamine moiety in addition to the fluorine on the aniline ring. RL-81 was found to be three times more potent than SF0034 in activating $K_v7.2/7.3$ channels while maintaining selectivity for these subtypes over Kv7.4/7.5. Similar to SF0034, RL-81 requires the W236 residue for its activity, with mutations at this site abolishing drug-induced channel activation. Starting from RL-81 as a lead compound (Liu et al.,2019) synthesized 19 new analogues, with RL-36 and RL-12 showing enhanced selectivity and potency on $K_v7.2/7.3$ channels over other K_v7 subtypes. Additionally, RL-56 exhibited significantly higher potency than RL-81, underscoring its potential for further development.

SF0034 **RL-81**

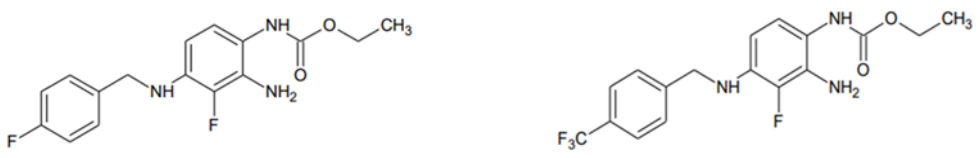

Figure 1.11 Molecular structures of SF0034 and RL-81 compounds

New K_V7.4/7.5-Selective Compounds

Another approach was to synthesize a tertiary butyl-substituted compound based on the P-retigabine structure. Compound 10g exhibited high selectivity for K_V7.4/7.5 channels, enhancing current amplitude without affecting voltage-dependent activation (Wang et al., 2018a).

Compound 10g

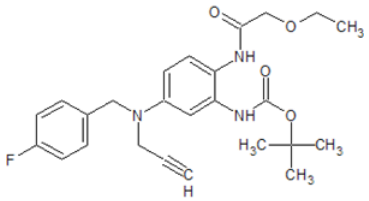

Figure 1.12 Molecular structure of Compound 10g

To develop more stable compounds, one strategy has been to replace the secondary amine linker with a sulfur atom. Using this approach, Bock and coll. (2019) synthesized a series of flupirtine/retigabine derivatives that demonstrated significantly reduced oxidative behavior while retaining or even enhancing pharmacological activity.

For instance, flupirtine analogue compound 48 exhibited increased potency on K_V7.2/7.3 channels, an improved toxicity-to-activity ratio, and the same efficacy as retigabine. Similarly, compound 36 matched the potency and efficacy of flupirtine, but presented reduced toxicity (Bock et al., 2019).

Another notable flupirtine/retigabine analogue is NS15370, a potent activator of K_V7.2–K_V7.5 channels. NS15370 has shown effectiveness in rodent models of partial epilepsy, including the 6 Hz seizure model and rat amygdala kindling, where it provided complete protection against epileptic discharges (Dalby-Brown et al., 2013).

Compound 48 **Compound 36** **NS15370**

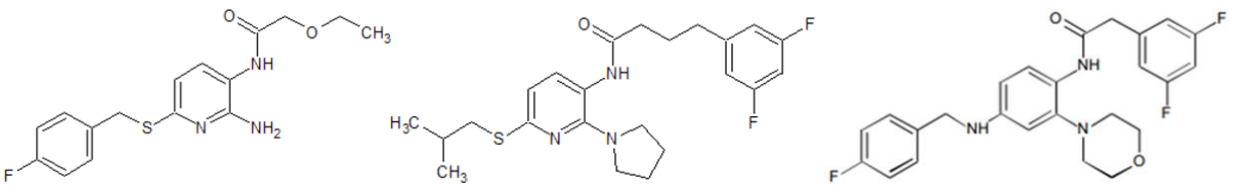

Figure 1.13 Molecular structures of Compound 48, 36 and NS15370

Dimethoxy-Pyrimidines and Hybrid Derivatives

To prevent dimer formation caused by the aniline group in retigabine, (Jennifer E. Davoren, 2015) synthesized PF-05020182, replacing the aniline structure with a 4,6-dimethoxypyrimidine. This compound demonstrated potent K_V7.2/7.3 activity, avoided cardiac K_V7.1 channel interactions, and showed anticonvulsant maximal electroshock seizure model (MES) in animals. Yang and coll. (2018a, 2018b) combined structural features of PF-05020182 and retigabine, yielding piperidine and N-phenylbutanamide derivatives. Compound 11 showed higher potency on K_V7.2 channels and better pharmacokinetics than retigabine, while compound 1 emerged as a more effective K_V7 opener, exhibiting anticonvulsant effects with no observed adverse effects.

PF-05020182 **Compound 11** **Compound 1**

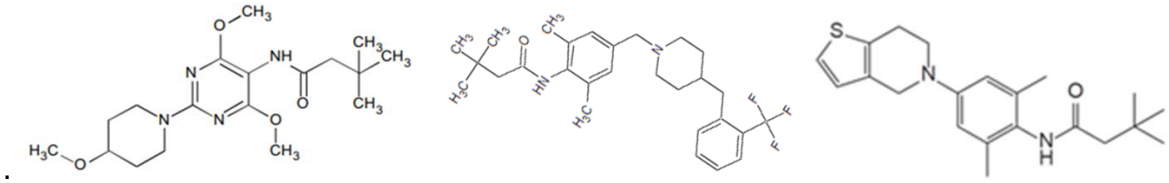

Figure 1.14 Molecular structures of Compound PF-05020182, 11 and 1

Surur and coll. (2019) used a retro-metabolic drug design strategy to reduce the formation of dimers, which are responsible for the mucocutaneous discoloration caused by long-term retigabine use. Starting with the dimer structure, they synthesized a series of 43 compounds in which the amino groups supposed to be involved in the dimerization reaction were modified. Two derivatives emerged: compound 22d was more effective than retigabine in activating K_V7.2/7.3 channels, but it revealed restricted water solubility; the compound 25b was less potent than compound 22d, but more soluble in aqueous solutions and showed a safe hepatoxicity profile in vitro. The same research group also tried a ligand-based design strategy, replacing amino substituents of the triaminoaryl core with alkyl substituents, generating led carba analogues of flupirtine and retigabine with improved oxidation resistance and negligible risk of quinoid metabolite formation, as observed the N-1/3 dicarba analogues 35a and 43b, displaying a good submicromolar K_V7.2/7.3 opening activity, no critical toxicity *in vitro and* improved oxidation stability (Wurm et al., 2022a). The author also attempted to separate retigabine and flupirtine activity from toxicity by using a pharmacological design technique that avoided harmful oxidation of the core aromatic ring.

The inversion of the amide group (forming a nicotinamide central scaffold) together with an additional methil group in ortho position respect to the amide group resulted in compound 36b, a flupirtine analogue that showed potent K_v7.2/7.3 opening activity, being six times as active as flupirtine itself, and is by design devoid of the potential for azaquinone diimine formation (Wurm et al., 2022b). The structure of compound 36b was further modified by adding a 2,2,2-trifluoroethoxy group and a morpholino substituent to improve the K_v7.2/7.3 opening capacity. In a fluorescence-based test, the resultant chemical 18c activated the K_v7.2/7.3 channel with 150 times the potency of flupirtine and 20 times the potency of retigabine. Compound 18c likewise had a poor water solubility while having a greater toxicity/activity ratio (Wurm et al.,2023).

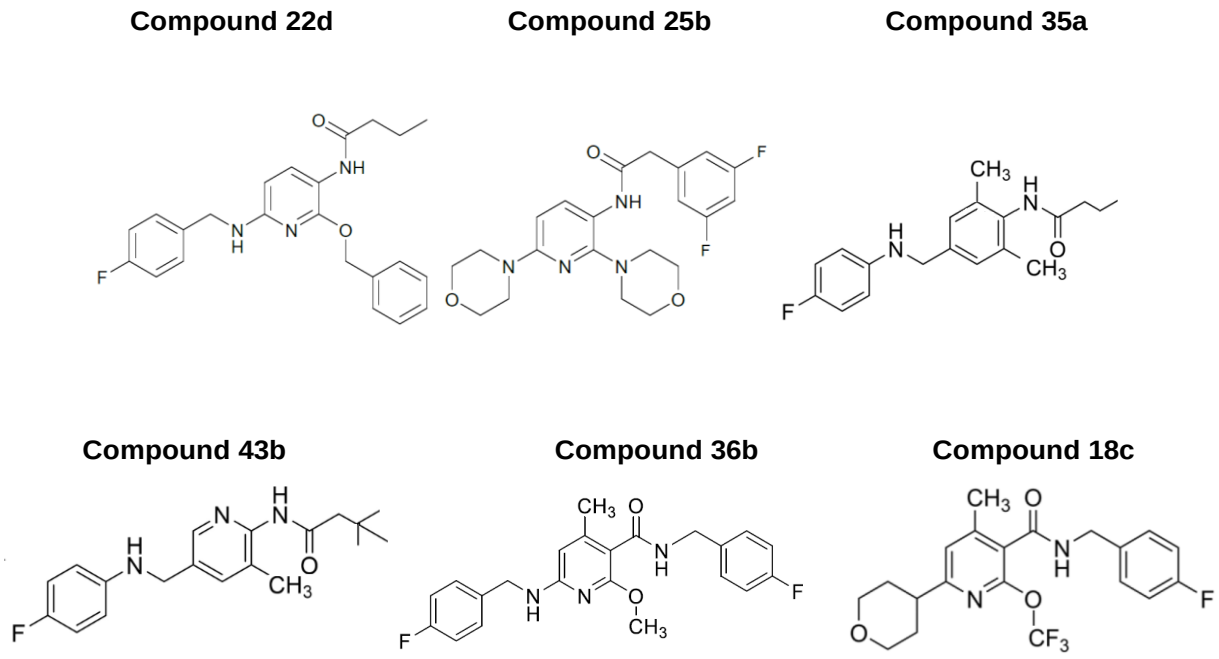

Figure 1.15 Molecular structures of 22d, 25b, 35a, 43b, 36b and 18c compounds.

Conformationally Restricted Analogues

Ostacolo and coll. (2020) synthesized conformationally restricted retigabine analogues, including compounds 23a and 24a, which demonstrated increased hydrophobicity, slower ON/OFF kinetics, and better brain permeability than retigabine. Compound 23a showed higher potency on $K_v7.2$ channels, while both 23a and 24a compounds exhibited better $K_v7.2/7.3$ activation than retigabine.

Compound 23a **Compound 24a**

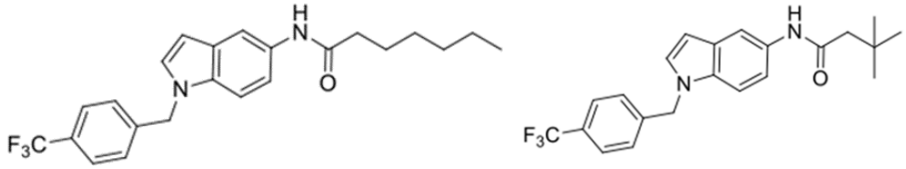

Figure 1.16 Molecular structures of 23a and 24a compounds.

Compound 60

To further address some of the limitations of retigabine, a small library of retigabine analogues was designed, synthesized, and evaluated by Musella and coll. (2022). Guided by molecular modeling and molecular dynamics studies, and based on the results obtained by RAS studies, a novel compound, referred to as compound 60, was identified. Compared to retigabine, compound 60 demonstrated higher potency and efficacy as a Kv7 channel activator in vitro, no photoinduced dimer formation, a higher brain-to-plasma ratio, and an extended plasma half-life in vivo.

Compound 60

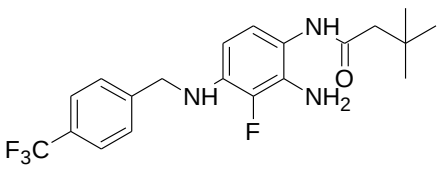

Figure 1.17 Molecular structure of Compound 60

Gabapentin and Cannabidiol

Gabapentin and cannabidiol (CBD) are both used clinically, though for different medical indications. Gabapentin is widely prescribed as an anticonvulsant and for the treatment of neuropathic pain. It is FDA-approved for epilepsy, specifically as an adjunct therapy for partial seizures (Beydoun et al., 1995), and for postherpetic neuralgia (PHN), a type of nerve pain following shingles (Rice et al., 2001). Additionally, it is frequently used off-label for conditions such as diabetic neuropathy, fibromyalgia, and anxiety disorders (Morello et al., 1999; Wiffen et al., 2017).

In contrast, CBD is primarily used for certain drug-resistant epilepsies. The FDA-approved formulation, Epidiolex, is indicated for Dravet syndrome and Lennox-Gastaut syndrome, both severe forms of childhood epilepsy, as well as for seizures associated with tuberous sclerosis complex (TSC) (Devinsky et al., 2017; Thiele et al., 2018). Recent clinical trials have further supported its efficacy in these conditions (Koo et al., 2020; Silvinato et al., 2022; Devinsky et al., 2018).

At the molecular level, both gabapentin and CBD modulate K_v7 channels, which play a key role in regulating neuronal excitability (Manville & Abbott, 2018; Soldovieri et al., 2020).

Gabapentin directly activates $K_v7.3$ and $K_v7.5$ potassium channels, reducing neuronal excitability and contributing to its anticonvulsant and analgesic properties (Manville & Abbott, 2018). Furthermore, Soldovieri and coll. (2020) provided clinical evidence of gabapentin's efficacy in treating a patient with DEE caused by a LoF variant in KCNQ2 (G310S). In vitro experiments demonstrated that gabapentin was able to restore the normal function of the mutated channels. Interestingly, this patient was treated with gabapentin and showed rapid and sustained clinical and electroencephalographic improvement, suggesting gabapentin as a potential precision therapy for DEEs linked to K_v7 dysfunction.

Gabapentin

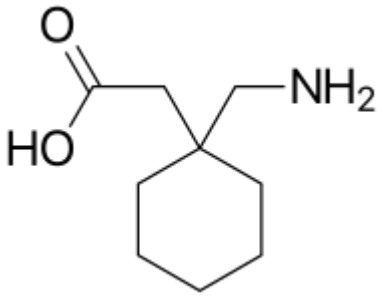

Figure 1.18 Molecular structure of Gabapentin

CBD, beyond its effects on various receptors and ion channels, also acts directly on K_v7.2/7.3 channels. Zhang and coll. (2022) demonstrated that CBD, at submicromolar concentrations (as low as 30 nM), shifts the voltage dependence of these channels in a hyperpolarizing direction, enhancing M-current in mouse superior cervical ganglion neurons and rat hippocampal neurons. This potent activation of K_v7.2/7.3 channels may contribute to its antiepileptic effects by reducing neuronal hyperexcitability.

In summary, gabapentin is widely used for epilepsy and neuropathic pain and is emerging as a potential treatment for genetic epileptic encephalopathies, while CBD is a promising therapy for specific drug-resistant epilepsies, partly due to its action on Kv7 channels and M-current modulation.

Cannabidiol

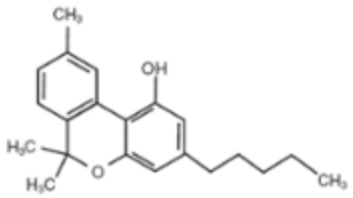

Figure 1.19 Molecular structure of Cannabidiol

XEN1101 and BHV-7000

Despite the promising results obtained in preclinical models, few K_v7 activators have reached the clinical phase of investigation. Among these:

-retigabine analogue HN37 progressed to clinical trials in China for epilepsy treatment;

-the compound XEN1101 is currently being studied in three different phase II/III clinical trials: 1. for the treatment of focal-onset seizures (ClinicalTrials.gov Identifier: NCT05614063), 2. as adjunctive therapy in primary generalized tonic-clonic seizures (ClinicalTrials.gov Identifier: NCT05667142), 3. for the treatment of major depressive disorder (ClinicalTrials.gov Identifier: NCT04827901).

-the compound BHV-7000 passed the phase I safety trials and a phase II/III trial for focal epilepsy and bipolar disorder was announced for 2023. Regarding the chemical structure of BHV-7000, detailed information has not been made public. However, it is known to be a small molecule belonging to the benzodiazepine class, designed to specifically modulate K_v7.2/7.3 channels (AdisInsight, 2024).

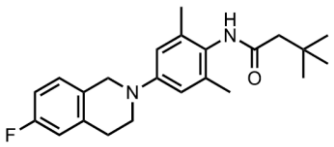

Figure 1.20 Molecular structure of XEN1101

P-Retigabine and Pynegabine (HN37): Improved Brain Penetration

To address retigabine's poor brain penetration, a propargyl group was introduced at the N4 position, creating P-retigabine. This derivative exhibited a 14-fold increase in the brain-to-plasma ratio (2.30 vs. 0.16 for retigabine) and demonstrated greater potency on $K_v7.2$ channels, as well as superior anticonvulsant activity with reduced toxicity in animal models (Zhou et al., 2015). Building on P-retigabine, Zhang and coll. (2021) developed HN37 (pynegabine) by removing the reactive ortho amino group and introducing two adjacent methyl groups to the carbamate motif. HN37 displayed improved K_v7 activation, reduced toxicity, and better stability, advancing to clinical trials in China for epilepsy treatment.

HN37 (pyne-retigabine)

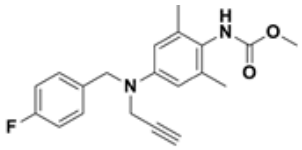

Figure 1.21 Molecular structure of HN37 (Pyne-retigabine)

Acrylamides

Acrylamide-based molecules have emerged as potent K_v7 channel activators. **BMS-204352**, developed by Bristol-Myers Squibb, was initially aimed at activating BK channels for stroke treatment, but it was also found to activate $K_v7.4$ channels with potency comparable to retigabine (Schroder et al., 2001).

The $K_v7.2$ activator (S)-1 demonstrated oral bioavailability and efficacy in a migraine model, while also blocking $K_v7.1$/KCNE1 and selectively

activating $K_v7.4$ and $K_v7.5$ currents (Bentzen et al., 2006). To overcome CYP3A4-mediated metabolism issues, the difluoro analogue **BMS-568274** (developed by the Bristol-Myers Squibb Pharmaceutical Research Institute) was synthesized with reduced pharmacokinetic interactions (Wu et al., 2003b). Advancements led to the synthesis of (S)-2, which shifted $K_v7.2$ activation and reduced hippocampal discharges. Modifications of (S)-2 produced (S)-3, (S)-4, and (S)-5, with (S)-4 and (S)-5 showing improved efficacy over (S)-2 and retigabine.

Only the (S)-enantiomers displayed activity, indicating strong stereoselectivity (Wu et al., 2004b)

Later, biaryl ether acrylamides (S)-6 and (S)-7 were developed, with (S)-6 showing efficacy in neuropathic pain treatment (Wu et al., 2013). The **BMS-1** analogue of (S)-2 displayed unique dual action by inhibiting $K_V7.2$ and activating $K_V7.4$ (Blom et al., 2014). Both **(S)-1** and **BMS-1** bind to the same pocket as retigabine, with $K_V7.4$ activation depending on a conserved tryptophan in the S5 segment (Bentzen et al., 2006).

Table 1.4. Acrylamides structures

Compound Name	Structure
BMS- 204352	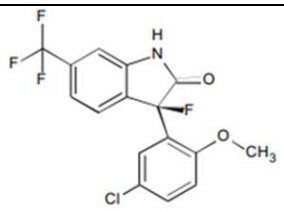
(S)-1	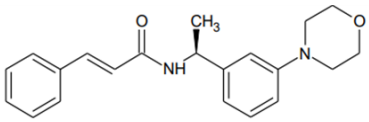
BMS-568274	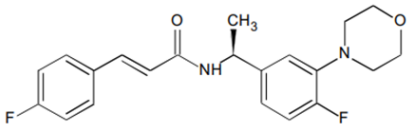
(S)-2	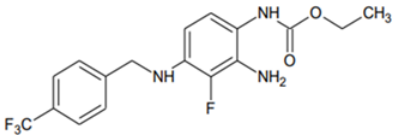
(S)-3	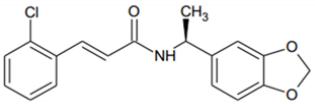
(S)-4	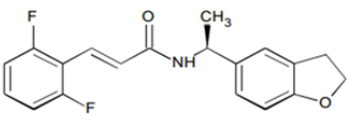
(S)-5	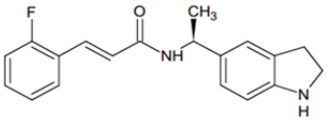

(S)-6	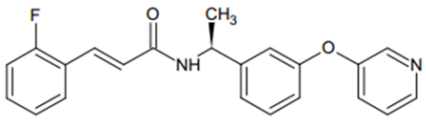
(S)-7	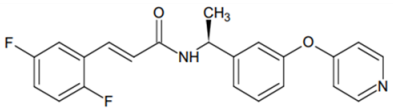
BMS-1	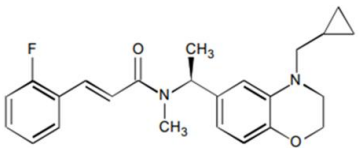

Benzamides as K_v7 Channel Activators

Benzamides are a class of potent K_v7 channel activators with distinct binding sites and mechanisms compared to retigabine and acrylamides. Among these:

- ICA-27243: the first benzamide identified as a K_v7 activator, it shifts the $K_v7.2/7.3$ activation curve leftward but has limited action on $K_v7.4$ and $K_v7.3/7.5$. It suppresses seizure-like activity in ex vivo hippocampal slices and exhibits anticonvulsant effects in several animal seizure models. However, toxicity studies revealed that prolonged administration causes non-hemolytic anemia (Wickenden et al., 2008);
- ICA-069673: a derivative of ICA-27243 with better pharmacokinetics and oral bioavailability. It selectively activates $K_v7.2/7.3$ over $K_v7.3/7.5$ and exhibits anticonvulsant effects in animal epilepsy models (Amato G, 2011);
- ICA-110381: this compound predominantly activates $K_v7.2$, causing a hyperpolarizing shift in activation and slowing deactivation. It shows anticonvulsant activity in the amygdala kindling model, reducing seizure severity and duration (Boehlen et al., 2013);
- ztz240: identified from a high-throughput screening of the ChemBridge Diverset™ library, ztz240 resembles ICA-27243 structurally. It increases $K_v7.2$ current amplitude and slows deactivation, but it also potentiates $K_v7.4$ and $K_v7.5$ currents more than $K_v7.2$. $K_v7.1$ and $K_v7.3$ remain insensitive to ztz240 (Gao et al., 2010).

Benzamides bind to the voltage-sensing domain (VSD) of K_v7 channels, unlike retigabine, which binds to the pore domain (PD) (Padilla K, 2009).The $K_v7.2$ W236L mutant remains

sensitive to ICA-27243, ICA-069673, and ztz240, confirming VSD binding (Padilla, 2009; Gao, 2010; Boehlen, 2013).

While retigabine requires a single subunit for maximal effect, benzamides like ICA-069673 need all four subunits to be sensitive, as even one insensitive subunit significantly reduces efficacy (Wang, 2018b).

Mutagenesis studies revealed essential residues in the VSD for benzamide binding:

- ztz240: critical residues include F137, I171, D172, R207, and R210. Mutating F137A, D172A, or R210Q reduced outward current amplitude and impaired the voltage shift induced by ztz240. Notably, these residues are less conserved in $K_V7.1$ and $K_V7.3$, explaining the reduced sensitivity of these subtypes to ztz240 (Li X et al., 2020);
- ICA-069673: residues F168 and A181 in the S3 segment are essential for its activity, as shown by Wang and coll. (2017).

Cryo-EM structures of $K_V7.2$ in complex with ztz240 confirmed that the binding site is between the S3 and S4 segments of the VSD, involving F137, I171, D172, R207, and R210, further supporting the mutagenesis data (Li X et al., 2020).

Benzamides, including ICA-27243, ICA-069673, ICA-110381, and ztz240, represent a unique class of K_V7 activators that bind to the VSD and require all four channel subunits for maximal efficacy. Their anticonvulsant effects and unique binding mechanism make them valuable therapeutic candidates, though toxicity and selectivity remain challenges for drug development.

Table 1.4. Benzamides structure

Compound Name	Structure
ICA-27243	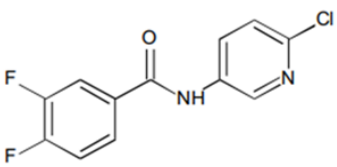
ICA-069673	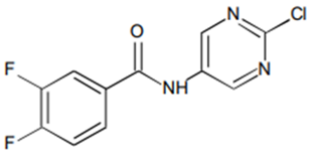

ICA-110381	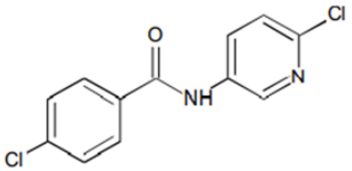
ztz240	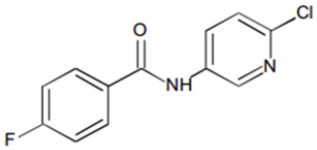

Fernamates

Fenamates, including well-known nonsteroidal anti-inflammatory drugs (NSAIDs) like meclofenamic acid and diclofenac, are non-selective inhibitors of COX-1 and COX-2 cyclooxygenases. They also activate K_v7 potassium channels, particularly $K_v7.2/7.3$ channels, by shifting their voltage-dependent gating to the left and slowing the deactivation kinetics, without affecting cardiac $K_v7.1$ channels (Peretz et al., 2005). Diclofenac also demonstrates anticonvulsant activity in the MES model.

To isolate the K_v7 activation from COX inhibition, derivatives of diclofenac have been developed. One such derivative, NH6, introduces a dietylene glycol tail to the molecule's carboxylic acid group. NH6 causes a hyperpolarizing shift in the voltage activation curve of $K_v7.2/7.3$ channels and slows deactivation kinetics, but it does not affect $K_v7.1$ currents. NH6 significantly reduces evoked and spontaneous action potentials in neurons, and in hippocampal slices, it decreases spike afterdepolarization in CA1 pyramidal neurons. It also reduces both excitatory and inhibitory postsynaptic currents without altering their amplitude or waveform (Peretz et al., 2007).

Another derivative, NH29, enhances $K_v7.2$ currents, shifts the gating of the channel to a hyperpolarized state, and speeds up both activation and deactivation kinetics of $K_v7.2$. Like NH6, it does not activate $K_v7.1$ channels. In DRG and hippocampal neurons, NH29 reduces evoked spikes and synaptic transmission. Importantly, NH29 is effective in $K_v7.2$ W236L channels, which are resistant to retigabine, suggesting it does not interact with the retigabine binding site on $K_v7.2$. Docking studies show that NH29 binds to a specific pocket in the voltage-sensing domain (VSD) of $K_v7.2$, with the nitro group of one aromatic ring forming a hydrogen bond with R207 and E130 (Peretz et al., 2007).

Table 1.5. Fenamates structure

Compound Name	Structure
Diclofenac	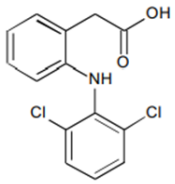
Meclofenamic acid	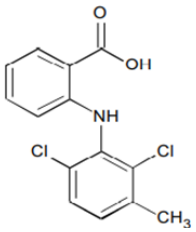
NH6	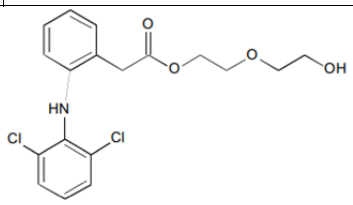
NH29	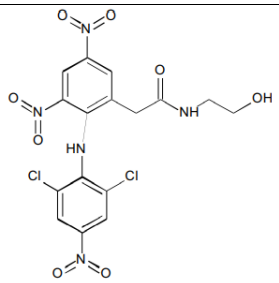

Other chemotypes of neuronal Kv7 activators

In 2011, Yu and coll. identified the compound ML-213 from the NIH Molecular Libraries Small Molecule Repository (MLSMR), a collection of 300,000 molecules. Initially, ML-213 was reported to selectively activate Kv7.2 and Kv7.4 channels (Yu, 2011), but further studies later revealed it to be a pan activator of Kv7.2-7.5 channels (Kanyo, 2020). In A7r5 vascular smooth muscle cells, ML-213 was found to strongly activate both homomeric K_v7.5 and heteromeric K_v7.4/7.5 channels. The compound increased their maximum conductance, shifted the activation curves negatively, and reduced the deactivation rates. Mutating the tryptophan residues at positions 235 and 242 in K_v7.5 and K_v7.4, respectively (W235L/W242L), abolished the effects of ML-213, indicating that it interacts with the same binding site as retigabine (Brueggemann, 2014).

Zinc pyrithione (ZnPy), a compound commonly used to treat psoriasis and control dandruff, has been shown to be a potent activator of most K_v7 channels, excluding K_v7.3 and K_v7.1/KCNE1 subunits. ZnPy enhances the open probability, shifts the activation curve to the left, and decreases deactivation rates. Unlike retigabine, ZnPy is effective in K_v7.2 W236L channels, suggesting that this residue is not critical for activity. Mutagenesis studies on Kv7.2 further revealed that residues L249 in S5, L275 between S5 and the pore region, and A306 in S6 play important roles in its action (Xiong et al., 2008; Gao et al., 2017).

A high-throughput screening (HTS) of 80,000 compounds led to the discovery of two novel K_v7.2 activators: ZG1732, an amide, and ZG2083, a benzothiophene. Both compounds significantly increased outward K_v7.2 currents and shifted the activation curve to the left at micromolar concentrations (Yue et al., 2016).

NS1643, originally identified as a K_v11 channel opener, is also an activator of K_v7 channels. It potentiates homomeric K_v7.2 and K_v7.4 channels, as well as heteromeric K_v7.2/7.3 channels, without affecting cardiac K_v7.1. NS1643 shifts the K_v7.2 activation curve leftward and slows deactivation (Li et al., 2014).

Benzbromarone (BBR), an inhibitor of urate transporters, has recently been shown to activate K_v7 channels. It exhibits promising antinociceptive effects, reducing inflammatory pain in rat and mouse models induced by bradykinin, formalin, or monosodium urate (Zheng et al., 2015).

At the 2019 American Epilepsy Society meeting, Knopp Biosciences presented KB-3061, a potent Kv7.2/7.3 channel activator being studied for the treatment of KCNQ2 neonatal epileptic encephalopathy (Picchione et al., 2019).

ZK-21, a 4-aminotetrahydroquinoline, was identified as a potent $K_v7.2$ activator through screening an in-house compound library. ZK-21 lost its activity in the $K_v7.2W236L$ mutant, suggesting it likely binds the same pore region (S5) as retigabine and the RL-series compounds (Hernandez et al., 2022).

GRT-X, a compound synthesized in the search for novel analgesics targeting Kv7 channels, was found to be an allosteric modulator of Kv7 channels. It also activates the mitochondrial translocator protein 18 kDa (TSPO) receptor, stimulating the synthesis of neurosteroids like allopregnanolone in the rat brain. This makes GRT-X the first drug to combine Kv7 and TSPO receptor agonism. In rodent epilepsy models, GRT-X demonstrated superior antiseizure efficacy compared to retigabine, especially in the 6-Hz seizure model (Bloms-Funke et al., 2022b).

Table 1.6. Structure of other chemotypes of neuronal K_v7 activators

Compound Name	Structure
ML213	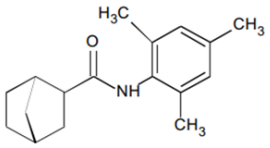
ZnPy	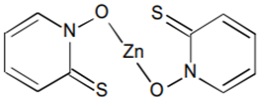
ZG1732	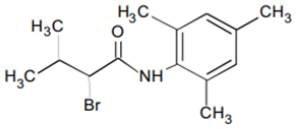
ZG2083	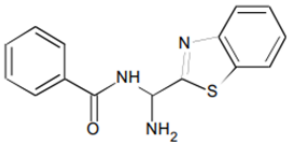
NS1643	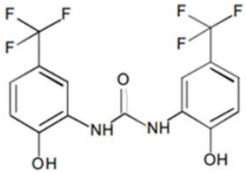
Benzbromarone	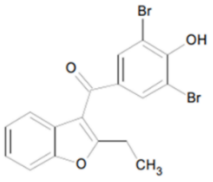

KB-3061	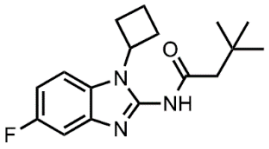
GRT-X	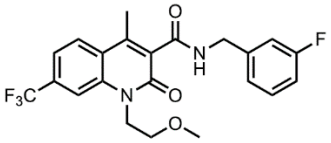
ZK-21	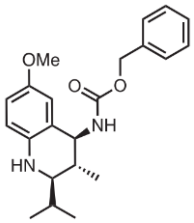

1.1.1.8.2 I_{KM} BLOCKERS

K_v7 blockers increase the cellular membrane potential to higher positive values by promoting a decrease in the outward K^+ currents. Linopirdine, a phenyl indolinone derivative developed in the 1980s (see Table 1.3 for all compounds structures), was the first specific K_v7 blocker. A cryo-EM structure showed that linopirdine's binding site is in a cytosolic pocket beneath the inner gate in $K_v7.4$. It is a non-selective K_v7 blocker, also active on cardiac $K_v7.1$ channels, although with lower potency when the channel co-assembles with KCNE1 accessory subunits (Aiken et al., 1995; Li T et al., 2021). In addition to raising dopamine, glutamate, aspartate, GABA, and serotonin levels, linopiridine was able to release acetylcholine in slices of the rat hippocampal, cortex, and caudate nuclei (Zaczek et al.,1993). Linopiridine has been suggested as a treatment for neurodegenerative diseases such as Alzheimer's disease due to its capacity to improve learning and memory function in several animal models (Brioni et al.,1993). However, clinical trials failed to demonstrate linopiridine's efficacy in treating Alzheimer's patients (Rockwood et al., 1997).

Linopiridine's short half-life and poor brain penetration may be the cause of its inability to improve human cognitive function. Numerous linopirdine analogues were designed to overcome these limitations. Among these, the XE-991 demonstrated a longer half-life, better brain-plasma ratio, and an increased potency in inhibiting K_v7 currents. Similar to linopirdine,

XE991 cannot distinguish between different K_v7 subunits (Wang et al., 2000). Their slow binding kinetics to the active conformation of K_v7 channels, which primarily block hyperexcited neurons, may account for the absence of seizures in an animal model following XE991 and linopirdine administration as well as their neuroprotective qualities (Greene et al., 2017). In contrast to non-selective K_v7 blockers, UCL2077 subtype-selectively blocks Kv7 channels, primarily $K_v7.1$ and $K_v7.2$ channels. It also inhibits $K_v7.3$ currents at greater depolarized values and increases them at negative membrane potentials. In addition, UCL2077 suppressed slow afterhyperpolarization (sAHP) at low micromolar concentrations without influencing medium afterhyperpolarization (Soh et al., 2022). This characteristic most likely results from a combination of UCL-2077's inhibitory effects on a wide range of channels, including a weak effect on large-conductance $Ca2^+$-activated K^+ (BK_{Ca}) channels, inhibition of intermediate-conductance $Ca2^+$-activated K^+ (IK_{Ca}) channels, suppression of hERG current, and selective inhibition of $K_v7.1$ and $K_v7.2$ (Hsu et al., 2020). ML252 is another strong K_v7 inhibitor that was just reported. Despite previous K_v7 channel blockers (XE991, linopiridine), this chemical is extremely powerful and exhibits an inhibitory effect at relatively low (nM) concentrations. Furthermore, it appears to be more selective than other inhibitors in blocking specifically $K_v7.2$ isoforms: in fact, the inhibitory action on $K_v7.2$ currents is about 40 times greater than that shown on $K_v7.1$ cardiac isoform. For $K_v7.2/7.3$ heteromeric channels or $K_v7.4$ channels, the ML252 exhibits decreased selectivity (Cheung et al., 2012). Additionally, SAR studies revealed that small structural changes of ML-252 (substitution of the ethyl group with a hydrogen; see compound structures in Table 1.7) are sufficient to cause a functional switch of its activity from an antagonist to an agonist. In a study of Richard and coll. (2023), ML-252 was characterized as a pore-targeted K_v7 channel inhibitor. It binds to a tryptophan residue in the pore domain of the $K_v7.2$ channel, causing a competitive inhibition with pore-targeted activators, such as ML213. This indicates that ML252 prevents the activation of the K_v7 channels by other molecules that typically induce channel opening. However, ML252 does not interfere with activators acting at the voltage sensor, such as ICA-069673, suggesting that while ML252 inhibits activators that directly target the pore, it does not block those that influence the channel's function through other domains (Kany at al., 2023).

A retigabine derivative acting as a Kv7 blocker, called HN38, was discovered.This compound is seven times more potent than XE991 in inhibiting $K_v7.2$ channels (Hu et al., 2013). Although its subtype selectivity for additional K_v7 family members is unknown, another blocker, the fenamate NH17, has been identified as a $K_v7.2$ channel inhibitor (Peretz

et al., 2007). A K_v7 blocker has recently been identified in fangchinoline, a naturally occurring alkaloid isolate from Stephania tetrandra that exhibits anti-inflammatory, anti-cancer, and antihypertensive properties. In heterologous expression, it blocked K_v7 currents without showing any preference for one family member over another. Additionally, fangchinoline blocked native M-channel currents of DRG neurons and slowed the activation of $K_v7.1$-7.5 channels (Li et al., 2022).

Table 1.7. K_v7 channel inhibitors.

Compound Name	Structure
Linopirdine	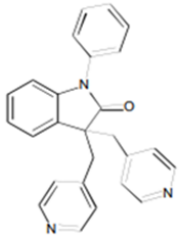
XE991	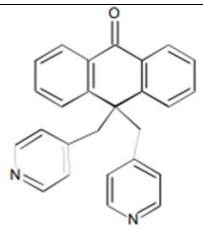
UCL-2077	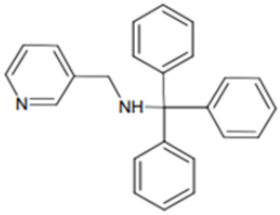
ML252	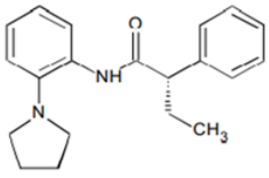
HN38	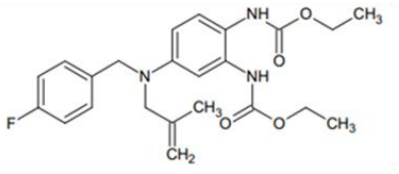

NH17	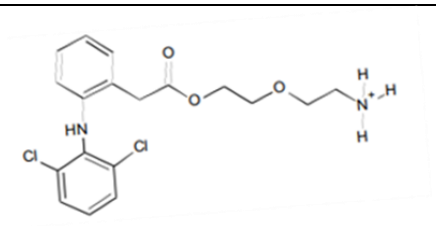
Fangchinoline	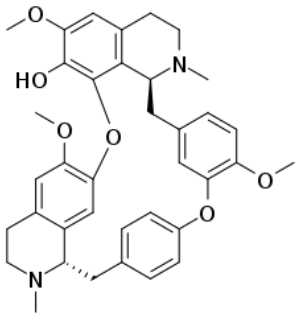

2 AIM OF WORK

Neuronal K_v7 potassium channels are promising pharmacological target for the treatment of various neurological disorders. In particular, neuronal K_v7 activators are believed to relieve disease states in which neuronal hyperexcitability is a relevant pathogenetic mechanism. In fact, potential therapeutic applications of neuronal K_v7 activators range from anti-nociceptive and anticonvulsant to the treatment of migraine, anxiety, mania, ADHD, addiction to psychostimulants and depression. By contrast compounds acting as neuronal K_v7 blockers, by increasing neuronal excitability and boosting the release of several neurotransmitters may ameliorate the cognitive decline occurring in neurodegenerative diseases in which deficits in specific neurotransmitters is considered a major pathogenetic event. Among K_v7 activators, retigabine was the first antiepileptic drug approved to target K_v7 channels; however, it exhibited several drawbacks, such as limited selectivity for K_v7 subtypes, a short half-life, poor brain penetration, and chemical instability. As a result, retigabine was withdrawn from the market in 2017. Currently, no selective K_v7 activators are available as a clinically approved anticonvulsant, underscoring the urgent need to identify novel modulators of K_v7 channels.

According to these premises, the aim of this work was to identify novel and safe K_v7 channel modulators. To this aim we exploited two different approaches:

1. a drug repurposing approach was undertaken to identify new K_v7 activators from drugs that have already undergone preclinical and clinical evaluations. This strategy aims to accelerate the development process and reduce costs, potentially bringing a clinically useful molecule to market more quickly. This work was carried out in collaboration with the Fraunhofer Institute for Translational Medicine and Pharmacology ITMP. To this aim, Dr Lidia Carotenuto, a PhD student from our research group, conducted a cell-based high-throughput screening (HTS) using the Fraunhofer repurposing library, about 5632 compounds from the Fraunhofer repurposing Library and the EU-Openscreen Pilot Bioactive Library on mammalian cells stably expressing the $K_v7.3$ A315T mutant channel by means of a fluorescence-based assay, the FluxOR Green Potassium Ion Channel assay. The most active compound identified from this screening was then functionally characterized by means of electrophysiological techniques, such as patch-clamp in whole-cell

configuration in Chinese hamster ovary (CHO) cell and hiPSC-derived neurons and multielectrode array recordings;

2. a structure-based drug design strategy was employed to develop, synthesize, and evaluate new retigabine analogues. Among these we have identified a novel K_V7 blocker that was functionally characterized by means of electrophysiological techniques. This project was a collaboration between our group and one at Department of Pharmacy at the University of Salerno led by Prof. Carmine Ostacolo for silico analyses and for synthesizing the analogues.

3 MATERIALS AND METHODS

3.1 BACTERIAL TRANSFORMATION AND PLASMIDIC DNA PREPARATION

The plasmids containing the cDNA coding for distinct K_v7 channels were transformed using the competent E. coli DH5α. After heat shock transformation 50-100 µl bacteria resuspended in 200 µl SOC medium (2% tryptone, 0.5% yeast extract, 10 mM NaCl, 2.5 mM KCl, 10 mM MgCl2, 10 mM MgSO4, 20 mM glucose) and incubated at 37°C for 45'. Then, the product was then plated on LB-Agar plates with 50 µm/ml of ampicillin (10 g/L tryptone, 5 g/L yeast extract, 5 g/L di NaCl, and 15 g/L of agar) and incubated overnight at 37°C upside down. After being plated with 5 ml of LB medium and 50 µg/ml of ampicillin, single colonies were cultured for an entire night at 37°C and 220 rpm. Starting from these, DNA plasmid was extracted using a commercially available kit (QIAprep Spin Miniprep, QIAGEN). Enzymatic digestion and DNA sequencing were used to identify positive vectors (Eurofins Genomics, Italy). One of the positive clones was amplified extensively to extract plasmidic DNA using a commercial kit (Plasmid Plus Maxi, QIAGEN) to get DNA in large quantities. In order to exclude any further alterations throughout the entire coding region and to confirm the existence of the desired mutation, the cDNA was sequenced once more.

3.2 CELL CULTURE

3.2.1 CHINESE HAMSTER OVARY CELLS(CHO)

In plastic Petri dishes measuring 100 mm, 60 mm, or 40 mm, depending on the specific requirements of the experiment, Chinese Hamster Ovary (CHO) cells were cultured in Dulbecco's Minimum Eagle Medium (DMEM) supplemented with 10% Fetal Bovine Serum, 1% L-glutamine (2 mM in 0.85% NaCl), 1% penicillin (50 U/mL), and 1% streptomycin (50 µg/mL). The cells were kept in a humid environment with 5% CO2 at 37°C. When the cells in the dishes were confluent, they were separated using 1% trypsin solution and gathered in fresh dishes diluted 1:3.

3.2.2 iPSC DERIVED-CORTICAL EXCITATORY NEURONS

iPSCs were differentiated into cortical glutamatergic neurons using a modified version of a protocol based on *Ngn2* overexpression (Zhang Y). Stem cells were dissociated as single cells using Accutase. Then, the cells were plated using accutase for 6-well plates (before applying Geltrex coated plates) with Stem Flex Medium (SF), plus doxycycline (2 µg/ml) and plus 500x Rock inhibitor. After two days, the SF was totally removed and replaced with fresh SF containing doxycycline. Next day, the cells could be freezed in knock-out serum (KOS) plus 10% of dimethylsulfoxide (DMSO) or used to start being differentiated themself. Coverslips were placed in 24 well plastic Petri dishes measuring 15.6 mm. Then, they were coated with 0.07% Polyethylenimine (PEI) for 1h at 37°C. Afterwards, PEI was removed, and every coverslip was washed 4 times with sterile water. Then, laminin was added (final concentration: 20 µg/ml to dissolve in sterile H_2O_2) and the plate incubated for 1h at 37°C. Subsequently, astrocyte cells were seeded (40.000 cells/well in a final volume of 500 µl) and cultured in Dulbecco's Minimum Eagle Medium (DMEM) supplemented with 10% Fetal Bovine Serum, 1% L-glutamax (100 mL), 1% penicillin (50 U/mL), and 1% streptomycin (50 µg/mL). The cells were kept in a humid environment with 5% CO2 at 37°C. When a confluent astrocyte layer is formed (after 2-3 days), the culture is ready for the neuron progenitor cell (NPC) seeding (40.000 cells/well in a final volume of 500 µl). The cells were cultured in Neurobasal (NB) Complete with factors (Doxycyclin 2 µg/ml, Human BDNF 10 ng/ml, Human NT3 10 ng/ml, 50x B-27 plus supplement), plus 10 µM of Rock inhibitor (5mM) and 2µM of ARA-C (2mM) for 2 days in a humid environment with 5% CO2 at 37°C. After, the cells were cultured in neurobasal medium only with factors and half medium was changed two times a week.

3.3 ELECTROPHYSIOLOGY

3.3.1 MANUAL PATCH-CLAMP

Whole-cell electrophysiology in transfected CHO cells.

Currents from CHO cells were recorded at room temperature (20–22°C) using the whole-cell configuration of the patch-clamp technique, with glass micropipettes of 3-5 MΩ resistance. During the recording, constant perfusion of extracellular solution was maintained. The extracellular solution contained (in mM): 138 NaCl, 2 $CaCl_2$, 5.4 KCl, 1 $MgCl_2$, 10 glucose, and 10 HEPES, at pH 7.4, with NaOH. The pipette (intracellular) solution contained (in mM): 140 KCl, 2 $MgCl_2$, 10 EGTA, 10 HEPES, 5 Mg^{2+}-ATP, at pH 7.3-7.4, with KOH (Miceli F., 2013). Current was recorded using an Axopatch-200A amplifier, filtered at

5 kHz, and digitized using a DigiData 1440A (Molecular Devices). The pCLAMP software (version 10.2) was used for data acquisition and analysis (Molecular Devices). To evaluate the activity of C4 compound on K_v7.3 A315T, K_v7.2+K_v7.3, K_v7.2 or K_v7.2 W236L currents, the cells were clamped at -80 mV and conductance-voltage curves (G/V curves; activation curves) were generated by normalizing to the maximal value of the instantaneous isopotential currents at 0 mV and expressing the normalized values as a function of the preceding voltages. Data were fit to a Boltzmann distribution of the following form: $y=max/[1+\exp(V_{1/2}-V)/k]$, where V is the test potential, $V_{1/2}$ the half-activation potential, and k the slope factor. The $\Delta V_{1/2}$ values, calculated as the difference between the $V_{1/2}$ for controls and after drug exposure, were plotted versus log[concentration] of the compound, fitted to the four-parameter logistic equation $y=min+(max-min)/(1+(x+EC_{50})^{-HillSlope})$ with SigmaPlot (version 12.3) to estimate EC_{50} values. Indicated EC_{50} values are the mean of at least three independent experiments ± standard error of the mean (SEM).

Whole-cell electrophysiology in iPSCs-derived neurons.

Currents from iPSCs-derived cortical excitatory neurons were recorded at room temperature (20–22°C) using the whole-cell configuration of the patch-clamp technique, with glass micropipettes of 5-7 MΩ resistance. During the recording, an oxygenated aCSF bath solution (in mM) was continuously perfused into neurons: 124 NaCl, 2.4 $CaCl_2$*$2H_2O$, 2.5 KCl, 1.25 NaH_2PO_4, 26 $NaHCO_3$, 2 $MgCl_2$*$7H_2O$, 15 glucoses, at pH 7.3-7.4, with NaOH and osmolality 305–310 mOsm/Kg. The pipette (intracellular) solution contained (in mM): 25 KCl, 125 K-gluconate, 4 Mg^{2+}ATP, 10 Na2 Phosphocreatine, 0.4 NaGTP, 10 HEPES, at pH 7.3-7.4, with KOH and osmolality 280–290 mOsm/Kg (Simkin, 2021). Current was recorded using an Axopatch-200A amplifier, filtered at 5 kHz, and digitized using a DigiData 1440A (Molecular Devices). The pCLAMP software (version 10.2) was used for data acquisition and analysis (Molecular Devices). Resting membrane potential (Em) and the number of spontaneous action potentials per second (APs/sec) measured through current-clamp mode. In addition, the neuronal basal activity was recorded for thirty seconds, after that 10 µM of retigabine (RET), C4 or D_2R antagonist was perfused during neuronal firing for sixty seconds.

Following RET and C4 treatments, an oxygenated co-perfusion with 10µM XE-991 (RET+XE991 or C4+XE991) was performed between thirty – sixty seconds. In this way the basal neuronal firing rate was rescued. The Clampfit software (version 11.3) was used for detected Em and number of APs, that were normalized by the occurrence of time (s).

Indicated values are the mean of at least three independent experiments ± standard error of the mean (SEM).

3.3.2 MULTI-ELECTRODES ARRAY (MEA) PLATFORM

Human iPSC-derived neurons' extracellular signals were captured using CMOS-based HD-MEAs (Ballini M, 2014) (Müller J, 2015). The entire sensing area of the HD-MEA is 3.85 x 2.10 mm^2, with 26 400 electrodes arranged in a 120 × 220 grid. With an electrode area of 9.3 × 5.45 μm^2 and a pitch of 17.5 µm from center to center, cell electrical activity can be recorded at subcellular resolution. A simultaneous recording from a user-selected set of 1024 electrodes is possible. With a customizable gain of up to 78 dB, the HD-MEA offers noise values of 2.4 µVrms in the action potential region of 0.3 – 10 kHz. There is a 20 kHz sampling frequency. MaxOne HD-MEA, manufactured by MaxWell Biosystems AG (www.mxwbio.com), and its laboratory version, which changes mainly in the printed circuit board (PCB) design, were used (Ronchi S, 2021).

3.4 STATISTICAL ANALYSIS

Significant differences in electrophysiological data were analyzed using the student t-test or ANOVA followed by the Student-Newman-Keuls test when comparing several groups, with a threshold of $p < 0.05$. Data were analyzed with SigmaPlot 12.3 for Windows (Systat Software Inc, San Jose, CA). Values are expressed as the mean ± standard error of the mean (SEM) of at least three cells recorded in at least two separate transfections.

4. RESULTS

4.1 Identification of novel K_v7 activators in the Fraunhofer repurposing library via high-throughput screening (HTS)

To discover new Kv7 channel activators among molecules at various stages of research and development, a high-throughput screening (HTS) was conducted using the Fraunhofer repurposing library and the Pilot Library from the European Chemical Biology Library (ECBL). The Fraunhofer repurposing library comprises 5,632 compounds, including 3,400 clinically utilized drugs covering 600 indications, and 1,582 preclinical compounds with varying levels of validation. The ECBL Pilot Library contains 2,464 biologically active small molecules curated from the EU-Openscreen compound library, targeting 1,039 distinct biological targets, and includes 654 approved drugs and 368 highly selective probes. To identify K_v7 activators, fluorescence-based thallium-flux assays have been widely used. Given the well-known permeability of potassium (K^+) channels to thallium (Tl^+), these assays exploit Tl^+ as surrogate for potassium K^+ and Tl^+-sensitive dyes, such as FluxOR, that are incubated in cell lines stably expressing the ion channel of interest. When Tl^+ is added to the external cellular solution, this flows through the open channels into the cytoplasm where it binds the Tl^+-sensitive dye, and this interaction generates a cytoplasmatic fluorescent signal proportional to the Tl^+ influx and therefore to the proportion of open channels. This assay was optimized in mammalian Chinese hamster ovary (CHO) cells stably expressing $K_v7.3$ A315T channels. The A315T mutation was introduced to enhance the macroscopic current density of $K_v7.3$ channels (Etxeberria et al., 2004), thereby improving the signal-to-background ratio and ensuring a robust screening assay, as evidenced by the assay quality parameter Z' factor, that is a statistical data quality indicator for a bioassay. Using this assay, compounds from the Fraunhofer and ECBL Pilot libraries were tested at a single concentration of 10 µM. Fluorescence signals were expressed as a percentage of drug-induced current increase relative to the effects prompted by 10 µM retigabine used as positive control, with minimum effect of 20% for identifying potential hits. Out of the 59 hits identified during this primary screening, 12 were confirmed under the same experimental conditions. During the subsequent profiling phase, seven compounds demonstrated an EC_{50} below 10 µM in activating the $K_v7.3$ A315T channel in the FluxOR assay. These compounds were ML-213, C4, C6, C12, C14, C26, and C54. However, because ML-213 is already well-known, it was eliminated from following electrophysiological studies, along with C12, which is no longer commercially available and difficult to obtain. The remaining five compounds were selected for further electrophysiological characterization.

4.2 ELECTROPHYSIOLOGICAL CHARACTERIZATION OF NEWLY-IDENTIFIED K_V7 ACTIVATORS

To validate the results obtained from the fluorescence-based screening, whole-cell patch-clamp recordings in CHO cells transiently transfected with Kv7.3 A315T cDNA were performed to investigate the effects prompted by the five selected molecules (C4, C6, C14, C26, and C54); in these experiments, retigabine was used as a comparator. Cells were clamped at -80 mV, and currents were elicited by 3-s voltage ramps from -80 mV to +20 mV (Figure 4.1 panel A, Control trace). The voltage-dependence of the $K_V7.3$ A315T current activation channel shifted to the left when 10 µM retigabine was applied (Figure 4.1, panel A, blue trace). This resulted in an increase of the ratio of currents measured in the presence of the drug to current in control conditions (Idrug/Icontrol) of roughly 12-fold at -40 mV (Figure 4.1, panel B). Using the same ramp protocol, only C4, C6 and C54 significantly increased $K_V7.3$ A315T currents ($p<0.05$, n=3-9), with C4 producing the largest effect (4-fold enhancement); instead, no current increase was detected with C14 and C26. Based on this results C4 was selected for further studies.

In order to better characterize the pharmacological properties of C$ we used a step protocol characterized by depolarized by consecutive voltage steps from -100/-80 to +20 mV, CHO cells transiently transfected with $K_V7.3$ A315T cDNA displayed robust outward K^+ currents with slow activation/deactivation kinetics, and a half activation potential (V½) of -30.8±1.3 mV (Figure 4.1. panels C and D). Perfusion with 1µM retigabine induced a -40 mV hyperpolarizing shift in V½ of $K_V7.3$ A315T currents; the same concentration of C4 only caused a -10 mV hyperpolarizing shift in V½ (Figure 4.1. panels C and D). For retigabine, as previously reported, an EC50 of 0.6±0.1 µM and a maximal $\Delta V_{1/2}$ of -60.9±6.1 mV was measured in concentration-response experiments (Figure 4.1 panel E). Instead, EC50 and maximal $\Delta V_{1/2}$ were 2.0±0.03 µM and of 37.0 ± 5.4 mV, respectively, for C4, showing that this compound, when compared to retigabine, displayed lower efficacy and potency in activating currents mediated by $K_V7.3$ A315T channels ($p<0.05$, n=3-9, Figure 4.1 panel E; Table 1).

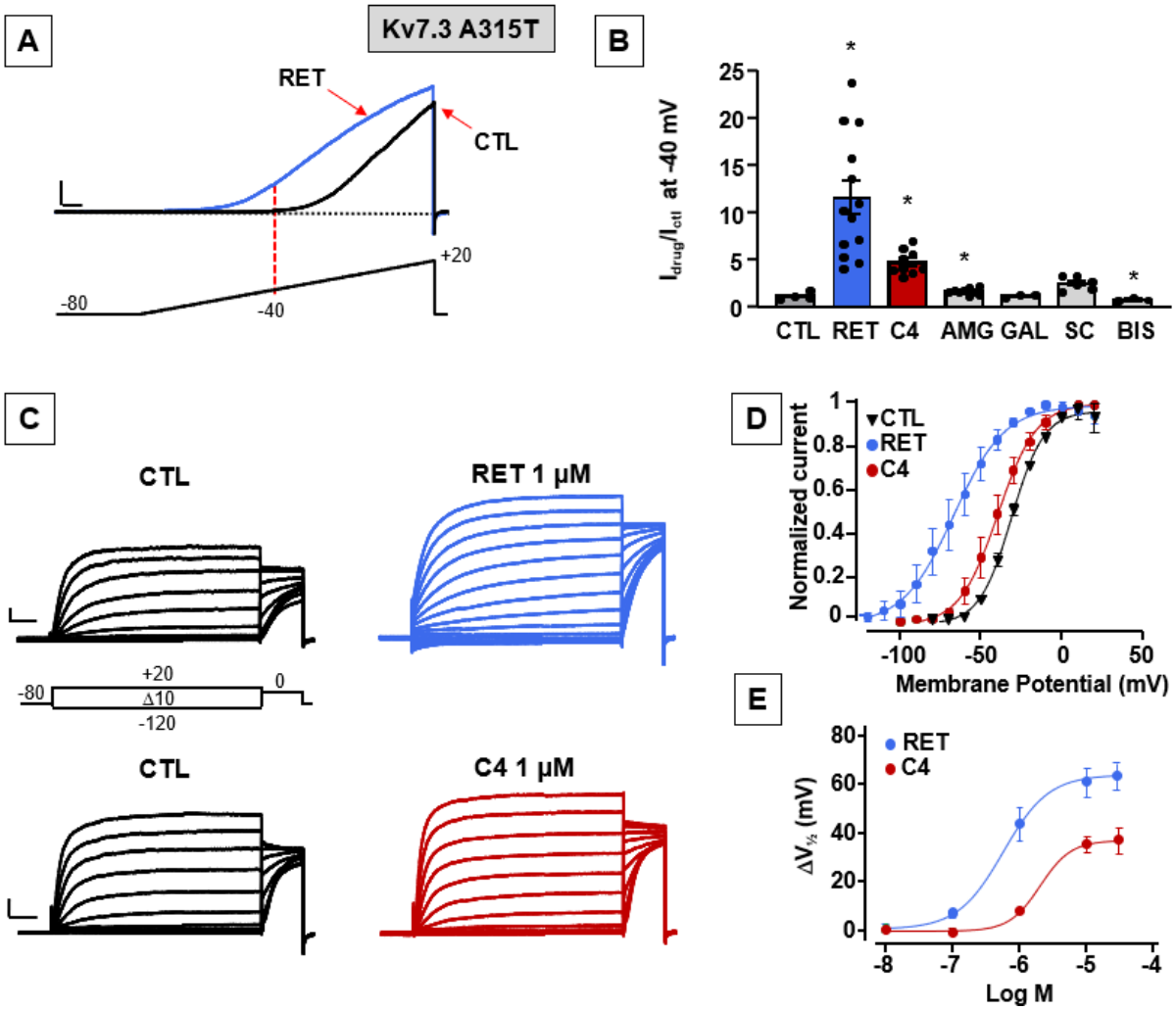

Figure 4.1. Electrophysiological characterization of newly identified K_v7 activators. (A) Representative current traces from CHO cells expressing Kv7.3 A315T channels before (CTL; black trace) and after (RET; blue trace) the administration of 10 µM RET in response to the specified ramp protocol. Time scale: 200 ms; current scale: 500 pA. **(B)** Quantification of the effects prompted by the indicated compounds on Kv7.3 A315T currents. A single asterisk indicates values significantly different versus control (CTL). **(C)** Representative macroscopic current traces recorded from Kv7.3 A315T channels in response to the indicated voltage protocol before (left) and after (right) application of 1 µM RET or 1 µM C4. Current scale, 500 pA; time scale, 0.2 s. **(D)** Conductance/voltage curves for Kv7.3 A315T channels in control condition or in the presence of 1 µM RET or 1 µM JNJ. Lines are Boltzmann fit experimental data. **(E)** Concentration-response curves for RET- and C4-induced activation of Kv7.3 A315T currents. Solid lines represent fits of the experimental data to the four-parameter logistic equation used to estimate EC50 values. Each data point is mean ± S.E.M. of 3-30 cells recorded in at least 3 separate experimental sessions. *p<0.05 vs CTL.

4.2.1 SELECTIVITY PROFILE OF C4 VERSUS DISTINCT K_V7 CHANNELS

Given that I_{KM} in most adult neurons primarily arises from the heteromeric assembly of $K_V7.2$ and $K_V7.3$ subunits, the effects of C4 were also compared with those of retigabine in CHO cells transiently co-transfected with $K_V7.2$ and $K_V7.3$ cDNAs. $K_V7.2/7.3$ voltage-dependent K^+ currents exhibited a threshold for activation at approximately -40 mV (Fig. 3A), with a $V_{1/2}$ of -30.2±0.7 mV.

Unlike $K_V7.3$ A317T currents, both retigabine and C4 induced a similar negative shift of approximately 15 mV in $K_V7.2/7.3$ channels (deltaV1/2: -15.3±2.2 mV for retigabine and -14.5±2.9 mV for C4, n=7-8, p>0.05). Concentration-response experiments (0.01-30 µM) showed comparable potencies for retigabine and C4 in activating $K_V7.2/7.3$ heteromeric channels, with EC50 values of 2.5±1.8 µM and 1.2±0.3 µM, respectively (n=3-9, p>0.05; Figure 4.2. panel C; Table 4).

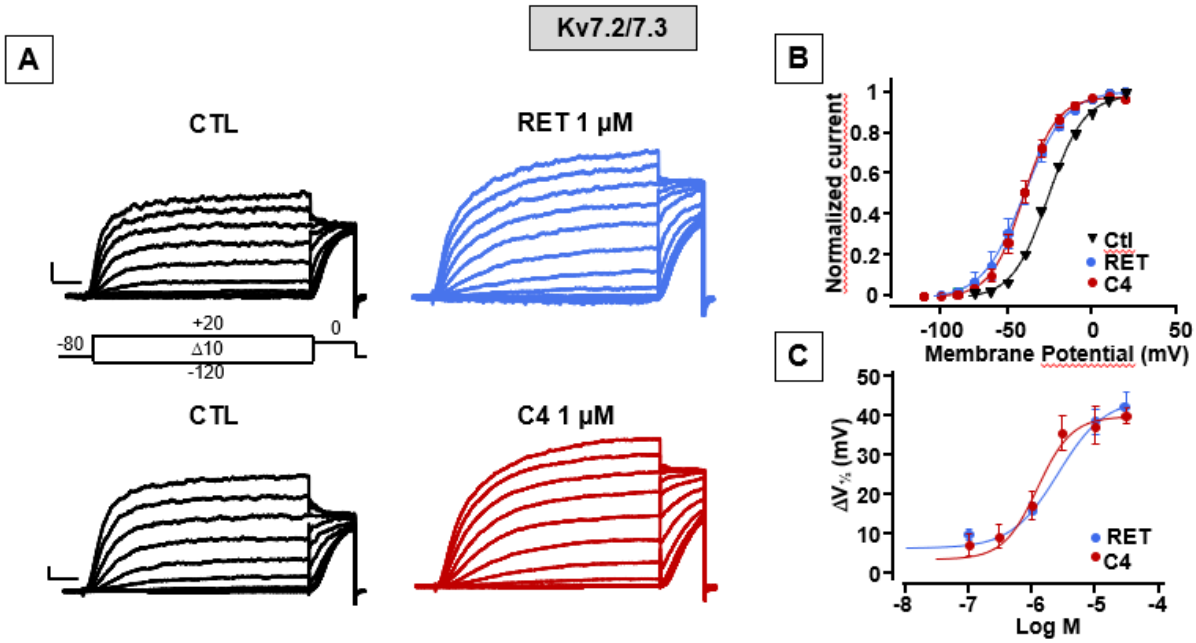

Figure 4.2. Effects of retigabine and C4 on Kv7.2/Kv7.3 currents expressed in CHO cells. (A) Representative macroscopic current traces measured in response to the indicated voltage protocol in cells expressing $K_V7.2/7.3$ channels both before (left traces) and after (right traces) the administration of 1 µM RET or 1 µM C4. **(B)** $K_V7.2/7.3$ conductance/voltage curves measured in control solution (CTL, black-filled triangles) or upon exposure to 1 µM RET (blue-filled circles), or 1 µM C4 (red-filled circles). Lines are Boltzmann fits of the experimental data. **(C)** Concentration-response curves showing the leftward shift in the voltage-dependence of leftward shift in the voltage-dependence of activation of heteromeric Kv7.2/7.3. Each data point is mean±S.E.M. of 10-30 cells recorded in at least 3 separate experimental sessions.

In order to determine whether C4, like retigabine, is able to activate the currents carried by homomeric $K_V7.2$, $K_V7.4$, and $K_V7.5$ channels, the corresponding cDNAs were expressed in CHO cells, and the resulting K^+ currents were recorded as above described, in the presence of varying concentrations (0.1-30 µM) of either C4 or retigabine. While both compounds

were equally effective in $K_v7.4$ and $K_v7.5$ channels, C4 was partially more effective than retigabine at activating $K_v7.2$ (Table 4.1). According to earlier reports, retigabine shifted the $V_{½}$ of $K_v7.2$, $K_v7.4$, and $K_v7.5$ currents with an EC50 of roughly 2 µM. C4 and retigabine had similar EC50 values in $K_v7.4$ and $K_v7.5$ channels (Figure 4.3 A-E, Table 1.3), while in $K_v7.2$ channels, C4 was marginally more potent than retigabine (n=7-11, $p<0.05$). The combined findings showed that C4 is a pan $K_v7.2$-5 channels opener with a profile of potency, effectiveness, and selectivity comparable to retigabine. Importantly, compound C4 do not modulate the cardiac $K_v7.1$ channels; indeed, application of 10µM retigabine or C4 do not significantly affect the $K_v7.1$ current recoded in control solution.

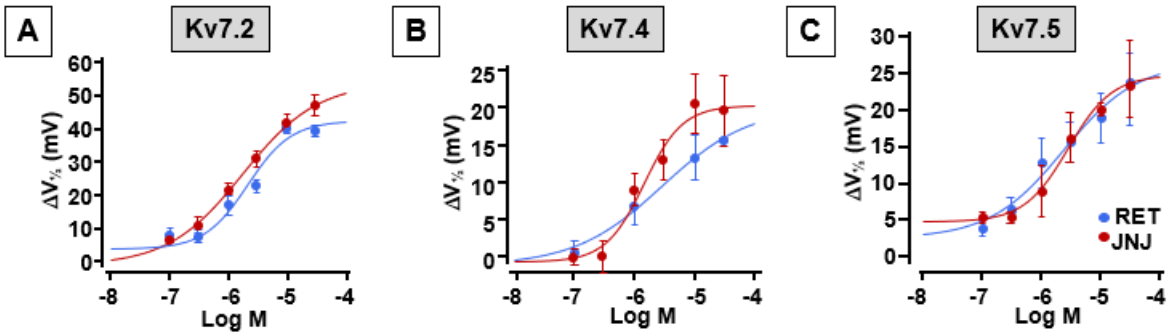

Figure 4.3. Effects of retigabine and C4 on $K_v7.2$, $K_v7.4$ or $K_v7.5$ currents measured in CHO cells. (A-C) Concentration-response curves showing the activation of homomeric Kv7.2 (A), Kv7.4 (B) or Kv7.5 (C) currents, caused by exposure to RET- (blue filled circles) or C4- (red full circles) compounds. Fits of the experimental data by using the four-parameter logistic equation to determine EC50 values. Each data point represents the mean ± standard error of 3–11 cells.

4.2.3 BINDING SITE OF C4 IN $K_V7.2$

Currently-available K_V7 activators bind to two distinct sites in K_V7 channels, one located in the VSD and recognized by benzamides like ICA-069673, and the other in the pore domain and recognized by retigabine. In the latter case, a H-bond between the carbamate group of retigabine and the indole nitrogen atom of a tryptophan residue in S5 within the pore domain (W236 in $K_V7.2$) is necessary for $K_V7.2$-$K_V7.5$ current potentiation (Wuttke TV, 2005) (Schenzer, et al., 2005). In order to identify the binding site of compound C4, we performed in silico docking simulations using the cryoEM structures of $K_V7.2$ (Li, et al., 2021). In $K_V7.2$, the critical H-bond interaction between retigabine carbamate and W236, and π-π interactions between the retigabine p-fluorophenyl moiety with the F305 and F240 residues were correctly predicted. Compound C4 mostly overlap with the binding site of retigabine on Kv7.2 channels. Using functional patch-clamp whole-cell tests in CHO expressing either retigabine-insensitive $K_V7.2$ W236L subunits or wild-type Kv7.2 subunits, in silico predictions were confirmed: indeed, C4 , as observed for retigabine, fails to potentiate activate $K_V7.2$ W236L currents, thus supporting the observation that C4 binds K_V7 channels at a position that is similar to retigabine (Figure 4.4).

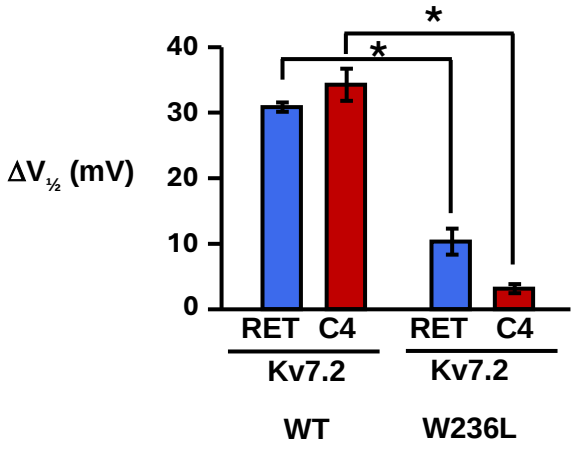

Figure 4.4. Effects of 10 µM RET or 10 µM C4 on $V_{1/2}$ of homomeric $K_V7.2$ or $K_V7.2$ W236L channels, as indicated. *p<0.05.

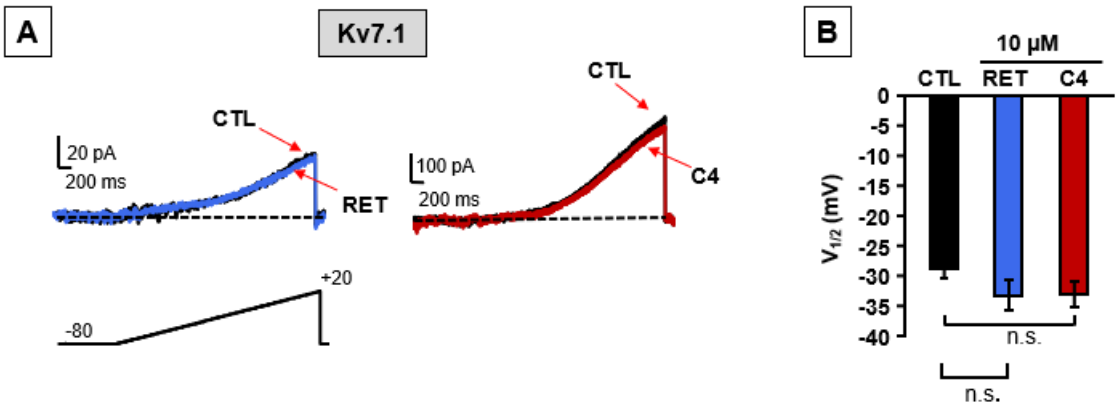

Figure 4.5. Effect of retigabine and C4 on Kv7.1 currents expressed in CHO cells. (A) Representative whole-cell current traces recorded in CHO cells expressing Kv7.1 channel subunits using the indicated ramp protocol before (CTL, black trace) and after exposure to 10 µM RET (blue trace) or C4 (red trace). **(B)** Quantification of Kv7.1 channels half activation potential (V½) in control solution (CTL) or in the presence of 10 µM retigabine (RET) or C4. Each data point is expressed as the mean ± SEM of at least three cells recorded in at least three independent experimental sessions.

Channels Subunits	n	$\Delta V_{½\ max}$ RET (mV)	$\Delta V_{½\ max}$ C4 (mV)	EC_{50} RET (µM)	EC_{50} C4 (µM)
Kv7.3 A315T	4-9	-60.9 ± 6.1	-37.0 ± 5.4*	0.6 ± 0.1	2.0 ± 0.03*
Kv7.2	7-11	-38.6 ±1.5	-46.5 ± 3.1**	2.1 ± 0.8	1.7 ± 0.2*
Kv7.2+Kv7.3	3-7	-38.9 ± 3.6	-37.8 ± 3.6	2.5 ± 1.8	1.2 ± 0.3
Kv7.4	3-6	-15.7 ± 0.2	-19.6 ± 4.7	2.9 ± 1.3	1.4 ± 0.3
Kv7.5	4-10	-26.3 ± 5.8	-23.3 ± 4.3	2.3 ± 0.9	2.8 ± 0.5
Kv7.1	7	-4.7 ± 2.1	-3.1 ± 1.1	--	--

*p<0.05 vs RET

Table 4.1. Profile of selectivity of retigabine and C4 versus distinct Kv7 channels.

4.2.4 EFFECTS OF C4 ON IPSC DERIVED-CORTICAL EXCITATORY NEURONS

Electrophysiological characterization of C4 revealed its ability to potentiate K_v7.2/Kv7.3 currents, which play a key role in neuronal excitability. Therefore, the acute effects of C4 on neuronal electrical activity was evaluated through whole-cell patch-clamp recordings in hiPSCs-derived cortical glutamatergic neurons (iNeurons), both in voltage- and current-clamp configurations. To obtain mature iNeurons, hiPSCs overexpressing NGN2 were cultured together with murine astrocytes and differentiated up to 36 days; electrophysiological recordings were performed on iNeurons in a timeframe between 21 and 36 days of differentiation. They produced spontaneous action potentials (APs) at a frequency of 2.1±0.3 APs/sec and had a resting membrane potential (Em) of -45.8±1.0 mV (Table 1.3). When iNeurons were perfused with either 10 µM retigabine or C4 for 60 seconds after neuronal firing was recorded for approximately 30 seconds, a significant decrease of firing frequency and hyperpolarized Em by approximately 8 mV (Figure 4.6, Table 4.2) were measured. The exposure to the K_v7 channel blocker XE-991 (10 µM) restored control values of Em and AP firing frequency. Since C4 is know as an antagonist of dopaminergic D_2 receptors (D_2R) (Langlois, et al., 2012), which are expressed in iNeurons, the effects of Sulpiride, a selective D_2R antagonist (Jenner & Marsden, 1984) was also examined. Neuronal firing and Em were unaffected by 10µM of Sulpiride (Figure 4.6, Table 4.2), indicating that C4 inhibited iNeuron firing through K_v7.2-5 channel activation rather than D_2R blockade.

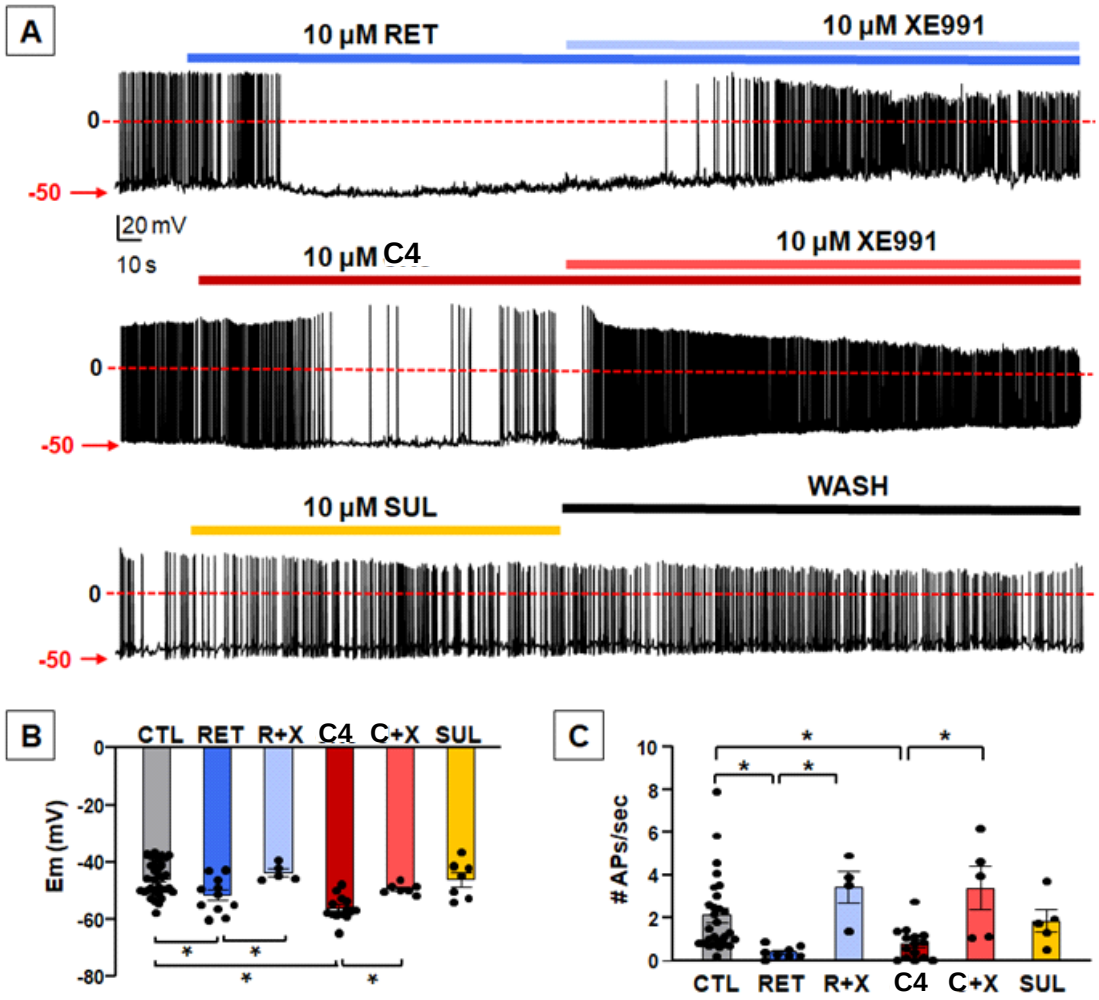

Figure 4.6. Sulpiride, C4, and retigabine's effects on the spontaneous electrical activity of neurons. **(A)** Representative traces of iNeurons recorded in whole-cell current clamp. The duration of drug applications is indicated by the lenght of the bars shown on top of each trace **(B-C)** Quantification of iNeurons Em (B) and spontaneous firing frequency (C) measured in control solution (CTL, black column) or in the presence of the indicated pharmacological treatments. Each drug was used at a 10 µM concentration. *p<0.05.

Treatment	n	Em (mV)	APs/sec
CTL	65	-45.22 ±0.67	2.12±0.34
RET	11	-51.54±1.95*	0.39±0.11*
C4	18	-53.97±1.23*	0.79±0.2*
RET + XE-991	5	-43.57±1.47$^{\#}$	3.41±0.56$^{\#}$
C4 + XE-991	7	-50.21±0.99$^{\alpha}$	3.39±1.13$^{\alpha}$
Sulpiride	7	-48.61±2.71	1.83±0.59

Table 4.2. Effects of retigabine, C4, and sulpiride on iNeurons' spontaneous action potentials (APs/sec) and membrane potential (Em). Retigabine (RET), C4, D_2R antagonist, and XE-991 were used at 10µM. Each data point is mean±S.E.M. of 4-65 cells recorded in at least 3 separate experimental sessions. *p<0.05 vs CTL; $^{\#}$p<0.05 vs RET; $^{\alpha}$p<0.05 vs C4.

Then, the impact of C4 was tested on neuronal network activity in iPSC-derived neurons (iNeurons) from a DEE patient carrying the LoF variant G290D (Orhan et al., 2014) and a CRISPR/Cas9 corrected isogenic control line. To compare the electrophysiological properties across the two cell lines, the percentage of active area, the mean firing rate (MFR), burst frequency and spike counts for burst were examined and compared up to 26 days. Spontaneous spiking activity rises around DIV10 in both lines and develops into robust synchronized bursting between DIV14 and DIV21. Instead, at DIV26, iNeurons^{G290D} showed hyperexcitability, as evidenced by greater spikes per burst, higher spontaneous mean firing rates, and a greater active area of the electrode array, with at that age of maturation no change in burst frequency. At DIV 26 different concentrations (0.03–10 µM) of retigabine and C4 have been tested in both cell lines. Both compounds reduced overall neuronal activity in a concentration-dependent manner, as reflected by a reduction of the normalized active area, which measures total amplitude and frequency of the recorded signal at each electrode and provides a reliable indicator of population-wide drug susceptibility, even in the absence of coordinated network bursting (Figure 4.7). Retigabine and C4 demonstrated similar potency in suppressing electrical activity in iNeurons^{Iso} and iNeurons^{G290D}, with IC50 values around 0.60 µM in the isogenic line and 1.2 µM in the mutant line (IC50s for retigabine and C4, respectively, were 0.61±0.09 and 0.60±0.12 in iNeurons^{Iso}, and 1.14±0.22 and 1.21±0.28 in iNeurons^{G290D}, n=6-8, p>0.05). The study found that retigabine and C4 silenced over 95% of active neurons at a concentration of 10 µM. Mean firing rate also decreased concentration-dependently after treatment with both drugs. Accordingly, a 30-minute pre-incubation with 20 µM XE991 reversed the induced neuronal silencing. To assess the possible participation of D2 receptor blockade in the inhibition of electrical activity by C4 in both iNeurons^{Iso} and iNeurons^{G290D}, the effect of (-)-Sulpiride, a selective D2 receptor antagonist, was also tested. 10µM (-)-Sulpiride did not affect the total active area, nor the firing rate, of iNeurons^{Iso} and iNeurons^{G290D} at DIV26. The activity pattern of C4 closely mirrored that of retigabine, with reduced excitability and suppressed synchronous burst activity.

Cell lines	Active area (%)	Firing rate (Hz)	Burst frequency (Hz)	Spike/Burst (count)
iNeurons^{ISO}	24.89 ± 2.46 (n=12)	0.4917 ± 0.011 (n=12)	0.019 ± 0.002 (n=12)	8976 ± 255 (n=12)
iNeurons^{G290D}	36.16± 1.50* (n=18)	0.6911 ± 0.063* (n=18)	0.018 ± 0.006 (n=18)	11819 ± 398* (n=18)

Table 4.3. Electrophysiological properties of iNeurons^{Iso} and iNeurons^{G290D} populations from HD MEA recordings at DIV26. Each data point is mean ± S.E.M of 12-18 MEA Chips recorded in 3 separate experimental sessions *p<0.05 iNeurons^{Iso} vs iNeurons^{G290D}

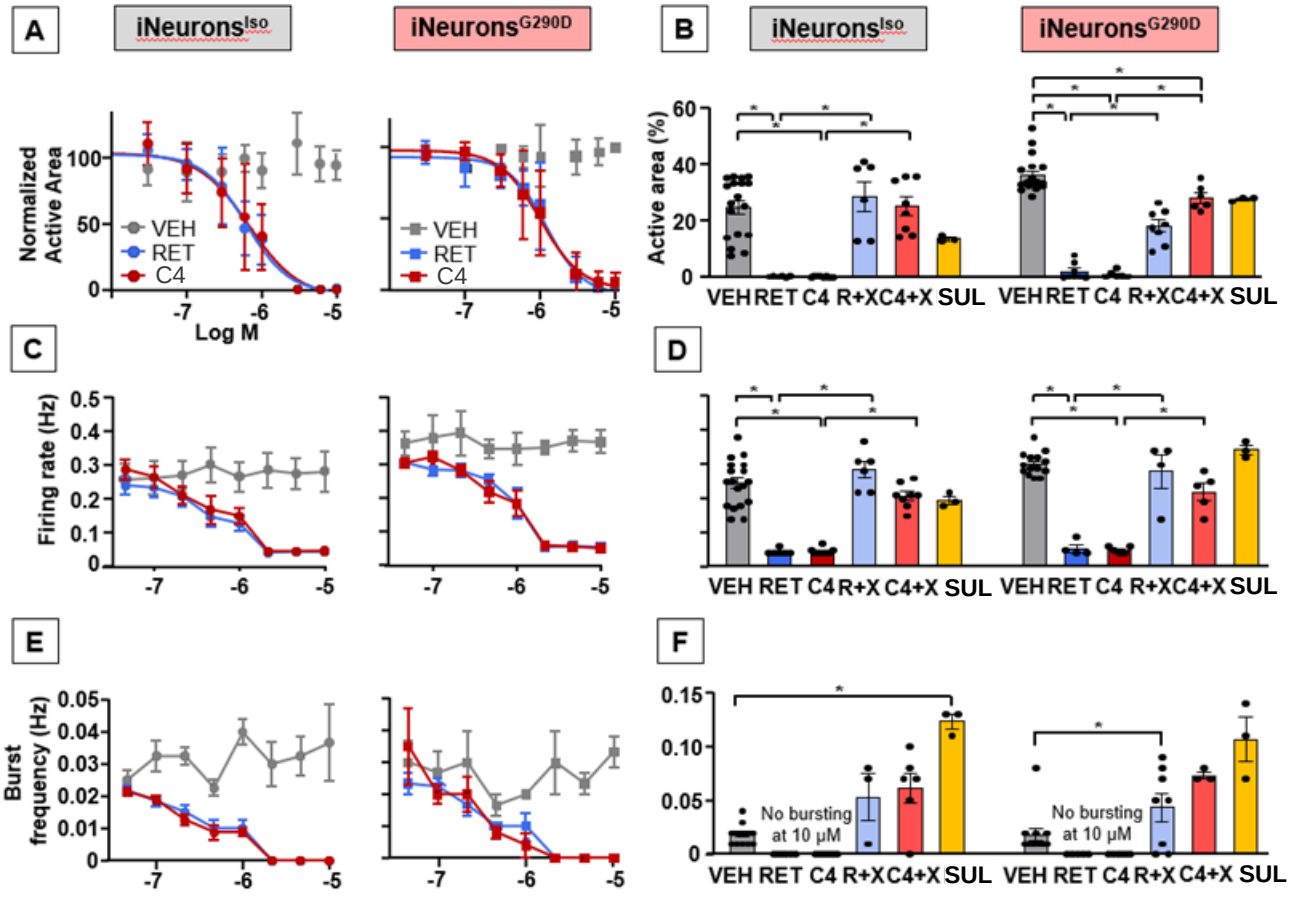

Figure 4.7. Effects of retigabine and C4 on single neurons and synchronized population activity of iNeurons^{Iso} and iNeurons^{G290D}. Concentration-response curves for retigabine- (RET, blue circles) and C4- (C4, red circles) on normalized active area (A), firing rate (C), and burst frequency (E) in iNeurons^{Iso} and iNeurons^{G290D} populations, as indicated. The effect of the vehicle (0.1% DMSO) was also assessed (in grey). In (A), solid lines represent fits of the experimental data to the four-parameter logistic equation used to estimate IC_{50} values. Quantification of active area (B), firing rate (D) and burst frequency (F) of iNeurons^{Iso} and iNeurons^{G290D} after treatment with vehicle (0.1% DMSO) or the following drugs: RET: 10 µM retigabine;10 µM C4; R+X: 10 µM retigabine + 20 µM XE991, C4+X: 10 µM C4 + 20 µM XE991, D2R: 10 µM D2R antagonist). Each data point is mean±S.E.M. of HD MEA recordings from 3-8 chips for each neuronal line. *p<0.05.

4.2.5 Anticonvulsant effects of C4 in two mouse models of seizures

In collaboration with the Department of Health Sciences at the University of Catanzaro led by Prof. Giovambattista De Sarro, the anticonvulsant properties of $K_V7.2/7.3$ channel activation by retigabine and C4 have been investigated in animal models of seizures:

1. acute exposure to the $GABA_A$ receptor antagonist pentylenetetrazol (PTZ), a mouse model of generalized tonic-clonic seizures;

2. audiogenic reflex seizures induced in genetically epilepsy-prone DBA/2 mice. In both models, retigabine effectiveness in reducing seizures severity score is well described (Rostock, et al., 1996) (De Sarro et al., 2001). Beside retigabine, other newer $K_V7.2/7.3$ activators effectively counteracted PTZ-induced seizures (Zhang, et al., 2021) (Grupe, et al., 2020) or sound-induced seizures in DBA/2 mice (Bloms-Funke et al., 2022), thus confirming the efficacy of these two animal models to evaluate the anticonvulsant efficacy of Kv7 channel activators. In both animal models, retigabine or C4 were administered i.p, 30 minutes before seizures induction.

In the PTZ model, retigabine (5–30 mg/kg, i.p) reduced the severity of both clonic and tonic phases of seizures, with ED_{50}s of 13 and 9 mg/kg, respectively. C4 (10–60 mg/kg, i.p) was effective in controlling both clonic and tonic phases of seizures with a potency comparable to that of retigabine (ED_{50}s were 15 mg/kg for clonus and 9 mg/kg for tonus). When animals were pretreated with the K_V7 antagonist XE-991 (Wang et al., 1998) (3 mg/kg, i.p), both retigabine and C4 anticonvulsant effects were reduced, thus suggesting that activation of K_V7 channels was responsible for C4-induced anticonvulsant effects in this animal model. Results are summarized in Table 4.

Treatments	ED_{50} Values (mg/kg)	
	Clonus	Tonus
RET (5-30 mg/Kg)	**13** (9.2-18.5)	**9** (7-12)
RET + XE-991 (3 mg/kg)	**17** (12.1-24.4)	**14** (9.6-21.2)#
C4 (10-60 mg/Kg)	**15** (12-18)	**9** (6-13)
C4 + XE-991 (3 mg/kg)	**20** (16-26)*	**14** (12-17)*

Table 4. **Anticonvulsant effects of retigabine and C4 against PTZ-induced seizures in C57BL mice.** Potency values (ED_{50}) expressed in milligram/kilogram (95% confidence limits) of retigabine (RET) and C4 on PTZ-induced seizures in C57BL/6J mice, with or without pretreatment with XE-991 (3 mg/kg) were calculated according to Litchfield and Wilcoxon (Litchfield & Wilcoxon, 1949) * and # $p<0.05$ versus RET or C4, respectively.

In the DBA/2 model, retigabine (3-20 mg/kg, i.p.) dose-dependently reduced sound-induced seizures, showing a protective effect against wild running, clonic and tonic phases with

calculated ED_{50s} of 12, 7 and 4.6 mg/kg, respectively. Compared to retigabine, C4 (5-40 mg/kg, i.p.) showed slightly higher potency in reducing wild running, clonic and tonic phases of seizures, with ED_{50s} of 11, 6 and 3 mg/kg, respectively. Pretreatment with the Kv7 antagonist XE-991 (Wang et al., 1998) (3 mg/kg, i.p) reverted the anticonvulsant effects shown by of both retigabine and C4, again suggesting that C4 antiseizures effects in DBA/2 mice are consequent to K_V7 current potentiation. These results are summarized in Table 5.

Treatments	ED_{50} Values (mg/kg)		
	Wild Running	Clonus	Tonus
RET (3-20 mg/kg)	**12.4** (9-17.3)	**6.9** (4.3-11)	**4.6** (3.6-6)
RET + XE-991 (3 mg/kg)	**25** (18-35)#	**9** (6.5-12.5)	**8** (6-10.5)#
C4 (5-40 mg/kg)	**10.6** (8.5-13.2)	**6** (5-9)	**3** (2-5)
C4 + XE-991 (3 mg/kg)	**15.4** (11.2-18.2)*	**10** (8-11)*	**7** (5-9)*

Table 5. **Anticonvulsant effects of retigabine and C4 against sound-induced seizures in genetically epilepsy-prone DBA/2 mice.** Potency values (ED_{50}) expressed in milligram/kilogram (95% confidence limits) of retigabine (RET) and C4 on audiogenic seizures in DBA/2 mice, with or without pretreatment with XE-991 (3 mg/kg), were calculated according to Litchfield and Wilcoxon (Litchfield & Wilcoxon, 1949)* # and * $p<0.05$ versus RET or C4, respectively.

4.3 IN SILICO-GUIDED SYNTHESIS OF NOVEL K_V7.2 MODULATORS

In a previous work, our research group have performed molecular docking and molecular dynamics (MD) studies to examine the characteristics of the retigabine binding site and to evaluate the chemical space available in the retigabine binding pocket. Using this strategy, we synthesized a series of retigabine derivatives that were subsequently tested on CHO cells stably expressing K_v7.2 and K_v7.3 channels. Among these, we have identified and characterized compound 60 as a potent K_v7.2/3 channel activators (Musella et al, 2022).

Starting from these results the group of Prof. Carmine Ostacolo from the University of Salerno designed and synthesized additional retigabine derivatives with the aim to identify additional K_v7 channel modulators. These compounds were then tested using an automated patch-clamp system on CHO cells stably expressing K_v7.2/K_v7.3 channels. The results revealed that several compounds were able to activate K_v7.2/3 channels and only one (called CPRET-106) completely blocked K_v7.2/3 channels. Considering that very few neuronal Kv7 channel blockers have been described and considering their potential use as “cognition enhancers”, we have focused our study to better characterize the pharmacological profile of the compound CPRET-106.

4.3.1 EFFECTS OF COMPOUND CPRET-106 ON K_V7.2/7.3 CURRENTS

Whole-cell patch-clamp electrophysiological tests have been conducted in CHO cells transiently transfected with cDNA encoding for different Kv7 channel subtypes. Cells were clamped at -80 mV, and 3-s voltage ramps from -80 mV to +20 mV were used to activate K_v7 currents (Figure 4.11). The CPRET-106 was tested on heteromeric configuration K_v7.2/ K_v7.3 as well as on homomeric K_v7.2, K_v7.3 A315T and K_v7.1 channels at different concentrations (0.001-10 μM). The results obtained revealed that CPRET-106 was a potent blocker of K_v7.2, K_v7.3 A315T and K_v7.2+K_v7.3 channels with an IC50 of about 20-40 nM (Figure 4.11). Noteworthy, CPRET-106 at 1 μM was inactive on the cardiac K_v7.1 channels, whereas the Kv7 channel blocker XE991 at the same concentration was able to block about 50% of these currents.

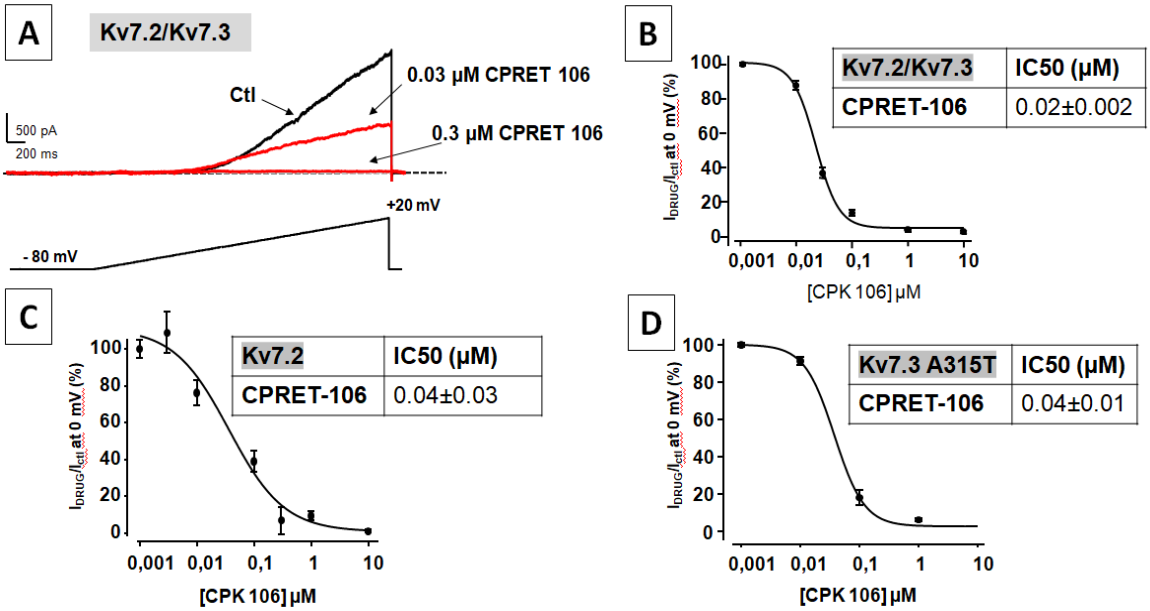

Figure 4.11. Pharmacological sensitivity of distinct Kv7 channels to the newly-identified Kv7 CPRET-106 compound. (A) Representative current traces from CHO cells expressing $K_v7.2$/ $K_v7.3$ channels before (black trace) and after (red trace) the exposure to 0.03 and 0.3 µM CPRET-106 in response to the specified ramp protocol. Time scale: 200 ms; current scale: 500 pA **(B)** Concentration-response curves of blocking effects prompted the the CPRET-106 compound heteromeric $K_v7.2/7.3$, $K_v7.3$ A315T currents. Each data point is mean±S.E.M. of 5-10 cells recorded in at least 3 separate experimental sessions.

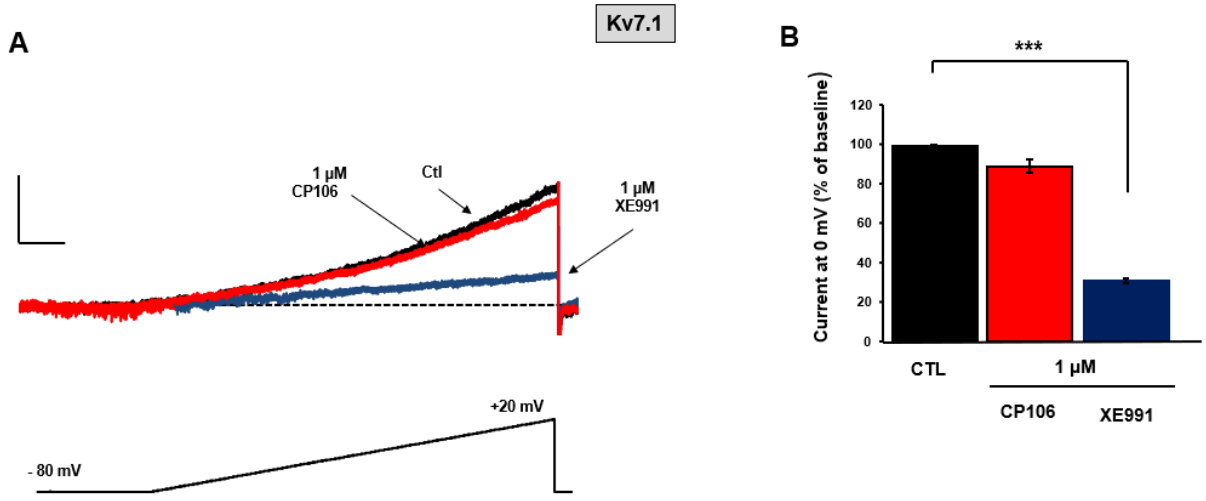

Figure 4.13. Effect of XE991 and C4 on Kv7.1 currents expressed in CHO cells. (A) Representative whole-cell current traces were obtained from CHO cells that expressed Kv7.1 channel subunits triggered by the voltage ramp technique before (CTL, black trace) and after being exposed to 1 µM XE991 (Blue trace) or CPRET-106 (Red trace). Time scale: 200 ms; current scale: 200 pA **(B)** Quantification of Kv7.1 channels half activation potential (V½) in control solution (CTL) or in presence of 1 µM XE991 or CPRET-106. Each data point is expressed as the mean ± SEM of 5-10 cells recorded in at least three independent transfections. ***p<0.001

4.3.2 BINDING SITE OF CPRET-106 ON K_V7.2 SUBUNITS

Retigabine recognises a binding site in the pore doman in of neuronal K_V7 channels. In particular, this molecula establish electostatic interactions with the W236 and S303 residues. In the next experiments, we performed mutagenesys and electrophysiological experiments to define the binding site of compond the CPRET-106 compound. To this aim, we evalaued the activity of compound 106 on the two K_V7.2 mutants W236L and S303A. CPRET-106 was completely inactive on currents expressed by Kv7.2 W236L mutant subunits, while it partially blocked those expressed by Kv7.2 S303A mutant subunits. These results suggest that CPRET-106 binds into the same pocked of retigabine. These results are confirmed by the cryo-EM studies of K_V7.2 channel in complex with CPRET-106.

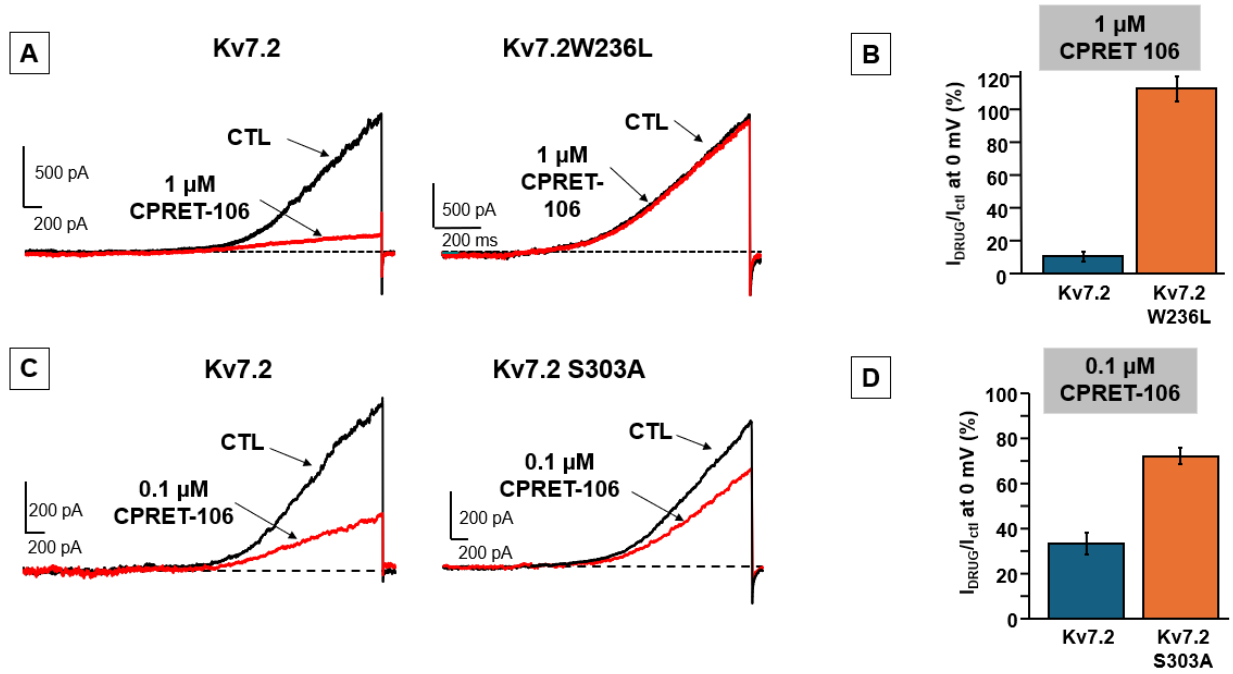

Figure 4.12. Effect of 1 µM RET or 1 µM CPRET-106 on $V_{1/2}$ of homomeric K_V7.2 and K_V7.2 W236L channels expressed in CHO cells. (A) Representative whole-cell current traces were obtained from CHO cells that expressed Kv7.2 or Kv7.2 W236L channel subunits triggered by the voltage ramp technique before (CTL, black trace) and after being exposed to 1 µM CPRET 106 (Red trace). **(B)** Quantification of Kv7.2 and Kv7.2 W236L channels current at 0 mV in control solution (CTL) or in presence of 1 µM CPRET-106. **(C)** Representative whole-cell current traces were obtained from CHO cells that expressed Kv7.2 or Kv7.2 S303A channel subunits triggered by the voltage ramp technique before (CTL, black trace) and after being exposed to 1 µM CPRET 106 (Red trace). **(D)** Quantification of Kv7.2 and Kv7.2 S303A channels current at 0 mV in control solution (CTL) or in presence of 0.1 µM CPRET-106. Each data point is expressed as the mean ± SEM of 7-10 cells recorded in at least three independent transfections. ****p<0.0001.

4.3.3 EFFECT OF CPRET-106 ON A GAIN-OF-FUNCTION VARIANT (GoF)

The K_v7.2 R201C variant is a pathogenic variant associated with DEE. This variant disrupts normal channel function by a GoF effect (Miceli et al., 2015). Compared to LoF of K_v7.2, patients carrying GoF variants suffer from a more complex clinical phenotype (Mulkey et al., 2017; Miceli et al., 2015). Considering that R201C is a GoF and that CPRET-106 produces functional effects opposite to those introduced by the mutation, in some experiments we evaluate the ability of CPRET-106 to counteract the mutation induced functional impairment. To this aim we performed electrophysiological experiments on CHO cells expressing heteromeric Kv7.2+Kv7.2 R201C+Kv7.3, channels. CPRET-106 concentration-dependently inhibits current wih an IC_{50}= 21 nM. Collectively, these data suggest that targeting the binding pocket with small-molecule inhibitors is an effective strategy to mitigate the functional effects of Kv7.2 GOF mutations. A value similar to that calculated for K_v7.2+K_v7.3.

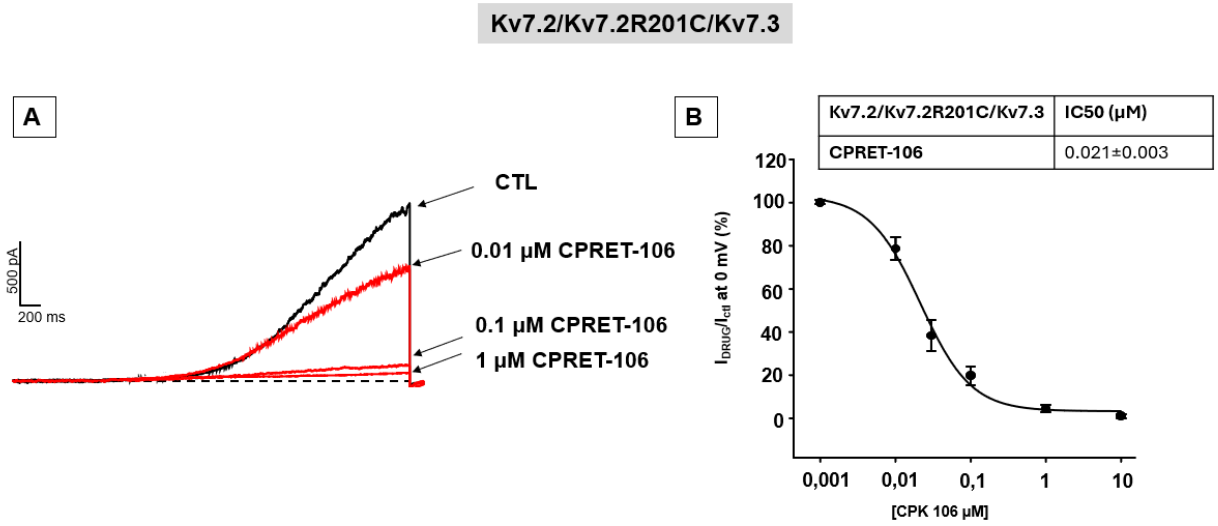

Figure 4.13. Pharmacological sensitivity of distinct Kv7.2/Kv7.2R201C/Kv7.3 channel to the newly-identified Kv7 CPRET-106 compound. (A) Representative current traces from CHO cells expressing K_v7.2/ K_v7.2R201C/K_v7.3 channels before (black trace) and after (red trace) the exposure to 0.01, 0.1 and 0.1 µM CPRET-106 in response to the specified ramp protocol. **(B)** Concentration-response curves of blocking effects prompted the the CPRET-106 compound heteromeric K_v7.2/ K_v7.2R201C/K_v7.3, currents. Each data point is mean±S.E.M. of 5-10 cells recorded in at least 3 separate experimental sessions.

5. DISCUSSION

The research presented in this Thesis is part of the European project "TreatKCNQ," an initiative aimed at developing innovative therapies for encephalopathies associated with K_v7 channels. These disorders, characterized by refractory epileptic seizures and severe developmental delays, represent a significant medical challenge. The "TreatKCNQ" project brought together a consortium of academic institutions and clinical partners of excellence, including the Fraunhofer Institute, University of Antwerp, Aix Marseille University, the University of Naples “Federico II”, and others, to address the many-sided aspects of these diseases. By leveraging multidisciplinary approaches, the project combined drug repurposing techniques, rational design of new compounds, and validation using state-of-the-art preclinical models.

K_v7 Channels as Therapeutic Targets for Epilepsy

Epilepsy is a neurological disorder that affects approximately 50 million individuals worldwide, making it one of the most prevalent neurological conditions (World Health Organization, 2019). The disorder can arise from various causes, including acquired brain injuries such as trauma, infections, strokes, or tumors (Hauser, 2008). Additionally, genetic mutations affecting ion channel or neurotransmitter-related genes and proteins—key regulators of brain excitability—can also lead to epilepsy (Helbig, 2008). Despite significant advancements in the development of antiepileptic drugs (AEDs), around 30% of epilepsy patients continue to experience drug-resistant seizures (Kwan, 2000). This persistent challenge highlights the urgent need for the identification of novel molecular targets and the development of new therapeutic strategies aimed at treating drug-resistant epilepsies (Sisodiya et al., 2013). Research in this area remains a high priority, as overcoming drug resistance could significantly improve the quality of life for millions of affected individuals (Chen et al., 2020). K_v7 potassium channels have gained significant attention as promising pharmacological targets for the treatment of various neurological disorders, including epilepsy (Barrese, 2018). These channels belong to a subfamily of voltage-gated potassium channels, comprising five members ($K_v7.1$–$K_v7.5$), which are encoded by the KCNQ gene family (KCNQ1–KCNQ5) (Jentsch et al., 2000). While $K_v7.1$ channels are predominantly expressed in cardiac tissue, $K_v7.2$, $K_v7.3$, and $K_v7.5$ are primarily found in the nervous system, where they play a critical role in regulating neuronal excitability (Miceli et al.,2008). In neurons, functional K_v7 channels are formed by tetrameric assemblies of $K_v7.2$, $K_v7.3$, and $K_v7.5$ (Schroeder et al.,1998). These channels are the molecular components responsible for the muscarinic-regulated M-current (I_{KM}), a non-inactivating potassium

current that stabilizes the resting membrane potential and limits repetitive neuronal firing (Wang et al.,1998; Shapiro et al.,2000). This current regulates repolarization of the membrane, dampens repetitive firing, and controls neuronal excitability (Brown and Passmore et al., 2006). In addition, an emerging number of studies pointed out that severe disruption of the function of $K_v7.2$, $K_v7.3$, and $K_v7.5$ subunits due to de pathogenic variants in the encoding gene leads to developmental and epileptic encephalopathy (Dirkx et al., 2020).

Therefore, pharmacological activation of K_v7 channels have become a target for treating epilepsy as well as other disorders in which neuronal hyperexcitability plays a critical role, such as neuropathic pain (Liu et al., 2021), ischemic stroke (Bierbower et al., 2015), and amyotrophic lateral sclerosis (Wainger et al., 2021).

Retigabine is the prototype K_v7 channel activator used as an antiseizure medication. Unfortunately, it was removed from the market for some limitations such as skin discoloration and no anti-seizure medications selectively acting on K_v7 channels are clinically available (Gunthorpe, Large, & Sankar et al., 2012) even though gabapentin and cannabidiol are compounds that potentiate K_v7 channels (Manville et al., 2018) (Soldovieri et al., 2020). However, three K_v7 channel activators — pynegabine (HN37) (Zhang et al., 2021), XEN1101 (French et al., 2023), and BHV-7000 (Bialer et al., 2024) — are currently undergoing clinical trials for the treatment of epilepsy. These compounds represent a promising new class of anticonvulsant drugs aimed at enhancing K_v7 channel activity to restore neuronal excitability to physiological levels. Simultaneously, the development of novel selective blockers for neuronal K_v7. channels are equally critical. Notably, also gain-of-function mutations in $K_v7.2$, $K_v7.3$ or $K_v7.5$, have been linked to DEE. In such cases, Kv7 blockers, rather than activators, could restore "normal" neuronal excitability and alleviate clinical symptoms.

In this context, the primary goal of the project was to develop new K_v7 channel activators. Among the strategies employed, drug repurposing enabled the identification of new bioactive molecules through the screening of existing drug libraries, such as the Fraunhofer set, which includes over 5600 compounds qualified for various pharmacological targets (Ashburn and Thor et al., 2004). Additionally, analogs of retigabine were designed to develop safer and more selective compounds.

Identification of C4, a novel Kv7 activator, though a Drug Repurposing strategy

The introduction of a new pharmaceutical drug to the market is a complex and lengthy process, spanning several stages that include basic research, discovery and optimization, preclinical development, human clinical trials, and ultimately, regulatory approval. On average, this journey exceeds a decade and incurs costs surpassing €1 billion (Hughes, 2011).

Drug repurposing refers to the strategic application of an already existing therapeutic agent to a novel disease indication. This approach offers considerable benefits, as clinically approved drugs that are repurposed can bypass the extensive early stages of drug development, proceeding directly to preclinical and clinical trials. This strategy significantly reduces both the time required and the costs associated with preclinical development.

In our efforts to identify novel K_v7.2/7.3 channel activators among approved drugs, a cell-based high-throughput screening (HTS) using the Fraunhofer repurposing library was conducted. This library comprises 5,632 compounds, including 3,400 clinically approved drugs spanning over 600 indications and 1,582 preclinical compounds with varying degrees of experimental validation. The origins of these compounds trace back to the Broad Repurposing Hub—a comprehensive and meticulously curated collection established through a collaborative effort by The Broad Institute of MIT and Harvard, located in Cambridge, Massachusetts. To develop the Broad Repurposing Hub, each drug was individually procured, annotated with its known biological activities and clinical indications, and rigorously analyzed to confirm its chemical identity and purity (Corsello et al., 2017). This systematic approach ensures a high-quality resource for accelerating drug discovery and repurposing initiatives.

To explore the library for novel K_v7.2/7.3 channel activators, in collaboration with Fraunhofer Institute, a PhD of our group, Dr. Lidia Carotenuto set up a fluorescence-based HTS assay (FluxOR assay) in CHO cells stably expressing the K_v7.3 A315T channel variant. The A315T mutation serves as an experimental tool to enhance current density by increasing the macroscopic current amplitude without affecting key functional properties, such as voltage dependence of activation, maximal open probability, or PIP_2 affinity (Zaika et al., 2008; Hernandez et al., 2009). In the initial screening phase, the compounds were tested at a concentration of 10 µM, normalizing their activity to that of retigabine, used as a positive

control (10 µM). To define potential hits, a threshold of 20% activity relative to retigabine was set. Out of the 59 hits identified during this primary screening, 12 were confirmed under the same experimental conditions.

During the subsequent profiling phase, seven compounds demonstrated an EC_{50} below 10 µM in activating $K_v7.3$ A315T channels in the FluxOR assay. These compounds were ML-213, C4, C6, C12, C14, C26, and C54. Among them, ML-213 stood out as a well-characterized K_v7 activator, previously studied and documented (Yu et al., 2011). The identification of ML-213 among approximately 5,600 compounds validated the effectiveness of our screening process in pinpointing K_v7 activators. However, since ML-213 is already well-known, it was excluded from further electrophysiological analyses, along with C12, which is no longer commercially available and difficult to source.

Then, we focused on electrophysiological characterization of the remaining five compounds—C4, C6, C14, C26, and C54—using patch-clamp recordings in CHO cells expressing the $K_v7.3$ A315T channel. While this approach is highly useful in experimental settings, it is important to note that the K_v7 channels physiologically expressed in the central nervous system (CNS) are primarily heteromeric $K_v7.2/7.3$ channels.

By applying a ramp protocol, we observed varying effects on the activity of the channel. At a resting membrane potential of -40 mV, retigabine increased $K_v7.3$ A315T currents by 12-fold, while C4 led to only a 4-fold increase, and C26 produced a 2-fold enhancement. The other compounds did not significantly increase $K_v7.3$ A315T currents, failing to confirm their efficacy as $K_v7.3$ A315T openers. These findings partially validated the results of the initial screening. While we successfully identified new K_v7 activators, some false-positive hits also emerged.

The effects of C4 on $K_v7.3$ A315T currents were also evaluated using a voltage-clamp protocol to investigate its dose-dependent activity and compare it directly with retigabine. Both compounds induced a shift in the voltage-dependence of activation and modestly increased the maximal currents of the $K_v7.3$ A315T channels, indicating their ability to enhance channel opening. However, the comparative analysis revealed that C4 is less potent and less effective than retigabine as a $K_v7.3$ A315T channel opener.

C4 revealed a reduced efficacy and potency compared to retigabine in shifting the voltage dependence of activation and modulating channel currents. This difference suggests that

the A315T mutation may affect the interaction of C4 with the channel, potentially altering its binding affinity or the conformational changes required for channel activation.

In addition, we investigated the effects of C4 on heteromeric K_v7.2/7.3 channels and homomeric K_v7.2, K_v7.4, and K_v7.5 channels. The findings demonstrate that C4 exhibits a pharmacological profile similar to that of retigabine, with notable similarities in efficacy and potency.

Both compounds shifted the voltage-dependence of activation of K_v7.2/7.3 channels in a comparable manner, indicating that C4 is equally able to modulate the activation threshold of these heteromeric channels. This modulation is consistent with the mechanisms by which K_v7 openers enhance neuronal excitability control. Moreover, concentration-response analyses confirmed that C4 and retigabine show similar potency in activating K_v7.2/7.3 channels, further supporting their functional similarity.

When the effects of C4 were examined on homomeric K_v7.2, K_v7.4, and K_v7.5 channels, it was observed that C4 displayed a slightly greater efficacy in activating K_v7.2 channels compared to retigabine. However, the two compounds exhibited similar efficacies and potencies in modulating K_v7.4 and K_v7.5 channels. These findings align with previously reported data on retigabine and suggest that C4, like retigabine, acts as a pan K_v7.2–K_v7.5 channel opener.

To explore the potential binding site of C4 on the K_v7.2 channels, we conducted molecular docking simulations using the cryo-EM structure of K_v7.2 in complex with retigabine (PDB ID: 7CR2; Li X et al., 2021). As described in Section 4.2.3, retigabine binds within the pore of the K_v7.2 channel at a site formed by three pockets. This binding site is largely conserved across K_v7.2–K_v7.5 channels, with only minor differences in the amino acids lining these pockets. A critic interaction involves a hydrogen bond between the carbamate group of retigabine and the indole nitrogen atom of a tryptophan residue (W236 in K_v7.2) located in the S5 domain. This interaction is crucial for retigabine's ability to open K_v7.2–K_v7.5 channels (Wuttke et al., 2005; Schenzer et al., 2005). In this context, the tryptophan residue serves as a hydrogen bond donor (HBD), while the carbamate group of retigabine acts as a hydrogen bond acceptor (HBA) (Kim et al., 2015). Our docking simulations suggested that C4 likely binds to the same pocket in K_v7.2 as retigabine. Specifically, the nitrogen atom in the piperazine ring of C4 appeared to act as a hydrogen bond acceptor, interacting with W236 as a hydrogen bond donor. Given the critical role of this interaction for retigabine's channel-opening effect, we conducted electrophysiological experiments to test this

hypothesis. The results showed that C4 was completely ineffective on currents expressed by K_v7.2 W236L mutant channel. These findings support the docking simulations and confirm that C4 binds to the same site as retigabine. Given the shared binding determinants, C4 is thought to facilitate channel opening through a similar mechanism to retigabine. Specifically, it likely triggers a clockwise rotation of the upper halves of the S5 and S6 segments, along with the pore helix. This conformational change increases the mobility of the voltage-sensing domain (VSD), thereby reducing the energy required for the VSD to transition from its resting state to an activated state. These structural rearrangements help explain the marked shift in voltage-dependent gating observed in electrophysiological experiments with both C4 and retigabine. Additionally, the ability of C4 to engage conserved structural features across K_v7 family members underscores its potential as a broad-spectrum modulator of neuronal K_v7 channels. This mechanism of action highlights the therapeutic relevance of targeting the shared hydrophobic binding pocket for the development of new anticonvulsant drugs and other treatments for excitability disorders.
An innovative aspect was the validation of the described compounds also in other cellular models derived from induced pluripotent stem cells (iPSCs). This model represents a crucial preclinical platform for studying neurological disorders, offering a human-relevant context for evaluating new drugs (Shi et al., 2017). In addition, cortical neurons derived from iPSCs of patients with pathogenic KCNQ2 variants exhibited neuronal hyperexcitability consistent with the clinical phenotype of KCNQ encephalopathies (Sands et al.,2019) (Kiskinis et al., 2021). To explore the effects of C4 on neuronal intrinsic excitability, we examined its acute effect on spontaneous firing in mature cortical-like glutamatergic neurons (iNeurons). For this purpose, in collaboration with Dr. Sarah Weckhuysen's lab at the University of Antwerp, we utilized neurons differentiated from CRISPR/Cas9-corrected (isogenic) induced-pluripotent stem cells (hiPSCs) derived from a patient carrying a pathogenic KCNQ2 variant associated with developmental and epileptic encephalopathy (KCNQ2 $^{G290D/+}$).

Differentiated iNeurons, identified morphologically by neurite extension, exhibited a resting membrane potential typical of mature neurons and generated spontaneous action potentials, indicative of their functional maturity. The spontaneous activity reflects the establishment of essential ionic mechanisms for neuronal excitability during the differentiation process.

Pharmacological modulation of iNeuron firing revealed distinct effects of K_v7 channel openers. Perfusion with retigabine or C4 caused a hyperpolarization of the membrane

potential and a marked reduction in firing frequency. These changes were reversible upon application of the K_v7 channel blocker XE-991, which restored both membrane potential and firing rates to baseline levels. These observations strongly suggest that the effects of C4, like those of retigabine, are mediated through activation of $K_v7.2$–$K_v7.5$ channels, a conclusion supported by the specificity of XE-991 in blocking these channels.

To exclude off-target effects, the impact of C4 on other pathways was investigated using the selective D_2R antagonist (-)-Sulpiride. The lack of any effect on neuronal firing or membrane potential by (-)-Sulpiride confirmed that the inhibition of firing induced by C4 was not attributable to interactions with D_2R blockade.

Altogether, these findings establish that the reduction in iNeuron firing by C4 is specifically mediated via K_v7 channel activation. This selective mechanism suggests the potential of C4 as a targeted modulator of neuronal excitability.

The effects of C4 on neuronal network activity were assessed using high-density microelectrode array (HD-MEA) recordings in iPSC-derived cortical-like glutamatergic neurons. The study utilized neurons from a patient with developmental and epileptic encephalopathy (DEE) due to the $K_v7.2$ G290D loss-of-function variant ($iNeurons^{G290D}$) and an isogenic control line corrected via CRISPR/Cas9 ($iNeurons^{Iso}$). Over 26 days of vitro, both cell lines displayed progressive neuronal maturation, with spiking activity emerging around day 10 and synchronized bursting developing by day 21. By day 26, $iNeurons^{G290D}$ demonstrated distinct hyperexcitability features, including increased active area coverage, elevated firing rates, and higher spike counts per burst, consistent with previous findings in models of K_v7-related cortical hyperexcitability.

Pharmacological experiments revealed that both retigabine and C4 reduced neuronal activity in a concentration-dependent manner in both cell lines. The reduction was observed across metrics such as the normalized active area and firing rates, suggesting widespread inhibition of network activity. These effects were largely reversed by the K_v7 channel blocker XE-991, confirming that both compounds modulate neuronal excitability through K_v7 channel activation. Importantly, no significant differences in potency or efficacy were detected between retigabine and C4 or between the two neuronal lines, highlighting the broad applicability of these modulators across different genotypes.

To rule out off-target effects, the selective dopamine D2 receptor (D_2R) antagonist (-)-Sulpiride was tested. Its lack of effect on network activity confirmed that the observed actions

of C4 were mediated through K_v7 channels rather than D_2R antagonism. Interestingly, while both retigabine and C4 effectively suppressed synchronized burst activity, XE991 fully restored bursting, and sulpiride modestly increased burst frequency in the isogenic control line, suggesting a minor role for D_2Rs in network modulation.

Moreover, as revealed by in vivo studied performed in collaboration with researchers at the University of Catanzaro, C4 demonstrates significant anticonvulsant properties in two animal models of acute seizures: generalized tonic-clonic seizures induced by pentylenetetrazol (PTZ) and audiogenic seizures in DBA/2 mice. These effects, comparable to those of retigabine and other $K_v7.2/7.3$ activators, were reversed by the K_v7 blocker XE991, indicating that anticonvulsant actions of C4 are mediated by through K_v7 channel activation rather than D_2 receptor antagonism. Supporting this, dopaminergic transmission enhancement (via agents like apomorphine or L-DOPA) is known to have anticonvulsant effects, whereas most D_2R antagonists worsen seizures in epilepsy-prone models.
The ED_{50} values for anticonvulsant effects of C4 align closely with its antipsychotic activity in rodent models, suggesting overlapping dose ranges. Importantly, none of the >20 D_2R-targeting compounds in screened libraries exhibited K_v7 activation, reinforcing the independence of these mechanisms. In iPSC-derived neurons expressing D_2R, C4 and retigabine induced XE991-sensitive hyperpolarization and firing inhibition, while the selective D_2R antagonist (-)-Sulpiride was ineffective. In KCNQ2-DEE patient-derived iNeurons and isogenic controls, C4 reduced both single-neuron and synchronized network activity with potency equivalent to retigabine, further confirming that K_v7 channel activation underlies its effects.
In the end, C4 offers greater specificity for K_v7 channels, making it a more promising candidate for treating KCNQ encephalopathies.

Development and Characterization of CPRET-106

In a previous work, our research group utilized molecular docking and molecular dynamics (MD) simulations to examine the retigabine binding site and explore the chemical space of its binding pocket. This approach facilitated the design and synthesis of several retigabine derivatives, which were tested on CHO cells expressing $K_v7.2$ and $K_v7.3$ channels. Among these compounds, one, compound 60, was identified as a potent $K_v7.2/ K_v7.3$ channel activator (Ostacolo et al., 2020). Building on this strategy, the team led by Prof. Carmine Ostacolo at the University of Salerno further synthesized and evaluated additional retigabine

derivatives. Using an automated patch-clamp technique, a compound named CPRET-106 was identified as a unique and potent blocker of K_v7.2/3 channels.

To assess the activity of CPRET-106 on K_v7 channels, whole-cell patch-clamp electrophysiology was performed on human CHO cells transiently transfected with cDNA encoding various K_v7 channel subtypes, including heteromeric K_v7.2/K_v7.3 and homomeric K_v7.2, K_v7.3 A315T, and K_v7.1 channels. The results showed that CPRET-106 is a potent blocker of K_v7.2, Kv7.3 A315T, and K_v7.2/K_v7.3 channels, with inhibition observed at low nanomolar concentrations. When compared to the other K_v7 channel blockers such as XE-991 (IC_{50} =0.98 µM; (Wang 1998)), ML252 (IC_{50}= 4.05 µM; (Kanyo et al.,2023)) (IC_{50}= 69 nM; (Cheung et al., 2012)) and the retigabine derivative HN38 (IC50=0.1 µM) compound CPRET-106 is the most potent. Interestingly, at a concentration of 1 µM, CPRET-106 showed no significant effect on K_v7.1 cardiac channels, in contrast to the known K_v7 channel blocker XE-991, which inhibited about 50% of the K_v7.1 current at the same concentration.

Retigabine binds to a specific site within the pore domain of neuronal K_v7 channels, interacting with key residues W236 and S303. To explore whether CPRET-106106 interacts with the same site, mutagenesis and electrophysiological experiments were conducted on two Kv7.2 mutants—W236L and S303A. The results demonstrated that the W236L mutation completely abolished the activity of CPRET-106, while the S303A mutation only partially reduced its efficacy. These findings strongly suggest that CPRET-106 occupies the same binding pocket as retigabine, contributing to its blockade of K_v7.2/3 channels.

Further supporting this hypothesis, cryo-EM studies of the K_v7.2 channel in complex with CPRET-106 revealed that the compound binds within the pore region of the channel. The cryo-EM structure of K_v7.2 in complex with CPRET-106 shows the channel in a decoupled state, with the voltage-sensing domain (VSD) activated and the pore closed, consistent with the blockade mechanism of action.

CPRET-106 represents a promising compound that targets the K_v7.2/ K_v7.3 channels, providing further insight into the binding mechanisms of K_v7 channel blockers. The similarity of its binding site to that of retigabine, along with its selective blockade of K_v7.2/ K_v7.3 channels, makes CPRET-106 a valuable tool for future studies on K_v7 channel function and its potential therapeutic applications in disorders related to K_v7 channel dysfunction. Indeed, upon experiements we observed that CPRET-106 at different concentrations showed a blocking effect (IC_{50}= 21 nM) on the heteromeric configuration K_v7.2 R201C combined with Kv7.2/7.3.

In conclusion, this work represents a successful example of integrating multidisciplinary approaches, combining drug repurposing, silico modeling, and advanced preclinical validations, opening new avenues for identification of novel K_V7 channel modulators for the treatment of hyperexcitability disorders such as pain and epilepsy and cognitive enhancement.

6. REFERENCES

Abbott. (2016). KCNE1 and KCNE3: The yin and yang of voltage-gated K(+) channel regulation. *Gene.*, 15;576.

Abbott (2021). KCNQ and KCNE Isoform-Dependent Pharmacology Rationalizes Native American Dual Use of Specific Plants as Both Analgesics and Gastrointestinal Therapeutics. . *Front Physiol.* , 12:777057.

Abbott (2016a). KCNE1 and KCNE3: The yin and yang of voltage-gated K(+) channel regulation. . *Gene.* , 576:1-13.

Abbott, (2015). The KCNE2 K+ channel regulatory subunit Ubiquitous influence, complex pathobiology. *Gene*, 569(2),162-172.

Abbott, (2016b). KCNE4 and KCNE5: K(+) channel regulation and cardiac arrhythmogenesis. *Gene.*, 593:249-60.

Abou-Khalil B, (2018). Genome-wide mega-analysis identifies 16 loci and highlights diverse biological mechanisms in the common epilepsies. *Nat Commun* , 9:5269.

AdisInsight, (2024). *https://adis.springer.com/drugs/800056133*.

Agency, (2018). *https://www.ema.europa.eu/en/news/withdrawal-pain-medicine-flupirtine-endorsed*. Retrieved from European Medicines Agency.

Aiken SP, (1995). Reduction of spike frequency adaptation and blockade of M-current in rat CA1 pyramidal neurones by linopirdine (DuP 996), a neurotransmitter release enhancer. . *Br J Pharmacol.* , 115:1163-8.

al, G. N. (n.d.). Subunit-Specific Modulation of KCNQ Potassium Channels .

Alaimo A, (2009). Calmodulin activation limits the rate of KCNQ2 K+ channel exit from the endoplasmic reticulum. . *J Biol Chem.* , 284:20668-75.

Amato G,(2011). N-Pyridyl and Pyrimidine Benzamides as KCNQ2/Q3 Potassium Channel Openers for the Treatment of Epilepsy. . *ACS Med Chem Lett.* .

Ambrosino P, (2018). Kv7.3 Compound Heterozygous Variants in Early Onset Encephalopathy Reveal Additive Contribution of C-Terminal Residues to PIP2-Dependent K+ Channel Gating. . *Mol Neurobiol.* , 55:7009-7024.

Angelo K, (2002). KCNE5 induces time- and voltage-dependent modulation of the KCNQ1 current. . *Biophys J.* , 83:1997-2006.

Bal , (2008). Homomeric and heteromeric assembly of KCNQ (Kv7) K+ channels assayed by total internal reflection fluorescence/fluorescence resonance energy transfer and patch clamp analysis. *J Biol Chem.*, 283:30668.

Balestrini, (2018). Pharmacogenomics in epilepsy. *Neurosci Lett* , 667: 27-39.

Ballini , (2014). A 1024-Channel CMOS Microelectrode Array With 26,400 Electrodes for Recording and Stimulation of Electrogenic Cells In Vitro. *IEEE J Solid-State Circuits.*, 49(11):2705-2719.

Barrese , (2010). Neuronal potassium channel openers in the management of epilepsy: role and potential of retigabine. . *Clin Pharmacol.* , 2:225-36.

Barrese ,(2018). KCNQ-Encoded Potassium Channels as Therapeutic Targets. . *Annu Rev Pharmacol Toxicol.*, 58:625-648.

Battefeld , (2014). Heteromeric Kv7.2/7.3 channels differentially regulate action potential initiation and conduction in neocortical myelinated axons. . *J Neurosci.* , 34:3719-32.

Bayat , (2021). Epilepsy Syndromes in the First Year of Life and Usefulness of Genetic Testing for Precision Therapy. . *Genes (Basel).* , 12:1051.

Beghi , (2019). Global, regional, and national burden of epilepsy, 1990- 2016: a systematic analysis for the Global Burden of Disease Study 2016. *Lancet Neurol* , 18:357–375.

Bentzen , (2006). The acrylamide (S)-1 differentially affects Kv7 (KCNQ) potassium channels. . *Neuropharmacology.*, 51:1068-77.

Berg , (2003). How long does it take for partial epilepsy to become intractable? *Neurology.* , 60:186-90.

Beydoun, A. &. (1995). Gabapentin: Pharmacokinetics, efficacy, and safety. *Clinical Neuropharmacology*, 18(6), 469-481.

Bialer, M., Johannessen, S. I., Koepp, M. J., Perucca, E., Perucca, P., Tomson, T., & White, H. S. (2024). Progress Report on New Medications for Seizures and Epilepsy: A Summary of the 17th Eilat Conference on New Antiepileptic Drugs and Devices (EILAT XVII). I. Drugs in Preclinical and Early Clinical Development. *Epilepsia* .

Bierbower, (2015). Augmentation of M-type (KCNQ) potassium channels as a novel strategy to reduce stroke-induced brain injury. . *J Neurosci.* , 35:2101-11.

Bloms-Funke, P., Bankstahl, M., Bankstahl, J., Kneip, C., Schröder, W., & Löscher, W. (2022). The Novel Dual-Mechanism Kv7 Potassium Channel/TSPO Receptor Activator GRT-X Is More Effective than the Kv7 Channel Opener Retigabine in the 6-Hz Refractory Seizure Mouse. *Neuropharmacology* .

Bock,(2019). Sulfide Analogues of Flupirtine and Retigabine with Nanomolar KV 7.2/KV 7.3 Channel Opening Activity. . *ChemMedChem.* , 14:952-964.

Boehlen (2013). The new KCNQ2 activator 4-Chlor-N-(6-chlor-pyridin-3-yl)-benzamid displays anticonvulsant potential. . *Br J Pharmacol.* .

Borgini ,(2021). Chemical modulation of Kv7 potassium channels. . *RSC Med Chem.*, 12(4):483-537.

Bosak , (2019). Implementation of the new ILAE classification of epilepsies into clinical practice - A cohort study. . *Epilepsy Behav.* , 96:28-32. .

Bosch , (2016). Novel genetic causes for cerebral visual impairment. . *Eur J Hum Genet.* , 24:660-5.

Boscia , (2006). Retigabine and flupirtine exert neuroprotective actions in organotypic hippocampal cultures. *Neuropharmacology.* , 51:283-94.

Brickel (2012). The urinary safety profile and secondary renal effects of retigabine (ezogabine): a first-in-class antiepileptic drug that targets KCNQ (K(v)7) potassium channels. . *Epilepsia.* , 53:606-12.

Brickel (2020). Safety of retigabine in adults with partial-onset seizures after long-term exposure: focus on unexpected ophthalmological and dermatological events. *Epilepsy Behav.*, 102:106580.

Brioni (1993). Linopirdine (DuP996) facilitates the retention of avoidance training and improves performance of septal-lesioned rats in the water maze. . *Pharmacol Biochem Behav.* , 44:37-43.

Brown, (1980). Muscarinic suppression of a novel voltage-sensitive K+ current in a vertebrate neurone. *Nature*, 283, 673–676.

Brown , & Passmore, G. M. (2009). Neural KCNQ (Kv7) Channels. . *British J Pharmacology* , 156 (8), 1185–1195. .

Brueggemann , (2014). Differential protein kinase C-dependent modulation of Kv7.4 and Kv7.5 subunits of vascular Kv7 channels. . *J Biol Chem.*, 289:2099-111.

Castaldo , (2002). Benign familial neonatal convulsions caused by altered gating of KCNQ2/KCNQ3 potassium channels. . *J Neurosci.* , 22:RC199.

Charlier , (1998). A pore mutation in a novel KQT-like potassium channel gene in an idiopathic epilepsy family. . *Nat Genet.* , 18:53-5.

Chen , (2018). Treatment Outcomes in Patients With Newly Diagnosed Epilepsy Treated With Established and New Antiepileptic Drugs: A 30-Year Longitudinal Cohort Study. . *JAMA Neurol.* , 75:279-286.

Chen (2020). What has been the impact of new drug treatments on epilepsy? *Curr Opin Neurol.* , 33:185-190.

Cheung (2012). Discovery of a series of 2-phenyl-N-(2-(pyrrolidin-1-yl)phenyl)acetamides as novel molecular switches that modulate modes of K(v)7.2 (KCNQ2) channel pharmacology: identification of (S)-2-phenyl-N-(2-(pyrrolidin-1-yl)phenyl)butanamide (ML252) as a potent, . *brain penetrant K(v)7.2 channel inhibitor. J Med Chem.* , 55(15):6975-9.

Clark,(2015). New antiepileptic medication linked to blue discoloration of the skin and eyes. . *Ther Adv Drug Saf.* , 6:15-9.

Clementi ,(2018). *Farmacologia generale e molecolare.* Edra.

Cooper, (2001). M channel KCNQ2 subunits are localized to key sites for control of neuronal network oscillations and synchronization in mouse brain. *J Neurosci.*, 21(24):9529-40.

Coppola ,(2019). Diagnostic implications of genetic copy number variation in epilepsy plus. . *Epilepsia* , 60: 689–706.

Cormack,(2007). The development of intellectual abilities in pediatric temporal lobe epilepsy. *Epilepsia.* , 48:201-4.

Davoren, (2015). Discovery of a novel Kv7 channel opener as a treatment for epilepsy,. *Bioorganic & Medicinal Chemistry Letters*.

D. Ma, (2022). Structural mechanisms for the activation of human cardiac KCNQ1 channel by electro-mechanical coupling enhancers. *Proc. Natl. Acad. Sci. U.S.A.*

D'Andrea Meira, (2019). Ketogenic Diet and Epilepsy: What We Know So Far. . *Front Neurosci.* , 13:5. .

De Sarro, (2001). Influence of Retigabine on the Anticonvulsant Activity of Some Antiepileptic Drugs against Audiogenic Seizures in DBA/2 Mice. . *Naunyn-Schmiedeberg's Archives of Pharmacology* .

Dedek (2001). Myokymia and neonatal epilepsy caused by a mutation in the voltage sensor of the KCNQ2 K+ channel. . *Proc Natl Acad Sci U S A.* , 98:12272-7.

Delmas (2005). Pathways modulating neural KCNQ/M (Kv7) potassium channels.. *Nat Rev Neurosci.* , 6:850-62.

Devaux (2017). A possible link between KCNQ2- and STXBP1-related encephalopathies: STXBP1 reduces the inhibitory impact of syntaxin-1A on M current. . *Epilepsia.*, 58:2073-2084.

Devinsky (2018). Randomized, dose-ranging safety trial of cannabidiol in Dravet syndrome. . *Neurology.* .

Devinsky, (2017). Trial of cannabidiol for drug-resistant seizures in the Dravet syndrome. *New England Journal of Medicine*, 376(21), 2011-2020.

Dirkx N, (2020). The Role of Kv7.2 in Neurodevelopment: Insights and Gaps in Our Understanding. . *Front Physiol.* .

Dupuis (2002). Activation of KCNQ5 channels stably expressed in HEK293 cells by BMS-204352. *Eur J Pharmacol.* , 437(3):129-37.

Dvir (2014). Recent molecular insights from mutated IKS channels in cardiac arrhythmia. . *Curr Opin Pharmacol.* , 15:74-82.

Ekberg (2007). Regulation of the voltage-gated K+ channels KCNQ2/3 and KCNQ3/5 by ubiquitination. Novel role for Nedd4-2. . *J Biol Chem* , 282:12135-12142.

Erdem (2017). Updating In Vivo and In Vitro Phosphorylation and Methylation Sites of Voltage-Gated Kv7.2 Potassium Channels. . *Proteomics.* , 17:10.1002/pmic.201700015.

Etxeberria (2008). Calmodulin regulates the trafficking of KCNQ2 potassium channels. *FASEB J.*, 22:1135-43.

Etxeberria, (2004). Three Mechanisms 770 Underlie KCNQ2/3 Heteromeric Potassium M-Channel Potentiation. The Journal of 771 Neuroscience, 24, 9146–9152).

Falco-Walter. (2020). Epilepsy-Definition, Classification, Pathophysiology, and Epidemiology. *Semin Neurol.*, 40:617-623.

Fareed (2024). XEN1101, a novel potassium channel opener: hope or hype for adults with focal seizure. . *Ann Med Surg (Lond).* , 86(5):2417-2419.

Feng (2019). Ultra-Rare Genetic Variation in the Epilepsies: A Whole-Exome Sequencing Study of 17,606 Individuals. . *American J Hum Genet* , 105: 267-82. .

Fiest (2017). Prevalence and incidence of epilepsy: A systematic review and meta-analysis of international studies. *Neurology* , 88:296-303.

Fisher (2014). ILAE official report: a practical clinical definition of epilepsy. . *Epilepsia.* , 55:475-82.

Fisher (2017). Operational classification of seizure types by the International League Against Epilepsy: Position Paper of the ILAE Commission for Classification and Terminology. *Epilepsia.* , 58:522-530.

Fisher (2005). Epileptic seizures and epilepsy: definitions proposed by the International League Against Epilepsy (ILAE) and the International Bureau for Epilepsy (IBE). . *Epilepsia*. , 46:470-2.

Fosmo (2017). The Kv7 Channel and Cardiovascular Risk Factors. *Front Cardiovasc Med.*, 5;4:75.

French, (2023). Efficacy and Safety of XEN1101, a Novel Potassium Channel Opener Channel Opener, in Adults With Focal Epilepsy: A Phase 2b Randomized Clinical Trial. . *JAMA Neurol* .

Gamper ,(2003). Calmodulin mediates Ca2+-dependent modulation of M-type K+ channels. *J. Gen. Physiol.*, 122:17–31.

Gamper ,(2005). Structural requirements for differential sensitivity of KCNQ K+ channels to modulation by Ca2+/calmodulin. . *Mol. Biol. Cell*, 16:3538–51.

Gamper ,(2003). Subunit-specific modulation of KCNQ potassium channels by Src tyrosine kinase. . *J Neurosci.*, 23(1):84-95.

Gamper ,(2015). KCNQ channels. In: Zheng J, Trudeau MC (eds) Handbook of ion channels. *CRC Press, Boca Raton*, 275–306.

Gamper,(2003). Calmodulin mediates Ca2+-dependent modulation of M-type K+ channels. *J. Gen. Physiol.*, 122:17–31.

Gamper, & Shapiro(2015,). KCNQ channels. Handbook of ion channels.

Gao, (2010). Isoform-specific prolongation of Kv7 (KCNQ) potassium channel opening mediated by new molecular determinants for drug-channel interactions. . *J. Biol. Chem*. .

Gao, (2017). Intracellular zinc activates KCNQ channels by reducing their dependence on phosphatidylinositol 4,5-bisphosphate. *Proc. Natl. Acad. Sci. U.S.A.*

Geiger, (2006). Immunohistochemical analysis of KCNQ3 potassium channels in mouse brain. *Neurosci Lett.*, 400:101–104.

Ghosh,(2006). KCNQ1 assembly and function is blocked by long-QT syndrome mutations that disrupt interaction with calmodulin. . *Circ. Res.* , 98:1048–1054.

Goff ,(2019). Vasoactive intestinal peptide-expressing interneurons are impaired in a mouse model of Dravet syndrome. . *Elife.* , 8:e46846.

Goswami, (2019). Current Perspectives On The Role Of The Ketogenic Diet In Epilepsy Management. *Neuropsychiatr Dis Treat.*, 15:3273-3285.

Goto , (2019). Characteristics of KCNQ2 variants causing either benign neonatal epilepsy or developmental and epileptic encephalopathy. *Epilepsia*. , 60:1870-1880.

Greene, (2017). Modulation of Kv7 channels and excitability in the brain. . *Cell Mol Life Sci.*, 74:495-508.

Grunnet , (2002). KCNE4 is an inhibitory subunit to the KCNQ1 channel. . *J Physiol.* , 542:119-30.

Grupe, (2020). In vitro and In vivo characterization: A Novel, Brain Penetrant, Pan-Selective Kv7 Potassium Channel Opener with Efficacy in Preclinical Models of Epileptic Seizures and Psychiatric Disorders. *European Journal of Pharmacology* .

Gunthorpe, (2012). The Mechanism of Action of Retigabine (Ezogabine), a First-in-class K + Channel Opener for the Treatment of Epilepsy. . *Epilepsia* , 53 (3), 412–424.

GW., (2020 Jun 23). KCNQs: Ligand- and Voltage-Gated Potassium Channels. . *Front Physiol.*, 11:583. .

Hadley (2003). Stoichiometry of expressed KCNQ2/KCNQ3 potassium channels and subunit composition of native ganglionic M channels deduced from block by tetraethylammonium. . *J Neurosci.*

Hauser, (2008). First seizure definitions and worldwide incidence and mortality. *Epilepsia*, 49(s1), 8-12.

Hebbar, (2020). Recent advances in epilepsy genomics and genetic testing. *F1000 Faculty Rev-185.*

Helbig, (2008). Navigating the channels and beyond: unravelling the genetic architecture of epilepsy. . *The Lancet Neurology*, 7(3), 231-245.

Hernandez ,(2009). Affinity for phosphatidylinositol 4,5-bisphosphate determines muscarinic agonist sensitivity of Kv7 K+ channels. *J Gen Physiol*, 134: 437–448.

Hoshi, (2003). AKAP150 signaling complex promotes suppression of the M-current by muscarinic agonists. . *Nat Neurosci* , 6: 564-571.

Housley, (1992). Ionic currents of outer hair cells isolated from the guinea-pig cochlea. . *J Physiol.* , 448:73-98.

Hsu HT, (2020). Characterization of Convergent Suppression by UCL-2077 (3-(Triphenylmethylaminomethyl)pyridine), Known to Inhibit Slow Afterhyperpolarization, of erg-Mediated Potassium Currents and Intermediate-Conductance Calcium-Activated Potassium Channels. *Int J Mol Sci.* , 21:1441.

Hu, (2002). Two forms of electrical resonance at theta frequencies, generated by M-current, h-current and persistent Na+ current in rat hippocampal pyramidal cells. *J Physiol.* , 545:783-805.

Hu, (2013). Discovery of a retigabine derivative that inhibits KCNQ2 potassium channels. . *Acta Pharmacol Sin.*, 34:1359-66.

Huang, (2023). Voltage-gated potassium channels KCNQs: Structures, mechanisms, and modulations. *Biochemical and Biophysical Research Communications*.

Hsu, (2020). Characterization of Convergent Suppression by UCL-2077 (3-(Triphenylmethylaminomethyl)pyridine), Known to Inhibit Slow Afterhyperpolarization, of erg-Mediated Potassium Currents and Intermediate-Conductance Calcium-Activated Potassium Channels. *Int J Mol Sci.* , 21:1441.

Iannotti , (2010). Expression, localization, and pharmacological role of Kv7 potassium channels in skeletal muscle proliferation, differentiation, and survival after myotoxic insults. *J Pharmacol Ex Ther.* , 332:811-20.

Iannotti, (2013). Specification of skeletal muscle differentiation by repressor element-1 silencing transcription factor (REST)-regulated Kv7.4 potassium channels. *Mol Biol Cell.*, 24:274-84.

Ipavec (2011). KV7 channels regulate muscle tone and nonadrenergic noncholinergic relaxation of the rat gastric fundus. *Pharmacol Res.* , 64:397-409.

Jenner, (1984). Multiple Dopamine Receptors in Brain and the Pharmacological Action of Substituted Benzamide Drugs: Pharmacology of Substituted Benzamide Druigs. . *Acta Psychiatr Scand* , 69 (S311), 109–123.

Jentsch, T. J. (2000). Neuronal KCNQ potassium channels: Physiology and role in disease. *Nature Reviews Neuroscience*, 1(1), 21-30.

Jepps ,(2011). Downregulation of Kv7.4 channel activity in primary and secondary hypertension. . *Circulation*. , 124(5):602-11.

Jespersen (2007). The KCNQ1 potassium channel is down-regulated by ubiquitylating enzymes of the Nedd4/Nedd4-like family. . *Cardiovasc Res*. , 74:64-74.

Kalappa , (2015 Jun). Potent KCNQ2/3-specific channel activator suppresses in vivo epileptic activity and prevents the development of tinnitus. *J Neurosci.*, 10;35(23):8829-42.

Kanaumi,(2008). Developmental changes in KCNQ2 and KCNQ3 expression in human brain: possible contribution to the age-dependent etiology of benign familial neonatal convulsions. . *Brain Dev*. , 30:362-9.

Kanyo, (2023). Site and Mechanism of ML252 Inhibition of Kv7 Voltage-Gated Potassium Channels. . *Function (Oxf).*, 4(4):zqad021.

Kasimova ,(2015). PIP_2-dependent coupling is prominent in Kv7.1 due to weakened interactions between S4-S5 and S6. . *Sci Rep*. , 5:7474.

Kato (2013). Clinical spectrum of early onset epileptic encephalopathies caused by KCNQ2 mutation. *Epilepsia.*, 54:1282-7.

Kim R (2015). Atomic basis for therapeutic activation of neuronal potassium channels. *Nat Commun*. , 6:8116.

Kim, (2015). Atomic basis for therapeutic activation of neuronal potassium channels. . *Nat. Commun*. , 6, 8116.

Kimitsuki ,(2010). Property of I(K,)(n) in inner hair cells isolated from guinea-pig cochlea. . *Hear Res*. , 261:57-62.

King , (2014). Kv7.2 regulates the function of peripheral sensory neurons. . *J Comp Neurol.*, 522:3262-80.

Kiskinis, (2021). Dyshomeostatic modulation of Ca2+-activated K+ channels in a human neuronal model of KCNQ2 encephalopathy . *elife*.

Klein, (2023). BHV-7000: A next-generation Kv7 activator with a focus on safety and efficacy. . *Epilepsy Research*, 192(4), 106934.

Koo CM, (2020). Cannabidiol for Treating Lennox-Gastaut Syndrome and Dravet Syndrome in Korea. . *J Korean Med Sci*. .

Kosenko , (2012). Coordinated signal integration at the M-type potassium channel upon muscarinic stimulation. . *EMBO J*, 3147–3156.

Kosenko , (2012). Coordinated signal integration at the M-type potassium channel upon muscarinic stimulation. *EMBO J*, 3147–3156.

Kothur K, (2018). Diagnostic yield of targeted massively parallel sequencing in children with epileptic encephalopathy. . *Seizure*. , 59:132-140.

Krzystanek , (2012). Deubiquitylating enzyme USP2 counteracts Nedd4-2-mediated downregulation of KCNQ1 potassium channels. . *Heart Rhythm*. , 9:440-8.

Kumar, (2016). Possible role of P-glycoprotein in the neuroprotective mechanism of berberine in intracerebroventricular streptozotocin-induced cognitive dysfunction. *Psychopharmacology* , 233, 137-152 .

Kurokawa . (2009). KCNE variants reveal a critical role of the beta subunit carboxyl terminus in PKA-dependent regulation of the IKs potassium channel. *Channels (Austin).*, 3:16-24.

Kurokawa ,(2003). Requirement of subunit expression for cAMP-mediated regulation of a heart potassium channel. *Proc Natl Acad Sci U S A.*, 100:2122-7.

Kurokawa, (2004). Regulatory actions of the A-kinase anchoring protein Yotiao on a heart potassium channel downstream of PKA phosphorylation. *Proc Natl Acad Sci U S A.*, 101:16374-8.

Kwan ,(2010). Definition of drug resistant epilepsy: consensus proposal by the ad hoc Task Force of the ILAE Commission on Therapeutic Strategies. *Epilepsia*. .

Kwan, (2000). Early identification of refractory epilepsy. . *New England Journal of Medicine.*, 342(5), 314-319.

Lange, (2009). "Refinement of the binding site and mode of action of the anticonvulsant Retigabine on KCNQ K+ channels.". *Molecular pharmacology 75.2*, 272-280.

Langlois, (2012). Pharmacology of JNJ-37822681, a Specific and Fast-Dissociating D 2 Antagonist for the Treatment oof Schizophrenia. . *J Pharmacol* , 342 (1), 91–105.

Lauritano .(2019). A novel homozygous KCNQ3 loss-of-function variant causes non-syndromic intellectual disability and neonatal-onset pharmacodependent epilepsy. *Epilepsia Open.*, 4:464-475.

Lehman (2017). Loss-of-Function and Gain-of-Function Mutations in KCNQ5 Cause Intellectual Disability or Epileptic Encephalopathy. *Am J Hum Genet.*, 101:65-74.

Lerche , (2000). Molecular cloning and functional expression of KCNQ5, a potassium channel subunit that may contribute to neuronal M-current diversity. . *J Biol Chem.* , 275:22395-400.

Li H, (2022). Inhibition of Kv7/M Channel Currents by Fangchinoline. . *Pharmacology.* , 14:1-9.

Li T, (2021). Structural Basis for the Modulation of Human KCNQ4 by Small-Molecule Drugs. . *Mol Cell.* , 81:25-37.e4.

Li Y, (2011). KCNE1 enhances phosphatidylinositol 4,5-bisphosphate (PIP2) sensitivity of IKs to modulate channel activity. . *Proc Natl Acad Sci U S A.*, 108:9095-100.

Li X., (2021). Molecular basis for ligand activation of the human KCNQ2 channel. *Cell Res*.

Li X., (2021). Molecular basis for ligand activation of the human KCNQ2 channel. . *Cell Res* , 31, 52–61.

Li, (2005). "Regulation of Kv7 (KCNQ) K+ channel open probability by phosphatidylinositol 4, 5-bisphosphate." . *Journal of Neuroscience* , 9825-9835.

Litchfield, J. T., & Wilcoxon, F. (1949). A Simplified Method of Evaluating Dose-Effect Experiments. . *J Pharmacol Exp Ther* .

Liu,(2019). Synthesis and Optimization of Kv7 (KCNQ) Potassium Channel Agonists: The Role of Fluorines in Potency and Selectivity. . *ACS Med Chem Lett.* , 10:929-935.

Liu ,(2014). Calmodulin orchestrates the heteromeric assembly and the trafficking of KCNQ2/3 (Kv7.2/3) channels in neurons. . *Mol Cell Neurosci.* , 58:40-52.

Liu, (2021). Pharmacological Activation of Neuronal Voltage-Gated Kv7/KCNQ/M-Channels for Potential Therapy of Epilepsy and Pain. . *Handb Exp Pharmacol.*, 267:231-251.

Liu, (2019)."Synthesis and optimization of Kv7 (KCNQ) potassium channel agonists: the role of fluorines in potency and selectivity." . *ACS Medicinal Chemistry Letters 10.6* , 929-935.

Lohrmann, (1995). A new class of inhibitors of cAMP-mediated Cl− secretion in rabbit colon, acting by the reduction of cAMP-activated K+ conductance. *Pflügers Archiv 429* , 517-530.

Long (2007). Atomic structure of a voltage-dependent K+ channel in a lipid membrane-like environment. *Nature.* , 450:376-82.

Löscher (2020). Drug Resistance in Epilepsy: Clinical Impact, Potential Mechanisms, and New Innovative Treatment Options. . *Pharmacol Rev.* , 72:606-638.

Ma, (2023). Ligand activation mechanisms of human KCNQ2 channel. *Nat Commun* .

Main,(2000). Modulation of KCNQ2/3 potassium channels by the novel anticonvulsant retigabine. *Mol Pharmacol.* , 58:253-62.

Malysz, (2020). Detrusor Smooth Muscle KV7 Channels: Emerging New Regulators of Urinary Bladder Function. . *Front Physiol.* , 11:1004.

Mandala, (2023). The membrane electric field regulates the PIP2-binding site to gate the KCNQ1 channel, . *Proc. Natl. Acad. Sci. U.S.A.*

Manville ,(2018). Gabapentin Is a Potent Activator of KCNQ3 and KCNQ5 Potassium Channels. . *Mol Pharmacol.*, 94(4):1155-1163.

Martire,(2004). M channels containing KCNQ2 subunits modulate norepinephrine, aspartate, and GABA release from hippocampal nerve terminals. . *J Neurosci.* , 24:592-7.

Martire, (2004). M channels containing KCNQ2 subunits modulate norepinephrine, aspartate, and GABA release from hippocampal nerve terminals. . *J Neurosci.* , 24:592-7.

Martire , (2007). Involvement of KCNQ2 subunits in [3H]dopamine release triggered by depolarization and pre-synaptic muscarinic receptor activation from rat striatal synaptosomes. *J Neurochem.* , 102:179-193.

Marx , (2002). Requirement of a macromolecular signaling complex for beta adrenergic receptor modulation of the KCNQ1-KCNE1 potassium channel. . *Science.* , 295:496-9.

Matthews ,(2020). Muscle and brain sodium channelopathies: genetic causes, clinical phenotypes, and management approaches. . *Lancet Child Adolesc Health* , 4: 536-47.

McRae , (2017). Prevalence and architecture of de novo mutations in developmental disorders. Deciphering Developmental Disorders Study. *Nature* , 542:433–438.

Melman , (2004). KCNE1 binds to the KCNQ1 pore to regulate potassium channel activity. . *Neuron* , 42:927–37.

Micel, (2009). Gating currents from neuronal K(V)7.4 channels: general features and correlation with the ionic conductance. . *Channels (Austin). Epub*, 3(4):274-83.

Miceli, (2015a). Early-onset epileptic encephalopathy caused by gain-of-function mutations in the voltage sensor of Kv7.2 and Kv7.3 potassium channel subunits. . *J Neurosci.*, 35:3.

Miceli, (2015). Early-onset epileptic encephalopathy caused by gain-of-function mutations in the voltage sensor of Kv7.2 and Kv7.3 potassium channel subunits. . *J Neurosci.*

Miceli, (2018). KCNQ2-related disorders. *In: Adam MP, Ardinger HH, Pagon RA et al (eds) , GeneReviews® [Internet]. Seattle University of Washington*.

Miceli, (2015b). A novel KCNQ3 mutation in familial epilepsy with focal seizures and intellectual disability. *Epilepsia.*, 56:e15-20.

Miceli,(2013). Genotype-phenotype correlations in neonatal epilepsies caused by mutations in the voltage sensor of K(v)7.2 potassium channel subunits. *Proc Natl Acad Sci U S A*.

Miceli,(2008). Molecular pharmacology and therapeutic potential of neuronal Kv7-modulating drugs. . *Current Opinion in Pharmacology*, 8(1), 65-74.

Milh,(2015). Variable clinical expression in patients with mosaicism for KCNQ2 mutations. *Am J Med Genet A.*, 167A:2314-8.

Millichap, (2017). Infantile spasms and encephalopathy without preceding neonatal seizures caused by KCNQ2 R198Q, a gain-of-function variant. . *Epilepsia.* , 58:e10-e15.

Millichap ,(2016). KCNQ2 encephalopathy: Features, mutational hot spots, and ezogabine treatment of 11 patients. . *Neurol Genet.*, 2:e96.

Misura , (2002). Three-dimensional structure of the amino-terminal domain of syntaxin 6, a SNAP-25 C homolog. *PNAS* , 99(14): 9184-9189.

Morello,(1999). Gabapentin for the treatment of painful diabetic neuropathy. *Clinical Therapeutics,* , 21(5), 814-827.

Mulkey ,(2017). Neonatal nonepileptic myoclonus is a prominent clinical feature of KCNQ2 gain-of-function variants R201C and R201H. *Epilepsia.*, 58:436-445.

Müller,(2015). High-resolution CMOS MEA platform to study neurons at subcellular, cellular, and network levels. . *Lab Chip.* .

Musella,(2022). Beyond Retigabine: Design, Synthesis, and Pharmacological Characterization of a Potent and Chemically Stable Neuronal Kv7 Channel Activator with Anticonvulsant Activity. *Med Chem.*, 65(16):11340-11364.

Nappi, (2022). Gain of function due to increased opening probability by two KCNQ5 pore variants causing developmental and epileptic encephalopathy. *Proc Natl Acad Sci U S A.*, 119:e2116887119.

Nappi, (2020 Jul). Epileptic channelopathies caused by neuronal Kv7 (KCNQ) channel dysfunction. . *Pflugers Arch.*, 472(7):881-898. .

Gamper, (2021). *Pharmacology of Potassium Channels*.

Oliveras, (2014). Functional assembly of Kv7.1/Kv7.5 channels with emerging properties on vascular muscle physiology. . *Arterioscler Thromb Vasc Biol.* , 34:1522-30.

Orhan, (2014). Dominant-negative effects of KCNQ2 mutations are associated with epileptic encephalopathy. . *Ann Neurol.* , 75(3):382-94.

Ostacolo, (2020). Synthesis and pharmacological characterization of conformationally restricted retigabine analogues as novel neuronal Kv7 channel activators. *J. Med. Chem.* , 63, 163–185.

Padilla ,(2009). The KCNQ2/3 selective channel opener ICA-27243 binds to a novel voltage-sensor domain site. . *Neurosci Lett.* .

Pan, (2006). A common ankyrin-G-based mechanism retains KCNQ and NaV channels at electrically active domains of the axon. . *J Neurosci* , 26:2599–2613.

Paventi, (2022). Kv7.4 channels regulate potassium permeability in neuronal mitochondria,. *Biochemical Pharmacology*.

Peretz, (2005). Meclofenamic acid and diclofenac, novel templates of KCNQ2/Q3 potassium channel openers, depress cortical neuron activity and exhibit anticonvulsant properties. *Mol Pharmacol.*, 67:1.

Peretz ,(2007). A tale of switched functions: from cyclooxygenase inhibition to M-channel modulation in new diphenylamine derivatives. . *PLoS One.* , 2:e1332.

Peters,(2005). Conditional transgenic suppression of M channels in mouse brain reveals functions in neuronal excitability, resonance and behavior. . *Nat Neurosci.* , 8:51-60.

Pharmaceuticals, B. (2023). Biohaven's BHV-7000: A next-generation therapy for epilepsy and neurological disorders. *Biohaven Press*.

Poduri. (2017). When Should Genetic Testing Be Performed in Epilepsy Patients? *Epilepsy Curr.*, 17:16-22.

Poduri ,(2011). Epilepsy genetics--past, present, and future. . *Curr Opin Genet Dev.* , 21:325-32.

Pohlmann-Eden, (2013). The puzzle(s) of pharmacoresistant epilepsy. *Epilepsia.*, 54 Suppl 2:1-4.

Preston, (2010). Disruption of the K+ channel beta-subunit KCNE3 reveals an important role in intestinal and tracheal Cl- transport. . *J. Biol. Chem.* .

Raol , (2009). A KCNQ channel opener for experimental neonatal seizures and status epilepticus. . *Ann Neurol.* , 65:326-36.

Regev , (2009). Selective interaction of syntaxin 1A with KCNQ2: possible implications for specific modulation of presynaptic activity. *Plos One*, 4:e6586.

Rice, (2001). Gabapentin in postherpetic neuralgia. *JAMA*, 285(7), 913-921.

Richards,(2015). Standards and guidelines for the interpretation of sequence variants: a joint consensus recommendation of the American College of Medical Genetics and Genomics and the Association for Molecular Pathology. . *Genet Med* , 17:405-24.

Robbins, (2001 Apr). KCNQ potassium channels: physiology, pathophysiology, and pharmacology. *Pharmacol Ther.*, 90(1):1-19.

Rockwood ,(1997). A randomized, controlled trial of linopirdine in the treatment of Alzheimer's disease. . *Can J Neurol Sci.* , 24:140-5.

Roepke ,(2006). The KCNE2 potassium channel ancillary subunit is essential for gastric acid secretion. . *J Biol Chem.* , 281:23740-7.

Ronchi, (2021). Electrophysiological Phenotype Characterization of Human iPSC-Derived Neuronal Cell Lines by Means of High-Density Microelectrode Arrays. . *Adv Biol (Weinh).* .

Rosti ,(2019). Intragenic duplication of KCNQ5 gene results in aberrant splicing leading to a premature termination codon in a patient with intellectual disability. *Eur J Med Genet.*, 62:103555.

Rostock, (1996). A New Anticonvulsant with a Broad Spectrum Activity in Animal Models of Epileptic Seizures. *Epilepsy Research* .

Ruggiero ,(2023). The current landscape of epilepsy genetics: where are we, and where are we going? . *Curr Opin Neurol.*, 36(2):86-94.

Saganich ,(2001). Differential expression of genes encoding subthreshold-operating voltage-gated K+ channels in brain. . *J Neurosci.* , 21:4609-24.

Salzer, (2017). Phosphorylation regulates the sensitivity of voltage-gated Kv7.2 channels towards phosphatidylinositol-4,5-bisphosphate. . *J Physiol.* , 595:759-776.

Sanders (2019). Implications of genetic diagnostics in epilepsy surgery candidates: A single-center cohort study. . *Epilepsia Open* , 4:609-17.

Sands (2019).. Autism and developmental disability caused by KCNQ3 gain-of-function variants. . *Ann Neurol.* , 86(2):181-192.

Sanguinetti (1996). Coassembly of K(V)LQT1 and minK (IsK) proteins to form cardiac I(Ks) potassium channel. . *Nature* , 384:80–83.

Sarnthein (1998). Synchronization between prefrontal and posterior association cortex during human working memory. *Proc Natl Acad Sci U S A.* ., 95:7092-6.

Scheffer (2017). ILAE classification of the epilepsies: Position paper of the ILAE Commission for Classification and Terminology. . *Epilepsia.* , 58:512-521. .

Scheffer, (2016). Classification of the epilepsies: New concepts for discussion and debate-Special report of the ILAE Classification Task Force of the Commission for Classification and Terminology. *Epilepsia Open.* , 1(1-2):37-44.

Schenzer,(2005). Molecular determinants of KCNQ (Kv7) K+ channel sensitivity to the anticonvulsant retigabine. . *J Neurosci.* , 25:5051-60.

Schenzer,.(2005). Determinants of KCNQ (K v 7) K + Channel Sensitivity to the Anticonvulsant Retigabine. . *J. Neurosci.* , 25 (20), 5051–5060.

Schmidt ,(2005). Drug resistance in epilepsy: putative neurobiologic and clinical mechanisms. . *Epilepsia.* , 46:858-77.

Schroeder (2000). KCNQ5, a novel potassium channel broadly expressed in brain, mediates M-type currents. . *J Biol Chem.* , 275:24089-95.

Schroeder (1998). Moderate loss of function of cyclic-AMP-modulated KCNQ2/KCNQ3 K+ channels causes epilepsy. . *Nature.* , 396:687-90.

Schroeder, (1998). KCNQ family of K+ channels: Novel insights into functional diversity and neuronal excitability. . *The EMBO Journal*, 17(7), 1869-1876.

Schwake ,(2006). Structural determinants of M-type KCNQ (Kv7) K+ channel assembly. . *J Neurosci.* , 26:3757-66.

Schwake ,(2003). A carboxy-terminal domain determines the subunit specificity of KCNQ K(+) channel assembly. . *EMBO Rep*, 4:76–81.

Schwake (2000). Surface expression and single channel properties of KCNQ2/KCNQ3, M-type K+ channels involved in epilepsy. *J Biol Chem.*, 275:13343-8.

Schwarz,(2006). KCNQ channels mediate IKs, a slow K+ current regulating excitability in the rat node of Ranvier. *J Physiol.*, 573:17-34.

Seebohm, (2006). Differential roles of S6 domain hinges in the gating of KCNQ potassium channels. Biophys J. *Biophys J.*, 90:2235-2244.

Selyanko, (2001). Properties of single M-type KCNQ2/KCNQ3 potassium channels expressed in mammalian cells. *J Physiol.*, 534(Pt 1):15-24. .

Shamgar, (2006). Calmodulin is essential for cardiac IKS channel gating and assembly: impaired function in long-QT mutations. *Circ Res.* , 98:1055-63.

Shapiro,(2000). Reconstitution of muscarinic modulation of the KCNQ2/KCNQ3 K(+) channels that underlie the neuronal M current. *J Neurosci* , 20:1710–1721.

Shi,(2020). Molecular Mechanisms and Structural Basis of Retigabine Analogues in Regulating KCNQ2 Channel. *J Membr Biol.*, 253:167-181.

Silvinato, (2022). Use of cannabidiol in the treatment of epilepsy: Lennox-Gastaut syndrome, Dravet syndrome, and tuberous sclerosis complex. . *Rev Assoc Med Bras (1992)*.

Simkin, (2021). Dyshomeostatic modulation of Ca^{2+}-activated K^{+} channels in a human neuronal model of KCNQ2 encephalopathy. *eLife*.

Singh ,(1998). A novel potassium channel gene, KCNQ2, is mutated in an inherited epilepsy of newborns. *Nat Genet.*, 18:25-9.

Sisodiya,(2013). Precision medicine and therapies of the future. . *Epilepsia.*, 54(s2), 35-39.

Søgaard,(2001). KCNQ4 channels expressed in mammalian cells: functional characteristics and pharmacology. . *Am J Physiol Cell Physiol* , 280:C859–C866.

Soh,(2022). KCNQ2 and KCNQ5 form heteromeric channels independent of KCNQ3. *Proc Natl Acad Sci U S A.*, 19:e2117640119.

Soldovieri, (2014). Novel KCNQ2 and KCNQ3 mutations in a large cohort of families with benign neonatal epilepsy: first evidence for an altered channel regulation by syntaxin-1A. *Hum Mutat.*, 35:356-67.

Soldovieri,(2020). Gabapentin treatment in a patient with KCNQ2 developmental epileptic encephalopathy. . . *Pharmacol Res.*, 160:105200.

Soldovieri,(2011). Driving with no brakes: molecular pathophysiology of Kv7 potassium channels. . *Physiology* , Oct;26(5):365-76.

Soldovieri,(2020). Gabapentin treatment in a patient with KCNQ2 developmental epileptic encephalopathy. *Pharmacol Res.*, 160:105200.

Sorge, (2010). Epilepsy and chromosomal abnormalities. *Ital J Pediatr.* , 3;36:36.

Specchio, (2022). International League Against Epilepsy classification and definition of epilepsy syndromes with onset in childhood: Position paper by the ILAE Task Force on Nosology and Definitions. . *Epilepsia*. , 63:1398-1442.

Steinlein, (1995). A missense mutation in the neuronal nicotinic acetylcholine receptor alpha 4 subunit is associated with autosomal dominant nocturnal frontal lobe epilepsy. *Nat Genet 1995 11:201-3*, 11:201-3.

Stott, (2014). K(V)7 potassium channels: a new therapeutic target in smooth muscle disorders. . *Drug Discov Today*. , 19:413-24.

Striano, (2020). From Genetic Testing to Precision Medicine in Epilepsy. . *Neurotherapeutics*. , 17:609-615.

Sun, (2019). KCNQ/M-channels regulate mouse vagal bronchopulmonary C-fiber excitability and cough sensitivity. . *JCI Insight*. , 4:e124467.

Sun, (2017). Cryo-EM Structure of a KCNQ1/CaM Complex Reveals Insights into Congenital Long QT Syndrome. *Cell.*, 169(6):1042-1050.e9.

Sun, (2020). Structural Basis of Human KCNQ1 Modulation and Gating. *Cell.*, 180:340-347.e9.

Sun, (2017). Cryo-EM Structure of a KCNQ1/CaM Complex Reveals Insights into Congenital Long QT Syndrome. *Cell*, 1042-1050.

Surur, (2019). Flupirtine and retigabine as templates for ligand-based drug design of KV7.2/3 activators. . *Org Biomol Chem.*, 17:4512-4522.

Svalø, (2013). Bladder contractility is modulated by Kv7 channels in pig detrusor. . *Eur J Pharmacol*. , 715:312-20.

Syeda, (2016). The Sensorless Pore Module of Voltage-gated K+ Channel Family 7 Embodies the Target Site for the Anticonvulsant Retigabine. . *J Biol Chem*. , 291:2931-7.

Syvertsen, (2015). Prevalence and incidence of epilepsy in the Nordic countries. . *Tidsskr Nor Laegeforen*. , 135:1641-5.

Szelenyi, (2013). Flupirtine, a re-discovered drug, revisited. *Inflamm Res.*, 62:251-8.

Taglietti,(2015). *Fisiologia e biofisica delle cellule*. Napoli: : EdiSES.

Tao, (2010). A gating charge transfer center in voltage sensors. . *Science*. , 328:67-73.

Tasic,(2016). Adult mouse cortical cell taxonomy revealed by single cell transcriptomics. . *Nat Neurosci*. , 19:335-46.

Tatulian, (2003). Effect of the KCNQ potassium channel opener retigabine on single KCNQ2/3 channels expressed in CHO cells. . *J Physiol*. , 549:57-63.

Tatulian, (2001). Activation of expressed KCNQ potassium currents and native neuronal M-type potassium currents by the anti-convulsant drug retigabine. . *J Neurosci*. , 21:5535-45.

Testai, (2016). Expression and function of Kv7.4 channels in rat cardiac mitochondria: possible targets for cardioprotection. *Cardiovasc Res*.

Thiele, (2018). Cannabidiol in patients with seizures associated with Lennox-Gastaut syndrome. . *New England Journal of Medicine*, 378(20), 1888-1897.

Tinel , (1998). The KCNQ2 potassium channel: splice variants, functional and developmental expression. Brain localization and comparison with KCNQ3. . *FEBS Lett.*, 438:171-6.

Tykocki (2019). The KV 7 channel activator retigabine suppresses mouse urinary bladder afferent nerve activity without affecting detrusor smooth muscle K+ channel currents. . *J Physiol.* , 597:935-950.

Tzingounis (2008). Contribution of KCNQ2 and KCNQ3 to the medium and slow afterhyperpolarization currents. . *Proc Natl Acad Sci U S A.* , 105:19974-9.

Tzingounis (2010). The KCNQ5 potassium channel mediates a component of the afterhyperpolarization current in mouse hippocampus. *Proc Natl Acad Sci U S A.*, 107:10232-7.

Tzingounis, (2008). Contribution of KCNQ2 and KCNQ3 to the medium and slow afterhyperpolarization currents. *Proc Natl Acad Sci U S A.*, 105:19974-9.

Verneuil (2020). The M-current works in tandem with the persistent sodium current to set the speed of locomotion. . *PLoS Biol.* , 18:e3000738.

Wainger (2021). Effect of Ezogabine on Cortical and Spinal Motor Neuron Excitability in Amyotrophic Lateral Sclerosis: A Randomized Clinical Trial. *JAMA Neurol.* .

Walsh (1988). Regulation of a heart potassium channel by protein kinase A and C. *Science.*, 242(4875).

Wang , (2000). Molecular basis for differential sensitivity of KCNQ and I(Ks) channels to the cognitive enhancer XE991. . *Mol Pharmacol.* , 57:1218-23.

Wang , (1998). KCNQ2 and KCNQ3 potassium channel subunits: molecular correlates of the M-channel. . *Science.* , 282:1890-3.

Wang, (2017). Sequence Determinants of Subtype-specific Actions of KCNQ Channel Openers. . *The Journal of Physiology* , 595 (3), 663–676.

Wang, (1998). KCNQ2 and KCNQ3 Potassium Channel Subunits: Molecular Correlates of the M-Channel. . *Science* .

Warth, (1996). The cAMP-regulated and 293B-inhibited K+ conductance of rat colonic crypt base cells. 432, 81–88.

Watanabe, (2000). Disruption of the epilepsy KCNQ2 gene results in neural hyperexcitability. . *J Neurochem.*, 75:28-33.

Weber, (2006). Immunohistochemical analysis of KCNQ2 potassium channels in adult and developing mouse brain. . *Brain Res.*, 1077:1–6.

Weckhuysen,(2022). KCNQ2- and KCNQ3-Associated Epilepsy (Elements in Genetics in Epilepsy) . *Cambridge: Cambridge University Press*.

Wei,(2022). Human KCNQ5 de novo mutations underlie epilepsy and intellectual disability. . *J Neurophysiol.* , 128:40-61.

Wei, (2024). A Randomized, Double-blind, Placebo-controlled, Dose-escalating Phase IIA Trial to Evaluate the Safety, Tolerability, Efficacy, and Pharmacokinetics of Multiple Oral Doses of

Pynegabine Tablets as Add-on Therapy in Patients with Focal Epilepsy. *CNS Neurosci Ther* , 30 (9), e70002.

Wells ,(2020). Efficacy and Safety of a Ketogenic Diet in Children and Adolescents with Refractory Epilepsy-A Review. *Nutrients*. , 12:1809. .

Wickenden (2008). N-(6-chloro-pyridin-3-yl)-3,4-difluoro-benzamide (ICA-27243): a novel, selective KCNQ2/Q3 potassium channel activator. *Mol Pharmacol*. .

Wiffen,(2017). Gabapentin for chronic neuropathic pain in adults. . *Cochrane Database of Systematic Reviews,*, 6, CD007938.

Willegems, (2022). Structural and electrophysiological basis for the modulation of KCNQ1 channel currents by ML277. *Nat Commun* .

Wrobel,(2012). The KCNE Tango - How KCNE1 Interacts with Kv7.1. . *Front Pharmacol.*, 3:142.

Wu,(2013). Discovery of (S,E)-3-(2-fluorophenyl)-N-(1-(3-(pyridin-3-yloxy)phenyl)ethyl)-acrylamide as a potent and efficacious KCNQ2 (Kv7.2) opener for the treatment of neuropathic pain. *Bioorg Med Chem Lett*. , 23:6188-91.

Wu,(2004b). Synthesis and KCNQ2 opener activity of N-(1-benzo[1,3]dioxol-5-yl-ethyl, N-[1-(2,3-dihydro-benzofuran-5-yl)-ethyl, and N-[1-(2,3-dihydro-1H-indol-5-yl)-ethyl acrylamides. . *Bioorg Med Chem Lett*. , 14:4533-7.

Wulff, (2009). Voltage-gated potassium channels as therapeutic targets. . *Nat Rev Drug Discov* , 8, 982–1001 .

Wurm,(2022b). Modifications of the Triaminoaryl Metabophore of Flupirtine and Retigabine Aimed at Avoiding Quinone Diimine Formation. *ACS Omega.*, 7:7989-8012.

Wurm,(2023). Replacing the oxidation-sensitive triaminoaryl chemotype of problematic KV7 channel openers: Exploration of a nicotinamide scaffold. . *Arch Pharm (Weinheim)*. , 356:e2200473.

Wuttke,(2005). The new anticonvulsant retigabine favors voltage-dependent opening of the Kv7.2 (KCNQ2) channel by binding to its activation gate. . *Mol Pharmacol*. , 67:1009-17.

Xiong ,(2008). Combinatorial augmentation of voltage-gated KCNQ potassium channels by chemical openers. Proc Natl Acad Sci U S A. 2008 Feb 26.

Xu, (2020). The auxiliary subunit KCNE1 regulates KCNQ1 channel response to sustained calcium-dependent PKC activation. . *PLoS One*. , 15:e0237591.

Yue C, (2004). KCNQ/M channels control spike afterdepolarization and burst generation in hippocampal neurons. . *J Neurosci.*, 24:4614-24.

Yus-Najera (2002). The identification and characterization of a noncontinuous calmodulin-binding site in noninactivating voltage-dependent KCNQ potassium channels. . *J Biol Chem*. , 277:28545-53.

Zaczek (1993). Unique properties of norepinephrine release from terminals arising from the locus coeruleus: high potassium sensitivity and lack of linopirdine (DuP 996) enhancement. . *Neurosci Lett*. , 155:107-11.

Zaydman (2013). Kv7.1 ion channels require a lipid to couple voltage sensing to pore opening. *Proc Natl Acad Sci U S A*. , 110:13180-5.

Zhang (2003). PIP2 activates KCNQ channels, and its hydrolysis underlies receptor-mediated inhibition of M currents. . *Neuron*. , 37:963-75.

Zhang (2022). Cannabidiol activates neuronal Kv7 channels. . *Elife*. .

Zhang (2013). Dynamic PIP2 interactions with voltage sensor elements contribute to KCNQ2 channel gating. Proc Natl Acad Sci U S A. 2013 110:20093-8. *Proc Natl Acad Sci U S A*. , 110:20093-8.

Zhang ,(2013). Rapid single-step induction of functional neurons from human pluripotent stem cells. *Neuron*. *Jun 5;78(5):785-98*.

Zhang, (2024). A small-molecule activation mechanism that directly opens the KCNQ2 channel. *Nature Chemical Biology* .

Zhang, (2021). Discovery of HN37 as a Potent and Chemically Stable Antiepileptic Drug Candidate. . *J. Med. Chem*. .

Zheng,(2022). Structural insights into the lipid and ligand regulation of a human neuronal KCNQ channel. . *Neuron*. , 110:237-247.e4.

Zhou, (2015). P-retigabine: an N-propargyled retigabine with improved brain distribution and enhanced antiepileptic activity. . *Mol Pharmacol*. , 87:31-8.

Zhuang, (2021). The S2-S3 Loop of Kv7.4 Channels Is Essential for Calmodulin Regulation of Channel Activation. . *Front Physiol.*, 11:604134.

RINGRAZIAMENTI

Negli ultimi tre anni, ho avuto il privilegio di intraprendere il mio percorso di dottorato nel Dipartimento di Neuroscienze dell'Università di Napoli Federico II. Sono stati anni estremamente stimolanti e formativi, caratterizzati da un'intensa crescita professionale e personale. Ho avuto la fortuna di incontrare numerosi ricercatori, ognuno dei quali mi ha ispirato con il proprio lavoro e la propria passione, e con molti di loro ho continuato a mantenere un rapporto di scambio e collaborazione. Tutto ciò è stato possibile grazie al Prof. Taglialatela, che mi ha accolto nel suo laboratorio con grande fiducia e mi ha saputo guidare con un approccio esemplare, nonostante fossi un ingegnere. La sua trasparenza, competenza e dedizione sono state per me non solo fonte di insegnamento, ma anche di grande motivazione. Ogni confronto con lui ha rappresentato un'opportunità per affinare la mia visione scientifica interdisciplinare, migliorare le mie capacità di analisi e crescere come ricercatrice. Il suo esempio ha avuto un impatto fondamentale su come affronto il lavoro e la ricerca, ispirandomi a perseguire l'eccellenza in ogni aspetto del mio percorso.

Un sentito ringraziamento va al Prof. Miceli, che mi ha letteralmente preso per mano, accompagnandomi con grande pazienza e competenza nei miei primi passi nel mondo della ricerca. È stata una figura di riferimento costante. Grazie al suo sostegno e fiducia, sono riuscita a superare i miei confini da ingegnere, ampliando le mie conoscenze e sviluppando nuove competenze. Inoltre, lavorare con lui è stato non solo un'esperienza formativa da allieva, ma anche estremamente piacevole: insieme abbiamo creato una squadra efficiente e affiatata. Gli sono grata per tutto ciò che ho imparato durante questo tempo insieme.

Un sentito ringraziamento va al Prof. Barrese, il cui coinvolgimento è stato fondamentale per la mia crescita professionale. Grazie a lui ho imparato a gestire con determinazione ed efficacia situazioni lavorative complesse e ad affrontare la pressione con maggiore sicurezza.

Un sentito ringraziamento va alla Dott.ssa Lidia Carotenuto, che mi ha accolto nel gruppo con entusiasmo e guidato con dedizione, superando di gran lunga il suo ruolo di dottoranda senior. Tra i tanti consigli che mi ha trasmesso, una frase rimarrà indelebile nella mia memoria: *"Siamo tutti uguali quando entriamo qui dentro, non ti spaventare, vedi di fare tu la differenza."* Non è stata solo un invito alla crescita, ma una sfida a distinguermi attraverso l'impegno, la responsabilità e la consapevolezza delle mie capacità. Grazie, per essere stata la prima persona ad aver creduto in me in tale contesto, per avermi guidato con fiducia e ispirato a dare il meglio di me stessa. Ti sarò sempre grata. È stato un onore e un privilegio

essere stata anche tua allieva e avere avuto la possibilità di imparare da te, di lavorare con te e per te.

Un sentito ringraziamento alla Dott.ssa Natascia Guida, la cui professionalità e dedizione sono state un costante punto di riferimento. Grazie, per essere stata una guida preziosa e un supporto in ogni fase di questo percorso.

I would also like to extend my heartfelt thanks to Marcus Kaji and Nina Dirkx for going beyond mere formalities and appreciating me for my skills and qualities. Beyond our professional relationship, we developed a bond built on mutual respect and genuine affection, which I truly value. Thank you for the time and energy you dedicated to our collaboration, for your willingness to listen, and for the invaluable insights you shared with me. The meetings we shared were not only productive but also filled with moments of camaraderie and encouragement that made a lasting impression on me. Your support and kindness have enriched my experience in countless ways, and I am deeply grateful to have had the opportunity to work alongside such remarkable individuals.

I would like to express my deepest gratitude to Prof. Holger Lerche and his team for generously hosting me in their lab for three months. This opportunity has been a defining experience in my academic journey, and I am incredibly grateful for the warm and supportive environment they created. A special thank you goes to Dr. Ulrike Hedrich, who not only welcomed me into her group but also made me feel like a valued part of the team. Being part of her group reminded me that science is truly for everyone—it thrives on passion, curiosity, and a willingness to learn. I am especially grateful for the way you treated me, not as an outsider, but as one of your PhD students. Your genuine care, encouragement, and mentorship were invaluable. From taking the time to guide me through new concepts to ensuring I felt supported in both my work and personal well-being, your kindness did not go unnoticed. I would also like to thank Stefano Iavarone, one of Ulrike's PhD students, who generously shared his time and expertise with me. Learning from him was an invaluable part of my experience, and his patience and guidance have had a significant impact on my understanding and growth. Thank you for fostering an environment where I could grow, learn, and feel confident in my contributions. These three months have not only enriched my knowledge but have also reminded me why I love science.

Un sincero ringraziamento va anche a tutti i colleghi dottorandi, assegnisti, ricercatori e professori del quindicesimo e del diciassettesimo piano, che sono sempre stati disponibili per confronti scientifici, rendendo ogni aspetto del lavoro più accessibile e stimolante.

Un ringraziamento alla Dott.ssa Elena Esposito e Dott.ssa Anna Imperatore per il loro efficiente supporto amministrativo ed emotivo.

Un sentito grazie a Vincenzo Santoro, il mio primo tesista, che in questo ultimo anno trascorso insieme ha contribuito a migliorare le mie capacità di guida e mentorship.

Trascorrere tanto tempo in laboratorio mi ha permesso di costruire legami che vanno ben oltre le mura del luogo di lavoro. Sono grata di aver incontrato persone straordinarie con cui ho condiviso esperienze e momenti indimenticabili. Vorrei dedicare un pensiero speciale a ciascuna di loro, per sottolineare quanto siano state importanti nel mio percorso.

Un sentito grazie a *Giusy Laudati*, che mi ha sempre accolta con disponibilità, sia per un confronto scientifico che per un consiglio personale. Sei stata un grande punto di riferimento. La tua competenza, la tua dedizione e la tua passione per la ricerca sono state per me una fonte di grande ispirazione. Grazie, per tutto ciò che hai condiviso con me e per il tuo sostegno umano in ogni momento. Sono sicura che continuerai a fare la differenza ovunque.

A *Silvia Ruggiero*, il mio grazie va per la tua contagiosa allegria, quel tuo spirito vivace capace di alleggerire ogni giornata e rendere speciali anche i momenti più semplici. La nostra complicità, con quel pizzico di follia che ci accomuna, è stata la chiave che ha trasformato ogni incontro in un'esperienza unica, in cui anche nei giorni più difficili tutto sembrava più leggero e sopportabile. Grazie per la tua sensibilità, che sa cogliere le sfumature più nascoste. Grazie, per la tua capacità di andare oltre le apparenze e le etichette, di vedere ciò che c'è davvero dietro ogni sorriso e ogni parola. Grazie, per aver visto in me ciò che pochi sono in grado di percepire, per avermi accettata come amica con tutte le mie fragilità e imperfezioni, nonostante non facessimo parte dello stesso gruppo di ricerca. Grazie, per essere sempre stata lì, anche nei momenti più inaspettati, con una parola gentile, un sorriso, un gesto che cambiava l'aria di una stanza. Grazie, per le passeggiate tranquille, per le pizze mangiate con leggerezza e i gelati condivisi nei pomeriggi più caldi. Grazie, per i pranzi in compagnia, le risate e le chiacchierate che hanno fatto volare il tempo senza accorgercene, rendendo ogni momento più bello, più vivido, e che porterò sempre con me. La tua amicizia è stata, è e sarà per sempre un dono raro e prezioso, un legame che custodirò nel cuore con gratitudine infinita.

To *Ingride Gaspar*, a daily discovery and an extraordinary companion on this journey. I first met you during your initial steps in the lab, a path that began with me as your guide (though I feared I might not fulfill the role as well as I hoped) and you as a learner, but quickly evolved into a genuine connection built on trust, understanding, and shared experiences. Day after day, we created something special: a deep friendship that rises above professional boundaries. Thank you for looking beyond the surface, beyond the shy, precise, sometimes overly serious control-freak person that I am. With you, I felt accepted for who I truly am, free to show even my vulnerabilities. Thank you for believing in me when I may have doubted myself, for being a true teammate, my favorite co-worker, and for making both of us stronger through your trust and support. Your insights and perspectives have constantly challenged me to grow, both professionally and personally. I am grateful for the way you pushed me to reach higher standards. Thank you for understanding my silence, which made me feel listened and less alone in a competitive environment. Being by your side has been a privilege, from which I have taken a piece of your independence and confidence. Thank you for the laughter, for the moments when you lightened my burdens, and for your ability to turn difficult situations into opportunities for growth and reflection. Thank you for the time we shared outside of the work environment, for welcoming me into your world, and for allowing me the chance to truly know you, discovering something new about you every day: a big heart full of loyalty and honestly. Each conversation, each challenge faced together, has added to the foundation of mutual respect and understanding we've built. I consider you one of my close friends. Even though time and distance may try to work against us, I hope they will never be able to break what we've built, because our bond might go far beyond all of that. I am certain that, despite everything, we will always be there for each other. *Always*.

Grazie a *Federica Marino*, una tesista che, nonostante non facessimo parte dello stesso gruppo di ricerca, è riuscita a costruire con naturalezza e spontaneità le fondamenta di un'amicizia. Grazie, per le risate sincere che ci hanno fatto sentire più vicine, per quelle passeggiate che sono diventate occasioni di scambio e di crescita, e per la semplice gioia di condividere momenti che rimarranno impressi nei miei ricordi. Grazie, soprattutto, per avermi ricordato il vero significato di forza e determinazione, quelle qualità che, insieme, abbiamo riscoperto nei momenti di sfida. Infine, grazie, per aver saputo andare oltre le apparenze, per aver visto in me molto più di ciò che l'etichetta avrebbe potuto suggerire. Grazie, perché nonostante la distanza ci siamo l'una per l'altra. La tua amicizia è un dono prezioso che porterò sempre con me.

Un sentito ringraziamento a *Michele Tufano, Silvia Sapienza, Rohan Patil, Raffaella Ciancio* ed *Elena Dapolito* per il supporto reciproco, i momenti di leggerezza e le risate condivise fuori dal laboratorio. La vostra compagnia ha reso speciale ogni occasione, regalandomi attimi di spensieratezza che conserverò con grande affetto.

Quando raggiungi un traguardo, ti rendi conto di quanto sia stata fondamentale la presenza delle persone che ti conoscono e ti sostengono in ogni scelta che hai affrontato. Vorrei dedicare alcune parole di gratitudine alla mia famiglia e alle mie amicizie, pilastri preziosi in questo percorso.

Vorrei dedicare un pensiero di profonda gratitudine *ai miei genitori*, che hanno rappresentato un porto sicuro in ogni momento della mia vita. Con la loro fiducia incrollabile, il loro sostegno incondizionato e il loro amore, mi hanno dato il coraggio di perseguire le mie scelte e di credere sempre nelle mie capacità. La loro presenza è stata e continua ad essere una guida preziosa e un esempio di forza e dedizione.

Un ringraziamento speciale va *ai miei fratelli*, che non sono solo parte della mia famiglia, ma anche i miei primi amici e i miei più grandi sostenitori. *Gianni* e *Salvatore*, con il loro modo unico di vedere la vita e il loro immancabile senso dell'umorismo, riescono sempre a portare leggerezza anche nei momenti più complessi. Grazie a loro, cerco di non prendere tutto troppo sul serio e a sorridere anche di fronte alle difficoltà.

Un pensiero particolarmente sentito è per *mia sorella Annamaria*, con cui condivido un legame speciale che supera qualsiasi differenza di età. Nonostante i dodici anni che ci separano, tra confidenze e momenti di sfogo, lei è una complice, un’amica e una presenza fondamentale nella mia vita. Crescere accanto a lei e accompagnarla nei suoi passi mi ha fatto scoprire lati di me stessa che non conoscevo. Aiutandola a crescere, mi sta insegnando molto: mi sta aiutando a essere più paziente, più attenta e più consapevole delle mie capacità. Inoltre, lei ha la straordinaria capacità di capirmi senza che io debba parlare, di leggere i miei umori con una sensibilità che pochi possiedono, e di offrirmi conforto o sostegno con una dolcezza che scalda il cuore. La sua curiosità e la sua intelligenza mi spingono a guardare il mondo con occhi nuovi e a trovare bellezza anche dove non avrei mai pensato di cercarla. Spero un giorno di essere per lei un punto di riferimento forte e stabile, come lei lo è già per me in modi che forse non immagina. Sono immensamente grata per il suo affetto e la sua presenza nella mia vita, che considero un dono inestimabile.

La loro presenza nella mia vita è un regalo che non smetterò mai di apprezzare, perché ho avuto la possibilità di essere figlia e sorella maggiore.

Adesso, tocca a voi, *amiche*:

Grazie a *Giovanna*, che con la sua vitalità e gioia riesce a cambiarti l'umore in un istante. Ha un talento unico nel rendere tutto più leggero, nonostante sia un ingegnere, e questo la rende ancora più speciale. Giovanna ha un cuore grande, pieno di generosità e amore per gli altri, e ogni volta che parliamo mi trasmette un coraggio contagioso e una straordinaria ispirazione a dare sempre il meglio. È una vera fonte di motivazione per me. Un grazie anche a suo marito Enzo, che con resilienza e precisione, qualità tipiche di un buon ingegnere, mi ha insegnato a vedere la cura dei dettagli come un pregio. E un pensiero speciale va al piccolo Luigi, che con i suoi sorrisi e il suo affetto incondizionato regala gioia a chiunque lo incontri. Grazie, famiglia Mignano, per essere un esempio di amore e sostegno. Vi voglio bene.

Grazie ad *Antonella*, che con la sua maturità e sensibilità mi ha permesso di essere sua amica. È una persona piena di coraggio, con un'anima gentile, e la sua fiducia in me è stata un dono prezioso. Nonostante la distanza, ha sempre creduto in me, e in molti momenti ho sentito la sua vicinanza come se fosse accanto a me, attraverso i nostri confronti. Sono grata per la nostra amicizia e spero di poter condividere con lei ancora tanti momenti di leggerezza e gioia. Ti voglio bene.

Grazie a *Marisa*, che con la sua riservatezza, semplicità ed onestà ha saputo abbattere le mie barriere di insicurezza, spronandomi a migliorarmi giorno dopo giorno.

Grazie a *Miriana*, che con la sua gentilezza e sensibilità mi ha accolto nella sua vita senza mai giudicarmi, facendomi sentire una persona speciale. Un ringraziamento speciale va anche a *Nando*, per la sua inesauribile disponibilità nel farmi da "tassista" e, soprattutto, per avermi insegnato con il suo esempio che non bisogna mai rinunciare ai propri sogni, qualunque essi siano. Grazie a entrambi per essere un modello da seguire e per aver arricchito la mia vita con la vostra presenza, il vostro supporto e la vostra straordinaria umanità.

Sia *Marisa* che *Miriana* sono state per me un sostegno fondamentale, grandi amiche e un punto di riferimento prezioso. Sempre disponibili, a qualsiasi ora. La nostra amicizia è un esempio straordinario di supporto reciproco: ci siamo sempre comprese e sostenute, anche nei momenti di sconforto. Forse non troverò mai le parole giuste per descrivere quanto sia

speciale il legame che ci unisce, ma mi sento incredibilmente fortunata ad averle incontrate. È come se ci conoscessimo da sempre. Abbiamo collezionato tanti ricordi insieme: affrontato ansie preesame, paure e momenti di vita importanti. Con il loro supporto, mi stanno aiutando a trasformare le mie insicurezze in punti di fiducia e forza. Sono certa che ci aspettano ancora tante avventure divertenti da vivere insieme, e non vedo l'ora di condividerle al loro fianco. Vi voglio bene.